THE REACTIONS OF FLAVIN-DEPENDENT THYMIDYLATE SYNTHASE FROM *THERMOTOGA MARITIMA*

by

John A. Conrad

A dissertation submitted in partial fulfillment
of the requirements for the degree of
Doctor of Philosophy
(Chemical Biology)
in the University of Michigan
2011

Doctoral Committee:

Associate Professor Bruce A. Palfey, Chair
Professor Dave P. Ballou
Professor E. Neil G. Marsh
Associate Professor Kristina I. Hakansson
Assistant Professor Patrick J. O'Brien

To Milo

ACKNOWLEDGEMENTS

I would like to first and foremost like to thank my advisor, Dr. Bruce Palfey. His deep understanding of enzymology not only guides but has inspired me. I would like to thank him for being so understanding of a grad student with a kid, it has meant such a great deal to me. I would also like to thank the Palfey lab. I would especially like to thank a former post-doc, Mariliz Johnson, who helped me in getting started in my thesis work. Mariliz also performed the acid quenching experiments that were discussed in Chapter 3. Also, Sam Hoppe for the HPLC analysis of dTMP from mutant enzymes discussed in Chapter 3.

Thanks to my committee – Dave Ballou, Neil Marsh, Kicki Hakansson, and Pat O'Brien. All have been extremely helpful in my research. Also, thanks to the Chemical Biology program. I could not have asked for a better group of fellow students share this experience with.

I would also like to thank Dr. Graham Moran, for giving me a place to do research while still being close to my family. I am indebted always.

Finally I would like to thank my family for their support and patients. They have always been there for me and it has been greatly appreciated. I would also like to thank my son, Milo, who can always bring a smile to my face.

TABLE OF CONTENTS

LIST OF FIGURES

LIST OF TABLES

TABLE

LIST OF ABBREVIATIONS

5F-dUMP, 5’-fluoro-2’-deoxyuridine-5’-monophosphate

dUMPS, 2’deoxyuridine-5’-monophosphate-monothioate

dUMP, 2’-deoxyuridine-5’-monophosphate

dTMP, 2’-deoxythymidine-5’-monophosphate

dATP, 2’-deoxyadenosine triphosphate

dCTP, 2’-deoxycytidine triphosphate

dGTP, 2’-deoxyguanosine triphosphate

dTTP, 2’-deoxythymidine triphosphate

ATP, adenosine triphsophate

CTP, cytidine triphosphate

GTP, guanosine triphosphate

ThyA, thymidylate synthase

ThyX, flavin-dependent thymidylate synthase

CH_2THF, *6R*-N^5,N^{10}-methylenetetrahydrofolate

DHF, 7,8-dihydrofolate

THF, 5,6,7,8-tetrahydrofolate

DHFR, dihydrofolate reductase

FolA, dihydrofolate reductase

TS, thymidylate synthase

k_{ox}, oxidative half-reaction rate constant

k_{red}, reductive half-reaction rate constant

K_i, inhibition constant

K_d, dissociation constant

KIE, kinetic isotope effect

EDTA, ethylenediaminetetraacetic acid

TRIS-HCl, tris (hydroxymethyl) aminomethane hydrochloride

TdK, thymidine kinase

NRT, nucleoside deoxyribosyltransferase

NADPH, reduced nicotinamide adenine dinucleotide phosphate

NADH, reduced nicotinamide adenine dinucleotide

FAD, flavin adenine dinucleotide

SDS, sodium dodecyl sulfate

H_2CO, formaldehyde

HPLC, high performance liquid chromatography

ABSTRACT

For decades the biosynthesis of thymidylate, a vital DNA precursor, was thought to be catalyzed solely by ThyA (the "classic" thymidylate synthase), which was thought to be found in all organisms. Recently a structurally unrelated new class of thymidylate synthase, ThyX, was found in many bacterial organisms including many pathogenic species. Both enzymes catalyze the reductive methylation of dUMP (deoxyuridine monophosphate) using CH_2THF (methylenetetrahydrofolate) as a carbon source to form dTMP (deoxythymidine monophosphate). However, the reductive mechanism is different between these two enzymes.

The "classic" thymidylate synthase uses CH_2THF as both the reductant and as the source of carbon forming both dTMP and dihydrofolate. ThyX catalyzes the reductive methylation of dUMP using CH_2THF as the carbon source, but requires a flavin prosthetic group and reducing equivalents from NADPH to form dTMP and THF (tetrahydrofolate). This reaction can be divided into two reactions. In the first reaction, the reductive half-reaction, the enzyme is reduced by NADPH. In the second reaction, the oxidative half-reaction, the reduced enzyme reacts with both dUMP and CH_2THF to form dTMP and THF.

The mechanisms of both the reductive and oxidative half-reactions were studied in detail by transient kinetics. The effect of the substrates on both reactions suggests a

preferred binding order. The substrate, dUMP, binds first followed by reduction of the enzyme by NADPH. The reduced enzyme•dUMP complex then reacts with CH_2THF to form dTMP and THF. Further experiments on the oxidative half-reaction by stopped-flow spectroscopy and rapid reaction acid quenching have revealed the accumulation of two as yet unidentified intermediates prior to oxidation of the flavin and product formation. Studies of the oxidative half-reaction using site directed mutagenesis, pH dependence, dUMP, and FAD analogues have let to a proposed detailed mechanism for the synthesis of dTMP by ThyX from *Thermotoga maritima*. This mechanism is different than the classical mechanism of ThyA. Strikingly, the activation of dUMP by ThyX does not occur by Michael addition, but occurs through the polarization of dUMP by binding to a polarized active site. The difference in these mechanisms, as well as there being no structural or sequence similarity in the proteins, makes ThyX an attractive target for antibiotic treatment of infections by many pathogens.

CHAPTER I

INTRODUCTION

Background

The survival of all organisms requires the replication of their genomes. The synthesis of DNA requires the incorporation of all four deoxynucleotide triphosphates. The deoxynucleotides, dATP, dCTP, and dGTP are synthesized from ATP, CTP, and GTP by ribonucleotide reductase. The deoxynucleotide, dTTP, first requires the reductive methylation of dUMP (2'-deoxyuridine-5'-monophosphate) to form dTMP (2'-deoxythymidine-5'-monophosphate) synthesized by thymidylate synthase. The 'classic' thymidylate synthase (ThyA) catalyzes this reduction methylation of dUMP using CH_2THF (*R*-N^5,N^{10}-methylenetetrahydrofolate) as both the carbon source and as the reductant forming dTMP and DHF (7,8-dihydrofolate) (*1*).

In human and in most microbial species this reaction is tightly coupled to two enzymes. The first enzyme, FolA (dihydrofolate reductase, or DHFR), catalyzes the reduction of DHF to THF (5,6,7,8-tetrahydrofolate). The tight coupling between TS and DHFR or FolA is required in order to maintain the pool of reduced folates. THF is required in a number of one-carbon reactions in DNA, RNA, and protein synthesis (*2*). These two enzymes have been the targets of numerous chemotherapeutic inhibitors,

specifically dUMP and folate analogues (*1*, *3*). The second enzyme, SHMT (serine hydroxymethyltransferase), catalyzes the transfer of a methylene from serine to DHF forming THF (Figure 1-1).

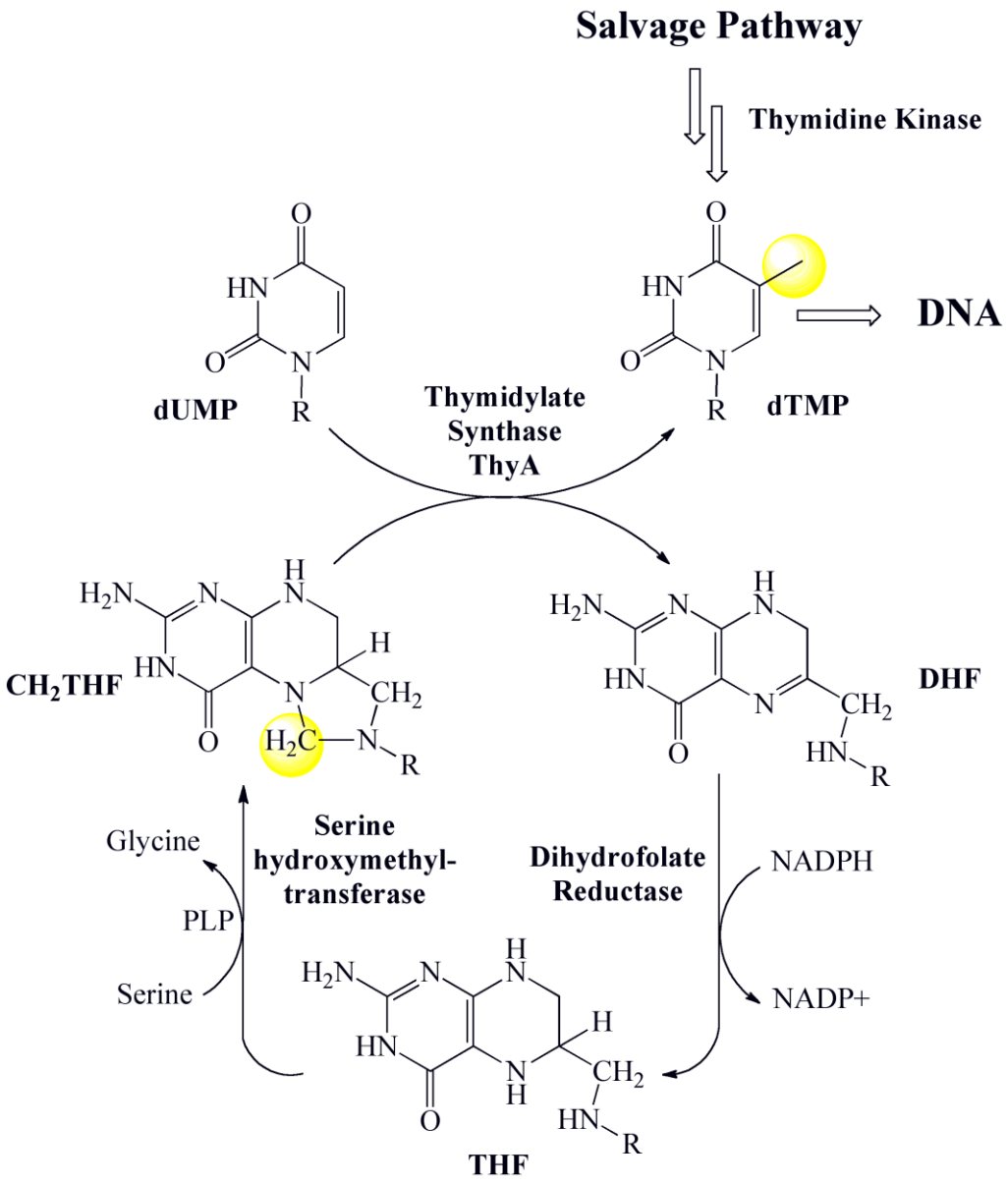

Figure 1-1. ***The Metabolic Pathway for the Synthesis of dTMP by ThyA***. The carbon atom that is transferred from CH_2THF to dUMP is highlighted in yellow.

For decades, the sole *de novo* biosynthesis of dTMP in all organisms was thought to be catalyzed either by ThyA, as mentioned above, or by the bifunctional enzyme TS-DHFR, which is found mostly in plants and protozoa (*1*). The enzyme TS-DHFR catalyzes the reductive methylation of dUMP, similarly to ThyA, but also has a second domain, DHFR, found on the same polypeptide, that catalyzes the reduction of DHF to THF (*4, 5*). Alternatively, thymine can be salvaged from growth medium by NRT (nucleoside deoxyribosytransferase) forming the nucleoside thymidine. Thymidine, formed from the previous reaction, or acquired extracellularly, is further modified by the phosphorylation reaction catalyzed by TdK (thymidine kinase) forming dTMP (*1*) (Figure 1-2).

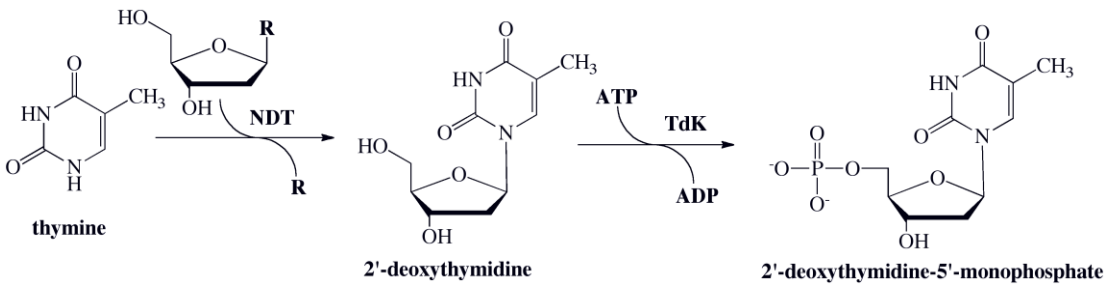

Figure 1-2. ***Salvage Pathway of dTMP***. The salvage of thymine or thymidine from extracellular growth medium is catalyzed by NDT (nucleoside deoxyribosytransferase) and TdK (thymidine kinase). R = pyrimidine base.

In 1989 Dynes and co-workers showed that the eukaryotic protist *Dictyostelium discoideum* lacks ThyA from its genome (*6*). They isolated a gene able to complement growth of *E. coli* lacking of its own ThyA. In 2000 the analysis of a large number of genomes showed that many organisms lack the gene that encodes for ThyA. Galperin and Koonin predicted that organisms lacking the thyA gene would use a novel thymidylate

synthase with sequence similarity to the gene discovered from *D. discoideum (7).* However, it was not until 2002 that Myllykallio and co-workers, also failing to find the gene for ThyA in a number of genomes, expressed and purified the first novel thymidylate synthase (ThyX) from *Helicobacter pylori* (*8*). They showed that this enzyme was able to synthesize dTMP from dUMP and CH_2THF, but required a flavin prosthetic group, FAD, and reduced pyridine nucleotide for catalysis (*8*). It was later discovered that the folate product from this reaction is THF, not DHF (*9*). The discovery of a novel thymidylate synthase shows two different ways to catalyzed the reductive methylation of dUMP have evolved.

Phylogenic Distribution

Recently, comparative genomics revealed that the genes encoding for ThyA and ThyX are widely distributed across all domains of life (*8, 10*). Roughly 35% of the 150 genomes sequenced at the time, encode the thyX gene (*10*). ThyX and ThyA are generally mutually exclusive - most genomes that have the thyX gene do not have the thyA gene. Interestingly, most of the organisms that express the gene for thyX usually lack the known genes for FolA and TdK (Table 1-1).

Species	thyA	DHFR	TdK	thyX	Ref.
Helicobacter pylori	-	-	-	+	(*8*)
Campylobacter jejuni	-	-	-	+	*(8)*
Borrelia burgdorferi	-	-	-	+	*(8)*
Dictyostelium discoideum	-	-	-	+	*(8)*
Paramecium borella Chlorea Virus-1	-	-	-	+	*(8)*
Rhodobacter capsulta	-	-	+	+	*(14)*
Rhodobacter spaeroides	+	+	-	+	*(14)*
Mycobacterium tuberculosis	+	+	-	+	*(8)*
Corynebacterium glutamicum	+	-	-	+	*(13)*
Thermatoga maritima	-	+	-	+	*(8)*

Table 1-1. ***Comparison of ThyX Containing Organisms*.** The table shows several pathogenic organisms (bold text) that catalyze the synthesis of dTMP using ThyX.

The gene for ThyX is found in many pathogenic bacteria, including several double-stranded DNA containing viruses (*11*). Many of these bacteria are anaerobic and microanaerobic organisms, suggesting organisms suggest that contain ThyX usually found in organisms where oxygen is limited. However, the gene for thyX can also found in a number of aerobic and mesophilic organisms, suggesting environmental factors cannot predict the distribution of thyX genes.

Interestingly, there are many organisms that encode genes for both ThyX and ThyA. For example, in the closely relates species, *M. tuberculosis* and *C. glutamicum,* have fully conserved genes for both ThyA and ThyX; however, the requirement for ThyX varies. In *M. tuberculosis* only the thyX gene is required for optimal growth (*12*), while

in the *C. glutamicum* the thyX gene was found not to be essential for growth, but its expression during stationary growth phase is presumed to be advantageous (*13*). Conversely, within the *Rhodobactor* family, *R. capsulatus* express thyX, while *R. sphaerodus* lacks the gene for ThyX; however, it encodes genes for both ThyA and FolA (*14*). This raises an important issue - why do these organisms have both genes?

It has been suggested that a lateral gene transfer event could account for the wide distribution of ThyX across all domains. The presence of microbial species that contain functional genes for both ThyX and ThyA has been suggested to have occurred recently and is presumably still in an intermediate phase of evolution (*11*). This conclusion was based on an analysis of a number of genomes that contain both thyX and thyA genes. The sequences of the thyX genes have a G + C % different than rest of the genome (*11*). Furthermore, a number of thyX genes, found in organisms that encode also for thyA, have been annotated as prophage sequences. This would suggest that viruses (*11*) could have facilitated a number of these lateral gene transfer events. Nevertheless, to date it is still unclear as to why some organisms have both ThyA and ThyX.

Sequence and Structure

The structure of ThyX from *Thermotoga maritima*, was solved in 2002 by the Joint Center for Structural Genomics, was the first for ThyX (*15*). Since then crystal structures have been solved for ThyX from *M. tuberculosis (16), C. glutamicum (17),* and *Paramecium bursilla* Chlorea Virus-1 ThyX (*18*). All crystal structures of ThyX are similar. ThyX is a homotetramer of 25-30 kDa per subunit with each subunit of

composed of 5 ß-strands and 10 helices. It and adopts a ternary structure not previously observed in other proteins. Each of the four active sites has an FAD prosthetic group, and each active site is composed of residues from three of the four subunits. The adenine of the FAD prosthetic group binds deep in the protein, while the isoalloxazine lies in the active site partially exposed to solvent. The structure of ThyX shows no similarity to the homodimeric ThyA enzyme, as can be seen in Figure 1-3.

Sequence alignments revealed a novel ThyX motif ($RHRX_{7-8}S$) that is conserved among all known ThyX sequences (Figure 1-4) (*8*). Site directed mutagenesis of numerous residues from *M. tuberculosis* ThyX and their effect on complementation of *E. coli* ΔThyA, has expanded this motif $(Y/W)X_{19-40}HX_{25-28}RHRX_{7-8}SXR(Y/R)X_{68-114}R$ (*20*). The amino acids that make up the ThyX motif are located in two of the three subunits and participate in hydrogen bonding distance to dUMP and/or FAD (Figure 1-5). However, no structure with any folate (CH_2THF, or THF) or pyridine nucleotide bound to the active site has been solved. Therefore it is still unclear where these substrates bind to the enzyme.

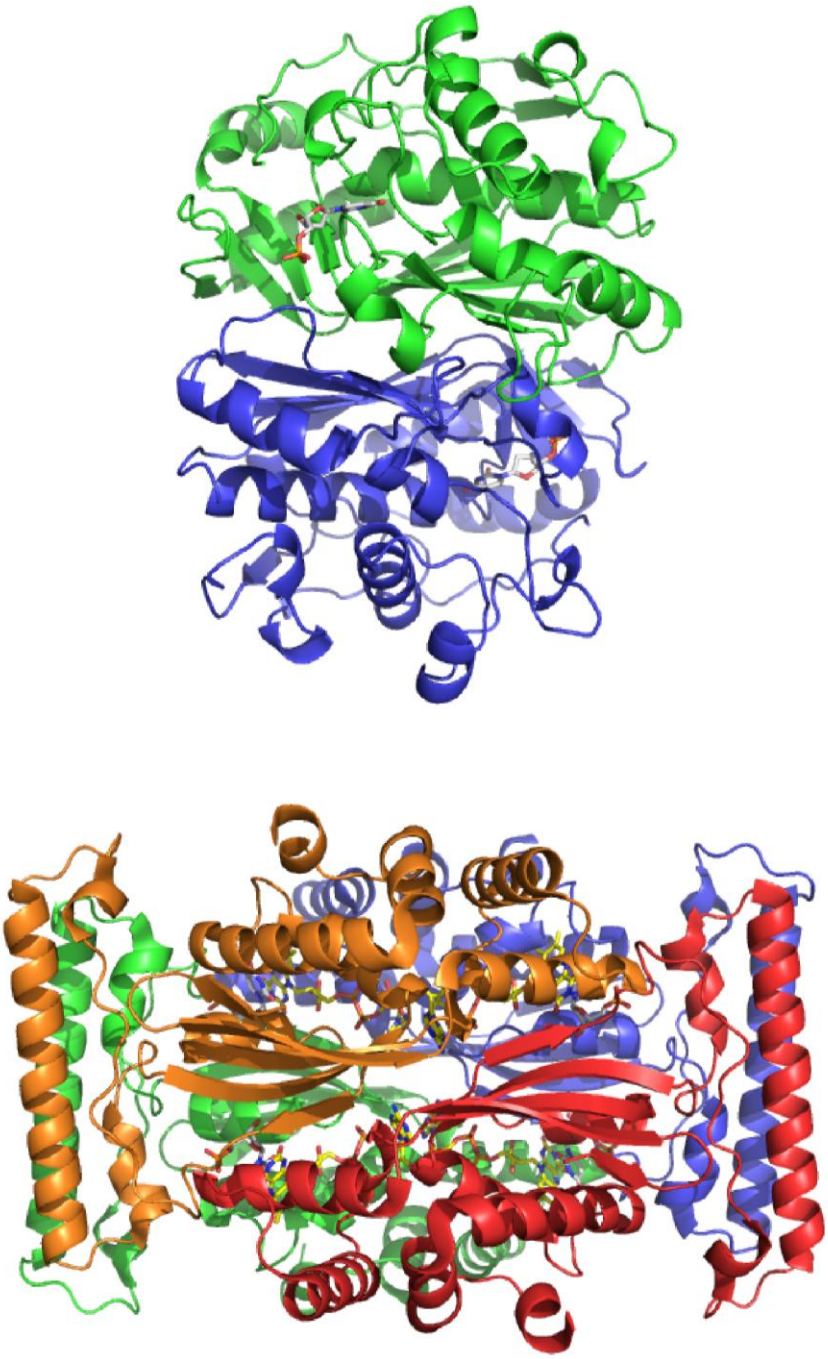

Figure 1-3. ***The Crystal Structures of ThyA and ThyX*****.** The top panel shows the structure of the ThyA•dUMP complex from *E. coli* (pdb 1BID – (*19*)). The bottom panel shows the ThyX•dUMP complex from *T. maritima* (pdb 1O26 – (*15*)). In both structures dUMP is shown in gray. The FAD prosthetic group is shown in yellow in the structure of the ThyX.

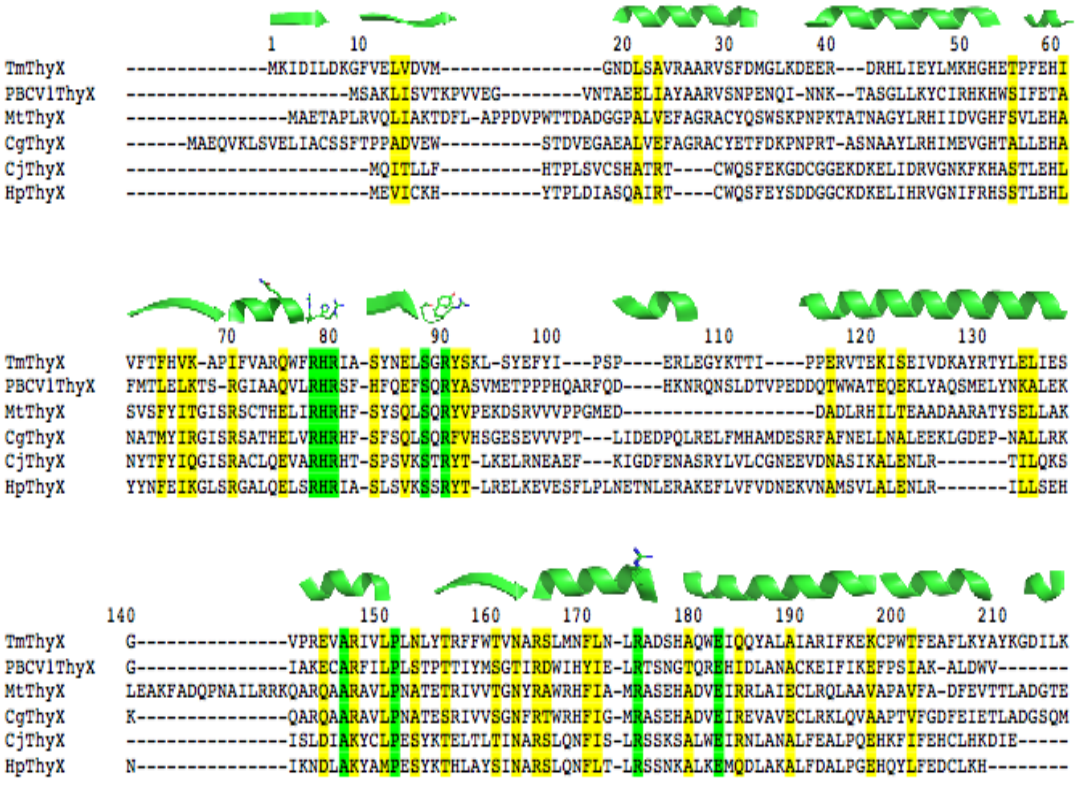

Figure 1-4. ***Sequence Alignment of Various Organisms Expressing thyX*.** The sequence alignment was made using CLUSTALW. The secondary structures from TmThyX are shown above the sequences. The residues that make up the ThyX motif are shown as sticks in the secondary structures above the sequences. The partially conserved residues are highlighted in yellow while the conserved residues are highlighted in green. Abbreviations: TmThyX, *T. maritima* ThyX; PBCV1-ThyX, *P. borella* Chlorea Virus-1; *M. tuberculosis* ThyX;CgThyX, *C. glutamicum* ThyX; CjThyX, *C. jejuni* ThyX; HpThyX, *H. pylori* ThyX.

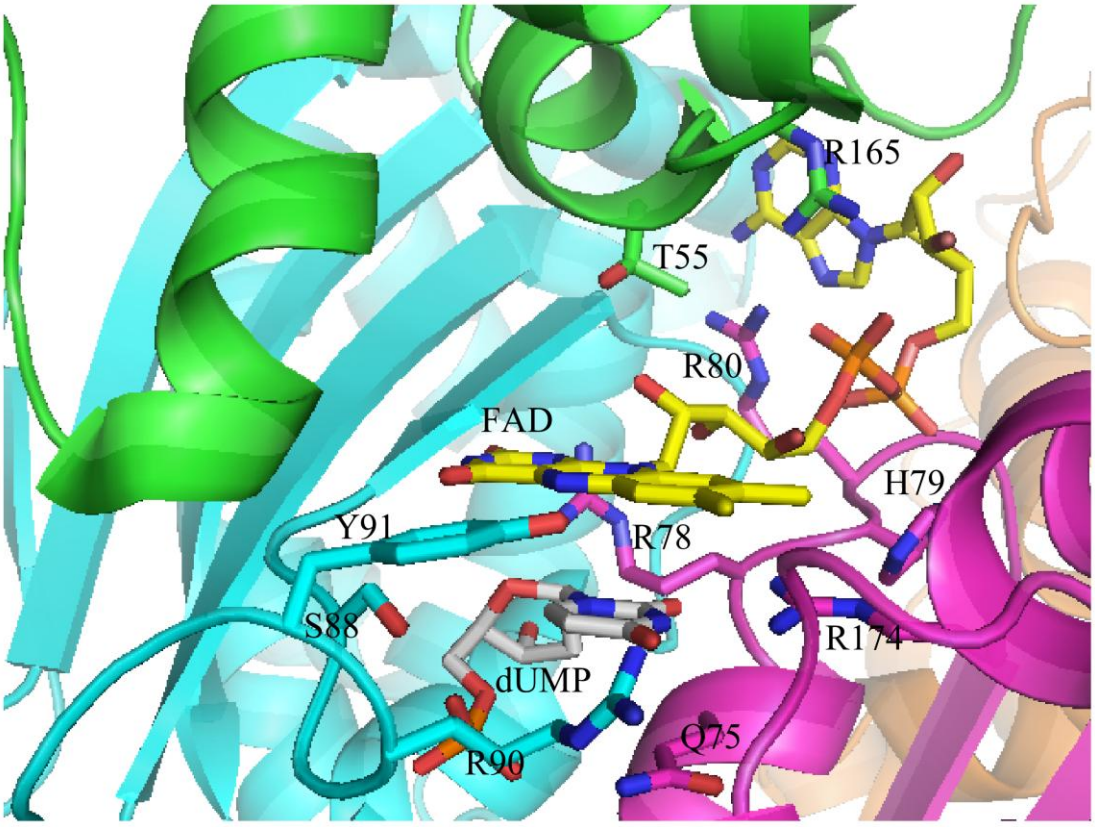

Figure 1-5. ***The Active Site of ThyX from T. maritima*** **(pdb 1O26)**. The active site is made up of three of the four subunits. The dUMP molecule is colored in gray and the FAD prosthetic group is colored in yellow. The residues shown as sticks make up the extended thyX motif, $(Y/W)X_{19\text{-}40}HX_{25\text{-}28}RHRX_{7\text{-}8}SXR(Y/R)X_{68\text{-}114}R$, proposed in reference (*20*).

Synthesis of dUMP by ThyX

ThyX and ThyA both catalyze the reductive methylation of dUMP; however, they have no sequence or structural similarity. ThyA uses CH_2THF as both carbon donor and

as the reductant with dTMP and DHF as its products. DHF must be reduced to THF by NADPH in a reaction catalyzed by DHFR. The ThyX enzyme also uses CH_2THF as a carbon donor, but requires an FAD prosthetic group, and it uses reducing equivalents from NADPH.

ThyX is a flavoprotein with one FAD per active site, and it utilizes the redox properties of the isoalloxazine moiety of FAD for catalysis. The overall reaction, like most flavoproteins, can be divided into two reactions. In the first reaction, the reductive half-reaction, the enzyme is reduced by NADPH. Agrawal and co-workers, using tritium labeled pyridine nucleotide, showed the enzyme prefers the proR hydrogen of NADPH, although this is not an absolute requirement (*21*). In the second reaction, the oxidative half-reaction, the reduced enzyme reacts with dUMP and CH_2THF to form dTMP and THF (Figure 1-6).

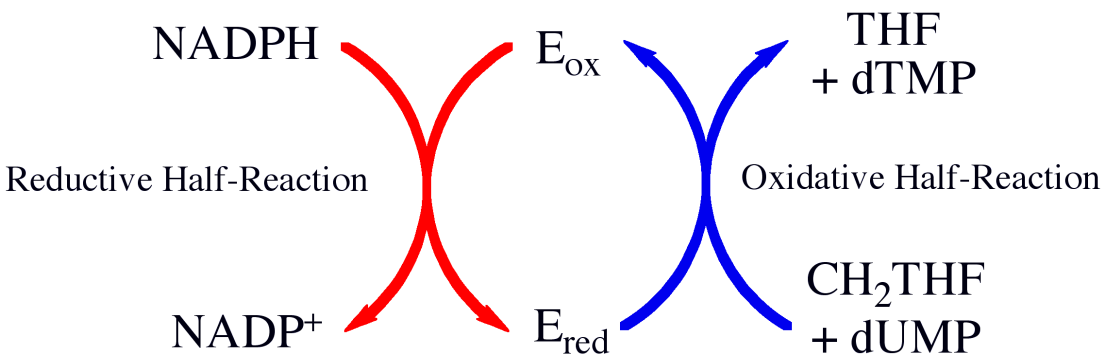

Figure 1-6. ***The Reactions of ThyX*.** The reaction of ThyX can be divided in two reactions. The first reaction, the reductive half-reaction shown in red, the enzyme is reduced with NADPH. In the second reaction, the oxidative half-reaction, shown in blue, the reduced enzyme reacts with dUMP and CH_2THF to form dTMP and THF.

Kinetic Mechanism of ThyX

Proposed kinetic mechanisms for ThyX from several organisms are shown in Figure 1-7. While the differences in kinetic mechanisms could be due to actual differences in ThyX from various organisms, they are likely due to be due to the experimental conditions employed. The kinetic mechanisms, shown in figure 1-7, were all determined under steady-state conditions aerobically. Our laboratory, and others (*22*), have shown that molecular oxygen at atmospheric conditions reacts readily with the reduced enzyme, forming H_2O_2, at rates (0.7 s^{-1}) that would compete catalytically. In fact the addition of dUMP increase the rate of oxidation by ~5-fold (*23*).

While the experimental conditions need to be reexamined for ThyX, it is clear that ThyX enzymes from various species have relatively low turnover numbers (ranging from 0.08 s^{-1} to 0.7 s^{-1}) (*9, 21, 24, 25, 27*) compared to the human ThyA, which has turnover number of 2.5 s^{-1} (*1*). It is not clear why these enzymes have such low turnover numbers. However, many organisms that use ThyX to synthesis dTMP have slower replication speeds than organisms that use ThyA (*28*). Similarly, it has been suggested in *M. tuberculosis*, which has both ThyX and ThyA, the low turnover numbers observed for both enzymes of 0.07 s^{-1} and 0.3 s^{-1}, respectively, are due to *M. tuberculosis* being a slow growing organism such that the requirements for dTMP may be relatively low (*27*). Alternatively, the reduction of ThyX, from *C. jejuni*, by NADPH is ~10,000-fold slower than the reduction of *T. maritima* ThyX using same reductant (*23*). It may be that NADPH might not be the natural substrate for many of these organisms.

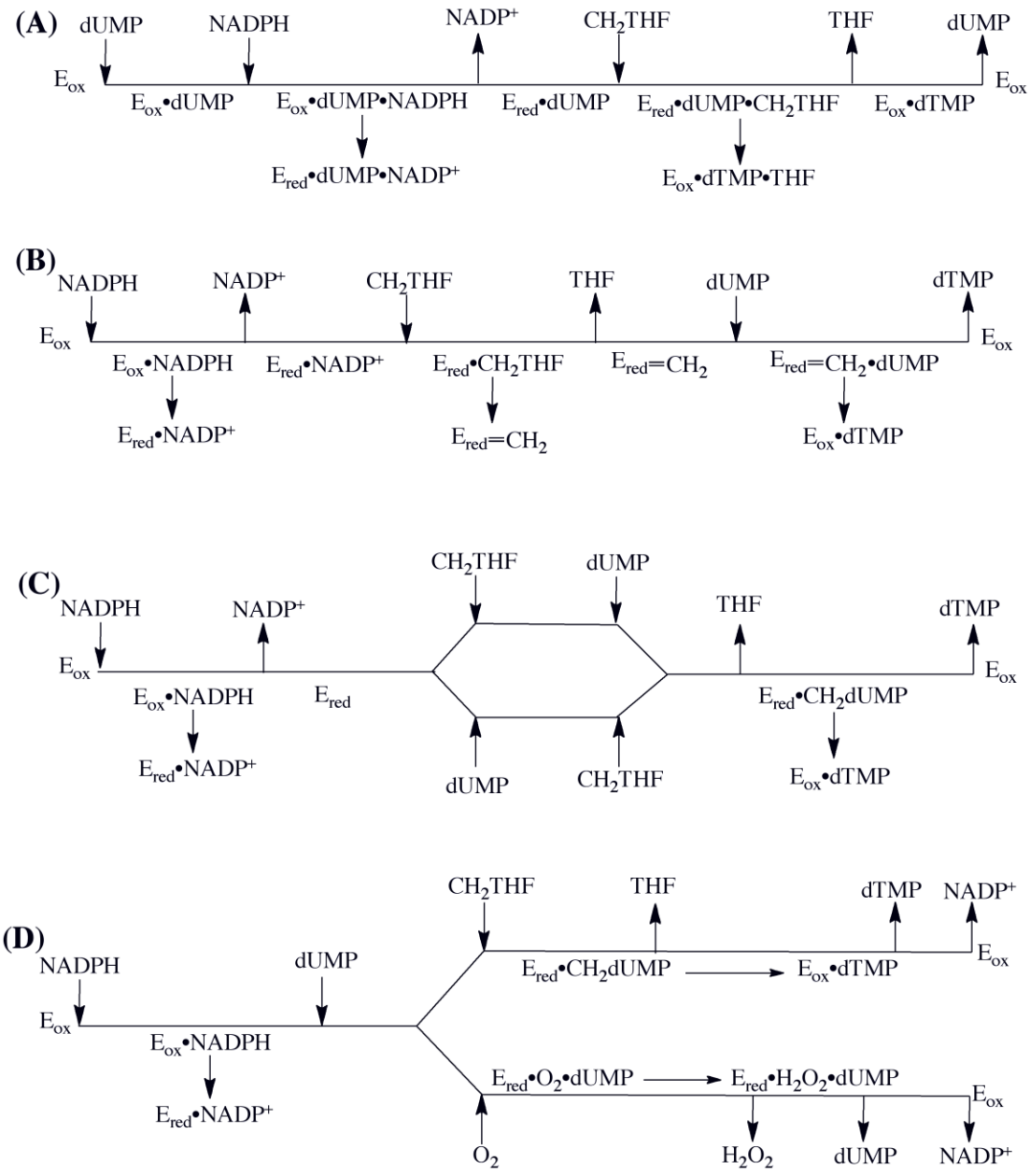

Figure 1-7. ***The Various Kinetic Mechanisms Proposed for ThyX***. The proposed mechanism for (A) PBCV1-ThyX (*24*), (B) *C. glutamicum* ThyX (*25*), (C) *T. maritima* ThyX (*21*) , and (D) *T. maritima* ThyX (*26*).

The existence of a novel TS found in many pathogenic organisms is very appealing drug target. The difference in sequence, structure, and mechanism, along with many of these pathogenic organisms sole reliance on ThyX for the synthesis of dTMP, make this quite an attractive target for the design of antibiotics. The dUMP analogue, 5F-dUMP, has been shown to inhibit *M. tuberculosis* (*27*), *C. jejuni* (*29*), and PBCV-1 ThyX (*24*), but in low micromolar concentrations. A few novel inhibitors have been designed by Önen and co-workers, based on an ethyl thiazolidine-4-carboxylate ring, and have been shown to inhibit PBCV-1 ThyX in submicromolar concentrations (*30*). However, the design of novel ThyX inhibitors still remains in its infancy. The work presented in this thesis can potentially aid the design of specific mechanism based ThyX inhibitors.

Chemical Mechanism

The chemical mechanism of ThyA has been extensively studied for decades, and the consensus mechanism is shown in Figure 1-8. This mechanism provides a basis for the thinking about the mechanism for ThyX. The differences in the reductive methylation of dUMP for the two enzyme that might be uses to design class specific inhibitors for ThyX. All thymidylate synthases must accomplish a number of tasks to synthesize dTMP. The synthesis of dTMP synthesis is described below and is divided into four major steps. Each step described is related as to what is known about the mechanisms for ThyA and ThyX.

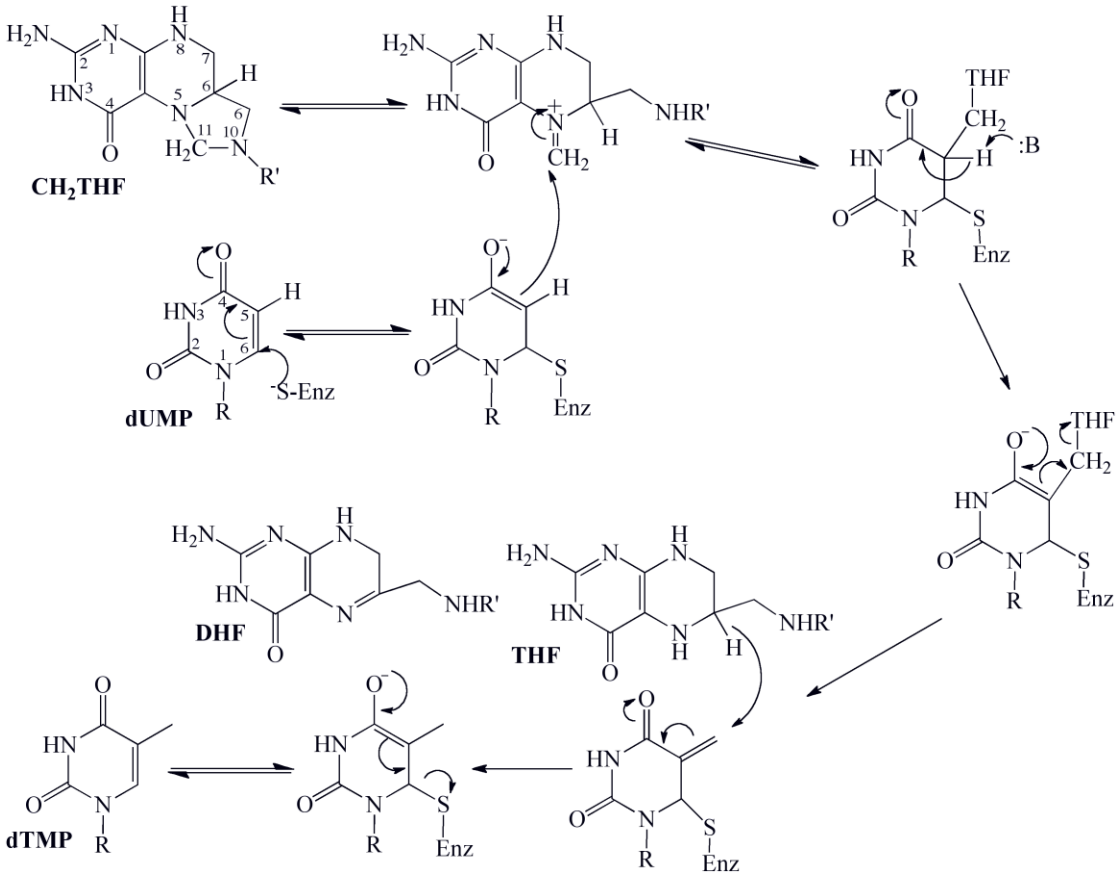

Figure 1-8. ***The Chemical Mechanism of ThyA (1).*** R = 2'-deoxyribose-5'-phosphate. R' =(*p*-aminobezoyl)-gultamate

1. *Activation of dUMP*. The C5 of the uracil moiety is not inherently nucleophilic and requires activation. ThyA accomplishes this task using an active site cysteine thiolate, which activates dUMP through a Michael addition at C6, resulting in increased nucleophilicity of the C5 carbon. No active site cysteine is found in ThyX. However, a conserved active site serine has been proposed as the active site nucleophile. This suggestion was supported by mutagenesis studies with both *M. tuberculosis* ThyX and *H. pylori* ThyX. In *M. tuberculosis* ThyX when this serine (S105) was substituted to a

glutamate, it did not retain activity (*20*). While the mutation of the analogous serine (S84) to an alanine did not result in loss of activity in *H. pyloi* ThyX, it was suggested that a neighboring serine (S85) was able to rescue the activity. In fact, the double mutant, S84A and S85A, showed no activity (*9*). However, it is not clear whether the loss of activity was the result of the disruption of the active site or due to loss of affinity for the substrates. Furthermore, a close examination of the crystal structures of ThyX shows this serine residue is in plane with the uracil ring (Figure 1-9 right panel). If this serine were to participate in a Michael addition, it would require the serine hydroxyl to be positioned directly above the uracil ring to enable a nucleophilic attack at C6 (Figure 1-9 shows the correct position of the cystine in ThyA that participates in a Michael addition). Additionally, no active site base, near the serine, is found that could activate the serine, which would be required if serine was the nucleophile.

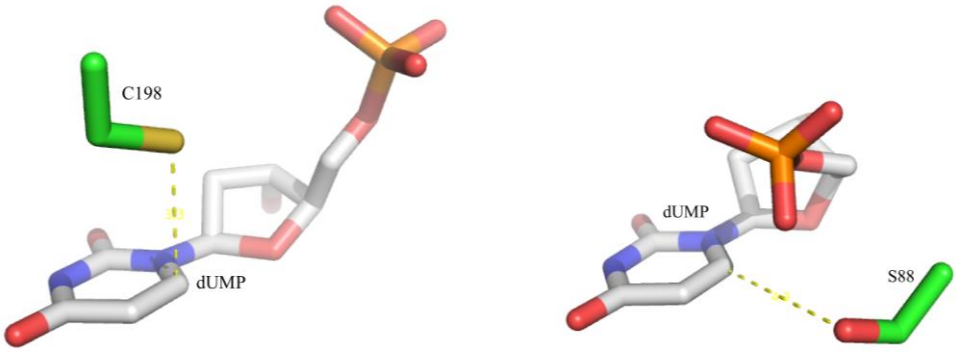

Figure 1-9. ***Proposed Activation of dUMP***. The structure on the left, from E. coli ThyA, shows the C198 thiolate directly above C6 of dUMP in a position that would facilitate a Michael addition (*19*). The structure on the right shows the proposed S88 hydroxyl, in *T. maritima* ThyX, not in a position that could easily participate in a Michael addition (*31*).

In collaboration with Kohen and co-workers we performed site directed mutagenesis to substitute this serine with an alanine, i.e. S88 in *T. maritima* (*32*). We saw only relatively small effects on this reaction, concluding this residue does not activate

dUMP through a Michael addition. In the same paper we suggested that a hydride transfer from the reduced flavin is responsible for the activation of dUMP. However this is inconsistent with our data on the oxidative half-reaction (Chapter 3), which shows at least two intermediates occurring prior to oxidation of the flavin.

2. *Activation of CH_2THF.* Activation of CH_2THF is accomplished by the opening of the imidazolidine ring of CH_2THF to form of the electrophilic iminium ion. The iminium ion of CH_2THF does not form free in aqueous solution (*33*) and thus it must form after it is bound to the enzyme so that it can react with the nucleophilic C5 of dUMP. In ThyA the formation of the iminium ion of CH_2THF, which occurs concomitantly with its binding to the active site, is assisted by the protonation of N10 of CH_2THF (*1*). This notion was also confirmed using a 5-deaza-CH_2THF, an analogue incapable of forming the iminium ion, which binds poorly to the active site (*34*).

3. *Transfer of methylene group.* The nucleophilic C5 of activated dUMP attacks the iminium carbon of CH_2THF to bridge the nucleotide and the folate, thus forming a ternary complex between the enzyme, nucleotide, and the folate. Using the nucleotide analogue 5F-dUMP this complex was observed both by mass spectroscopy and by crystallography (*1*). A proton is removed from C5 followed by a ß-elimination of THF, resulting in the completed transfer of the methylene group. It was proposed in *C. glutamicum* ThyX that the methylene is transferred to an active site arginine (*25*), suggested by mass spectroscopy results showing an increase in 14 Da after incubation of the reduced enzyme with CH_2THF. However, this conclusion is inconsistent with the

crystal structure of ThyX with bound nucleotide, which shows that the nucleotide would have to rotate 180º in order for transfer from the arginine to C6 of the nucleotide. Experiments were repeated with both PBCV-1 ThyX (*18*) and *T. maritima* ThyX (*35*), but neither could find any evidence for a methylated arginine.

4. *Reduction of the methylene*. The reduction of the methylene, in ThyA, is accomplished by a hydride transfer from THF to the exocyclic methylene of dUMP, forming both dTMP and DHF (*1*). In ThyX the reduction of the methylene by THF was examined with the use of tritium labeled THF. After the reaction with ThyX all of the tritium remained bound to THF (*21*), suggesting that THF does not reduce the transferred methylene group. Conversely, when the reaction was performed in D_2O, deuterium was incorporated from solvent into dTMP, suggesting that the reduced flavin is responsible for the reduction of the methylene (*21*). Kohen and co-workers further demonstrated that the reduction of the transferred methylene occurs through a 1,3-sigmatropic rearrangement (Figure 1-9), after transfer of hydride transfer from the reduced flavin to C6 of dUMP (*32*).

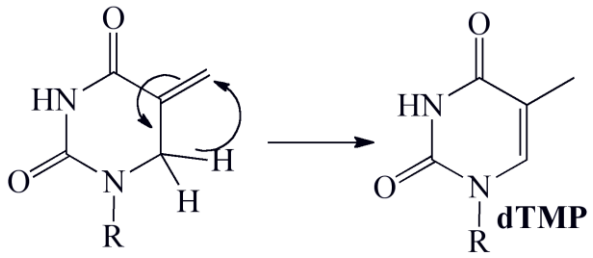

Figure 1-9. ***The Reduction of The Exocyclic Methylene by ThyX***. The reduction of the transferred methylene is accomplished by a 1,3-sigmatropic rearrangement.

Thesis Overview

My thesis research was designed to determine the mechanism of ThyX. Using Figure 1-6 as a guide, synthesis of dTMP by ThyX can be divided in to two half-reactions, the reductive and oxidative half-reactions. In Chapter 2 I describe studies directed at the reductive half-reaction. By carrying out the reduction of the enzyme by NADPH with either dUMP or CH_2THF present, and in the absence of oxygen, the reductive half-reaction can be examined and the complications of complete turnover and off pathway reactions with the reduced enzyme and molecular oxygen can be avoided. The reduction reaction were studied with NADPH and the effects of dUMP and CH_2THF on this reaction were used to determine the preferred binding order. A number of active site mutants were also used to determine roles of particular residues in the reductive half-reaction and in substrate binding. In Chapter 3 the focus was on the oxidative half-reaction. By starting with the reduced enzyme, and in the absence of molecular oxygen, we can look specifically at the oxidative half-reaction. The effects of dUMP and CH_2THF on this reaction suggested a preferred binding order that was consistent with the preferred binding order determined in the reductive half-reaction. Rapid reaction experiments revealed the accumulation of two intermediates prior to the oxidation of the flavin. The details of the chemical mechanism were also examined using active site mutants, nucleotide and FAD analogues, and variety of pH values. The details of these experiments suggested a novel mechanism for activation of dUMP and allowed me to propose a detailed mechanism for the synthesis of dTMP.

References

1. Carreras, C. W., and Santi, D. V. (1995) The catalytic mechanism and structure of thymidylate synthase, *Annu Rev Biochem 64*, 721-762.
2. Matthews, R. G. (1996) One carbon metabolism., in *Escherichia Coli and Salmonella - Cellular and Molecular Biology* (Neidhardt, F. C., Ed.), pp 600-611, ASM Press.
3. Costi, M. P., Ferrari, S., Venturelli, A., Calo, S., Tondi, D., and Barlocco, D. (2005) Thymidylate synthase structure, function and implication in drug discovery, *Curr Med Chem 12*, 2241-2258.
4. Atreya, C. E., and Anderson, K. S. (2004) Kinetic characterization of bifunctional thymidylate synthase-dihydrofolate reductase (TS-DHFR) from Cryptosporidium hominis: a paradigm shift for ts activity and channeling behavior, *J Biol Chem 279*, 18314-18322.
5. Atreya, C. E., Johnson, E. F., Williamson, J., Chang, S. Y., Liang, P. H., and Anderson, K. S. (2003) Probing electrostatic channeling in protozoal bifunctional thymidylate synthase-dihydrofolate reductase using site-directed mutagenesis, *J Biol Chem 278*, 28901-28911.
6. Dynes, J. L., and Firtel, R. A. (1989) Molecular complementation of a genetic marker in Dictyostelium using a genomic DNA library, *Proc Natl Acad Sci U S A 86*, 7966-7970.

7. Galperin, M. Y., and Koonin, E. V. (2000) Who's your neighbor? New computational approaches for functional genomics, *Nat Biotechnol 18*, 609-613.

8. Myllykallio, H., Lipowski, G., Leduc, D., Filee, J., Forterre, P., and Liebl, U. (2002) An alternative flavin-dependent mechanism for thymidylate synthesis, *Science 297*, 105-107.

9. Leduc, D., Graziani, S., Lipowski, G., Marchand, C., Le Marechal, P., Liebl, U., and Myllykallio, H. (2004) Functional evidence for active site location of tetrameric thymidylate synthase X at the interphase of three monomers, *Proc Natl Acad Sci U S A 101*, 7252-7257.

10. Leduc, D., Graziani, S., Meslet-Cladiere, L., Sodolescu, A., Liebl, U., and Myllykallio, H. (2004) Two distinct pathways for thymidylate (dTMP) synthesis in (hyper)thermophilic Bacteria and Archaea, *Biochem Soc Trans 32*, 231-235.

11. Stern, A., Mayrose, I., Penn, O., Shaul, S., Gophna, U., and Pupko, T. An evolutionary analysis of lateral gene transfer in thymidylate synthase enzymes, *Syst Biol 59*, 212-225.

12. Sassetti, C. M., Boyd, D. H., and Rubin, E. J. (2003) Genes required for mycobacterial growth defined by high density mutagenesis, *Mol Microbiol 48*, 77-84.

13. Park, M., Cho, S., Lee, H., Sibley, C. H., and Rhie, H. Alternative thymidylate synthase, ThyX, involved in Corynebacterium glutamicum ATCC 13032 survival during stationary growth phase, *FEMS Microbiol Lett 307*, 128-134.

14. Leduc, D., Escartin, F., Nijhout, H. F., Reed, M. C., Liebl, U., Skouloubris, S., and Myllykallio, H. (2007) Flavin-dependent thymidylate synthase ThyX activity: implications for the folate cycle in bacteria, *J Bacteriol 189*, 8537-8545.

15. Lesley, S. A., Kuhn, P., Godzik, A., Deacon, A. M., Mathews, I., Kreusch, A., Spraggon, G., Klock, H. E., McMullan, D., Shin, T., Vincent, J., Robb, A., Brinen, L. S., Miller, M. D., McPhillips, T. M., Miller, M. A., Scheibe, D., Canaves, J. M., Guda, C., Jaroszewski, L., Selby, T. L., Elsliger, M. A., Wooley, J., Taylor, S. S., Hodgson, K. O., Wilson, I. A., Schultz, P. G., and Stevens, R. C. (2002) Structural genomics of the Thermotoga maritima proteome implemented in a high-throughput structure determination pipeline, *Proc Natl Acad Sci U S A 99*, 11664-11669.

16. Sampathkumar, P., Turley, S., Ulmer, J. E., Rhie, H. G., Sibley, C. H., and Hol, W. G. (2005) Structure of the Mycobacterium tuberculosis flavin dependent thymidylate synthase (MtbThyX) at 2.0A resolution, *J Mol Biol 352*, 1091-1104.

17. Kan, S. C., Liu, J. S., Hu, H. Y., Chang, C. M., Lin, W. D., Wang, W. C., and Hsu, W. H. Biochemical characterization of two thymidylate synthases in Corynebacterium glutamicum NCHU 87078, *Biochim Biophys Acta 1804*, 1751-1759.

18. Graziani, S., Bernauer, J., Skouloubris, S., Graille, M., Zhou, C. Z., Marchand, C., Decottignies, P., van Tilbeurgh, H., Myllykallio, H., and Liebl, U. (2006) Catalytic mechanism and structure of viral flavin-dependent thymidylate synthase ThyX, *J Biol Chem 281*, 24048-24057.

19. Stout, T. J., Sage, C. R., and Stroud, R. M. (1998) The additivity of substrate fragments in enzyme-ligand binding, *Structure 6*, 839-848.

20. Ulmer, J. E., Boum, Y., Thouvenel, C. D., Myllykallio, H., and Sibley, C. H. (2008) Functional analysis of the Mycobacterium tuberculosis FAD-dependent thymidylate synthase, ThyX, reveals new amino acid residues contributing to an extended ThyX motif, *J Bacteriol 190*, 2056-2064.

21. Agrawal, N., Lesley, S. A., Kuhn, P., and Kohen, A. (2004) Mechanistic studies of a flavin-dependent thymidylate synthase, *Biochemistry 43*, 10295-10301.

22. Wang, Z., Chernyshev, A., Koehn, E. M., Manuel, T. D., Lesley, S. A., and Kohen, A. (2009) Oxidase activity of a flavin-dependent thymidylate synthase, *FEBS J 276*, 2801-2810.

23. Palfey, B. A., Oritiz-Maldonado, M., Conrad, J.A. (2008) The Chemistry of Flavin-Depenedent Thymidylate Synthase, in *Flavins and Flavoproteins* (Frago, S., Gomez-Moreno, C., and Medina, M., Ed.), Prensas Universitarias de Zaragoza, Zaragoza, Spain.

24. Graziani, S., Xia, Y., Gurnon, J. R., Van Etten, J. L., Leduc, D., Skouloubris, S., Myllykallio, H., and Liebl, U. (2004) Functional analysis of FAD-dependent thymidylate synthase ThyX from Paramecium bursaria Chlorella virus-1, *J Biol Chem 279*, 54340-54347.

25. Griffin, J., Roshick, C., Iliffe-Lee, E., and McClarty, G. (2005) Catalytic mechanism of Chlamydia trachomatis flavin-dependent thymidylate synthase, *J Biol Chem 280*, 5456-5467.

26. Chernyshev, A., Fleischmann, T., Koehn, E. M., Lesley, S. A., and Kohen, A. (2007) The relationships between oxidase and synthase activities of flavin dependent thymidylate synthase (FDTS), *Chem Commun (Camb)*, 2861-2863.

27. Hunter, J. H., Gujjar, R., Pang, C. K., and Rathod, P. K. (2008) Kinetics and ligand-binding preferences of Mycobacterium tuberculosis thymidylate synthases, ThyA and ThyX, *PLoS One 3*, e2237.

28. Escartin, F., Skouloubris, S., Liebl, U., and Myllykallio, H. (2008) Flavin-dependent thymidylate synthase X limits chromosomal DNA replication, *Proc Natl Acad Sci U S A 105*, 9948-9952.

29. Gattis, S. G., and Palfey, B. A. (2005) Direct observation of the participation of flavin in product formation by thyX-encoded thymidylate synthase, *J Am Chem Soc 127*, 832-833.

30. Esra Onen, F., Boum, Y., Jacquement, C., Spanedda, M. V., Jaber, N., Scherman, D., Myllykallio, H., and Herscovici, J. (2008) Design, synthesis and evaluation of potent thymidylate synthase X inhibitors, *Bioorg Med Chem Lett 18*, 3628-3631.

31. Mathews, II, Deacon, A. M., Canaves, J. M., McMullan, D., Lesley, S. A., Agarwalla, S., and Kuhn, P. (2003) Functional analysis of substrate and cofactor complex structures of a thymidylate synthase-complementing protein, *Structure 11*, 677-690.

32. Koehn, E. M., Fleischmann, T., Conrad, J. A., Palfey, B. A., Lesley, S. A., Mathews, II, and Kohen, A. (2009) An unusual mechanism of thymidylate biosynthesis in organisms containing the thyX gene, *Nature 458*, 919-923.

33. Kallen, R. G., and Jencks, W. P. (1966) The mechanism of the condensation of formaldehyde with tetrahydrofolic acid, *J Biol Chem 241*, 5851-5863.

34. Gangjee, A., Patel, J., Kisliuk, R. L., and Gaumont, Y. (1992) 5,10-Methylenetetrahydro-5-deazafolic acid and analogues: synthesis and biological activities, *J Med Chem 35*, 3678-3685.

35. Chernyshev, A., Fleischmann, T., and Kohen, A. (2007) Thymidyl biosynthesis enzymes as antibiotic targets, *Appl Microbiol Biotechnol 74*, 282-289.

CHAPTER II

The Reductive Half-Reaction of Flavin-Dependent Thymidylate Synthase from *Thermatoga maritima*

Production of thymidylate (2'-deoxythymidine-5'-monophosphate, dTMP) is thought to be the rate-determining step in DNA synthesis (*1*). Until recently dTMP was thought to be catalyzed by either ThyA ("classic" thymidylate synthase) by the reductive methylation of dUMP (2'-deoxyuridine-5'-monophosphate) by CH_2THF (5,10 methylenethetrahydrofolate) to form dTMP and DHF (dihydrofolate), or by the salvage of thymidine from growth media by thymidine kinase (*2*). However, ThyA is absent in ~35 % of bacterial genomes (*3*). These organisms instead express ThyX

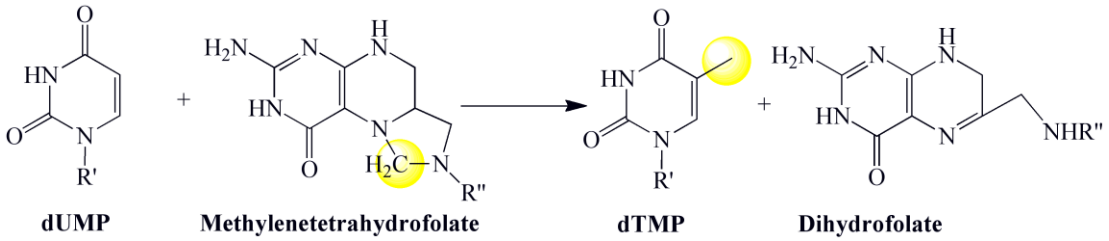

Figure 2-1. ***General ThyA Scheme***. ThyA catalyzes the reductive methylation of dUMP to form dTMP. The carbon from CH_2THF that is transferred to dUMP is highlighted in yellow.

(flavin-dependent thymidylate synthase). ThyX, like ThyA, synthesizes dTMP from dUMP and CH_2THF. However, THF (tetrahydrofolate) is formed instead of DHF. ThyX

requires an FAD prosthetic group and reducing equivalents from NADPH. Strikingly, the organisms that contain ThyX lack thymidine kinase and dihydrofolate reductase (*3*).

ThyX, unlike ThyA, is a homotetrameric flavo-protein with an FAD prosthetic group in each of the four active sites. Each active site uses residues from of three of the four subunits. Crystal structures of *T. maritima* ThyX with bound dUMP show the nucleotide stacked with the isoalloxazine of the flavin (Figure 2-2, (*4*)). When dUMP is bound, the active site is protected from solvent by the active site loop (residues 87-91 in *T. maritima* ThyX). However, when dUMP is absent this loop becomes disordered (*4*).

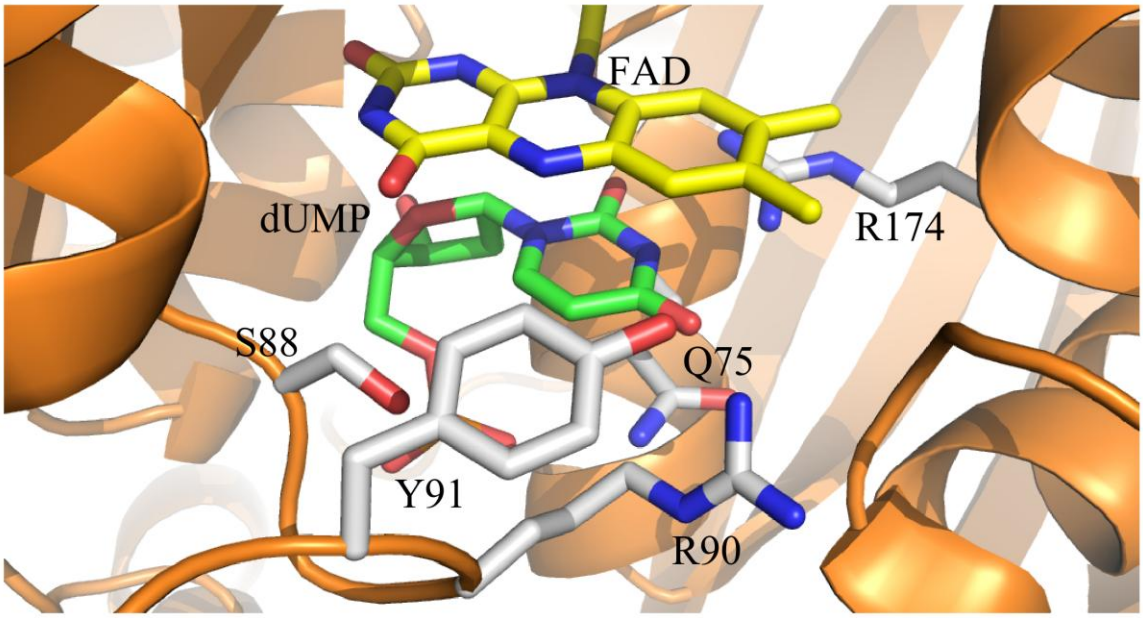

Figure 2-2. ***Active Site Structure of WT-ThyX•dUMP from T. maritima*** **(pdb 1O26).** Notice dUMP (in green) is stacked directly under the isoalloxazine moiety of the flavin. The active site residues (S88, Y91, R90, R174, and Q75) highlighted in gray are the ones substituted to alanine that have been studied in this work.

All known TSs (thymidylate synthases) synthesize dTMP from dUMP and CH_2THF. The mechanism of ThyA has been thoroughly examined and is the target of a number of chemotherapeutic inhibitors (*2*). This mechanism, like ThyX, must accomplish

a number of tasks for synthesis of dTMP. Both dUMP and CH_2THF must be activated to enable the transfer of the methylene to the nucleotide. Once transfer is complete the methylene is reduced to the methyl. A major difference between the ThyA reaction and the ThyX reaction is how the transferred methylene becomes reduced. ThyA accomplishes this task by utilizing the hydride from the transiently formed THF, while ThyX acquires the reducing equivalents from NADPH that ultimately reduce the methylene (*5*). It is of great interest therefore to determine the kinetics of reduction of ThyX.

We describe here the kinetic experiments of the reduction of the enzyme by NAD(P)H and show how dUMP stimulates and how CH_2THF inhibits the rate of reduction. Mutations were made to a substitute number of active site residues (S88A, Q75A, R90A, R174A, and Y91A) to test their roles in the reductive half-reaction and in substrate binding. These experiments imply a binding order of the substrates during catalysis.

EXPERIMENTAL PROCEDURES

Overexpression, Purification, and Preparation of S88A, Q75A, R90A, R174A, Y91A, and WT T. maritima ThyX. *Thermatoga maritima* ThyX (TM0449, GeneBank accession number NP228259) and each variant was overexpressed and purified as previously described (*6*) but with the following changes. Tris-HCl 50 mM pH 8.0 was used as lysis buffer. Enzyme was loaded on a Talon metal affinity column, pre-equilibrated with 50 mM Tris-HCl pH 8.0. The column was washed with 50 mM Tris-

HCl pH 8.0, 20 mM imidazole, and enzyme was eluted with 50 mM Tris-HCl pH 8.0, 200 mM imidazole. Enzyme was stored at 4 ºC as a 70 % ammonium sulfate slurry. Before experiments, enzyme was exchanged into the suitable buffer using Econo-Pac 10DG disposable desalting columns (Bio-Rad) and incubated at 70 ºC for 10 minutes. The solution was then centrifuged at 14,000 rpm for 10 minutes and supernatant was collected.

Extinction Coefficient. Enzyme concentrations were routinely determined by measuring the absorbance at 453 nm.The extinction coefficient of the enzyme-bound FAD at 453 nm was determined by adding a solution of SDS (1 % final) to a solution of enzyme. The extinction coefficient of the flavin bound to the enzyme was determined from the ratio of absorbance prior to denaturation and after liberation of FAD using ε_{450} = 11.3 mM^{-1} cm^{-1}. The extinction coefficient of the bound flavin at 453 nm was 11.1 mM^{-1} cm^{-1}.

Ligand Binding to WT-ThyX. Dissociation constants were determined for both dUMP and dTMP using a Hitachi F-4500 scanning fluorescence spectrophotometer. A solution of enzyme (337 nM), E_0 in Equation 1, at 25 ºC in 0.1 M Tris-HCl pH 8.0 was titrated with either a solution of dUMP or dTMP (0 – 1000 nM final concentration). The solution was excited at 450 nm and emission spectra were collected from 460 to 660 nm. The change in fluorescence at 525 nm was plotted versus total ligand (L_0) concentration and dissociation constants were determined using Equation 1, where ΔF is the

fluorescence change at any given ligand concentration and ΔF_{max} is the maximum fluorescence change at 525 nm.

$$\Delta F = \Delta F_{\max}\left[\frac{E_0 + L_0 + K_d - \sqrt{(E_0 + L_0 + K_d)^2 - 4E_0L_0}}{2}\right] \quad (1)$$

The kinetics of binding were also determined for dUMP, dTMP, CH_2THF, and THF. A solution of enzyme (6.6 µM after mixing) was mixed rapidly with various concentrations of dUMP, dTMP, CH_2THF, or THF (~30 – 300 µM after mixing) using a fluorescence stopped-flow instrument. The reaction was monitored by the change in flavin fluorescence after excitation at 450 nm with a 480 nm emission cut-off filter. The reaction traces were fit to a single exponential using KaleidaGraph (Synergy Software, PA). The bimolecular rate constants were determined for each of the substrates and products. All reactions were carried out in 0.1 M Tris-HCl, 1 mM EDTA pH 8.0 at 25 ºC. In order to stabilize CH_2THF, H_2CO (15 mM after mixing) was added. When experiments were carried out with CH_2THF and THF, all solutions were made anaerobic.

Ligand Binding to ThyX Mutants. Dissociation constants were determined for dUMP and CH_2THF for all mutants; however, methods varied from those used for WT. A solution of S88A-ThyX (20 µM) was titrated with dUMP (0 – 21 µM final concentration) and the change in absorbance was monitored at 450 nm using a Shimadzu UV-2450 spectrophotometer. The change in absorbance was plotted versus free dUMP concentration and the dissociation constant was determined from the hyperbolic dependence on dUMP concentration. A solution of R90A-ThyX (1 µM) was titrated with

a solution of dUMP (0 – 29 μM final concentration) using a fluorescence spectrophotometer. The solution was excited at 450 nm and the changes in fluoresce at 525 nm were fit to a square hyperbola to determine the dissociation constant. For the variants Q75A-ThyX and R174A-ThyX a different approach was required to determine the effective dissociation constant for dUMP. Catalytic amounts of either Q75A-ThyX or R174A-ThyX (1 μM) and NADPH (150 μM) with various concentrations of dUMP (0 – 200 μM) were placed in a cuvette, and oxidation of NADPH was monitored at 340 nm. The initial velocities were plotted versus total dUMP and were fit to a square hyperbola to determine the dissociation constants. The dissociation constant for dUMP with Y91A-ThyX could not be determined by the NADPH oxidase assay because the addition of dUMP (1 – 100 μM) did not alter the velocity.

Dissociation constants for CH_2THF with Q75A-ThyX, S88A-ThyX, R90A-ThyX, and R174A-ThyX were determined using a stopped-flow fluorometer. An anaerobic solution of enzyme (10 μM after mixing) was mixed with various concentrations of CH_2THF (0 – 724 μM after mixing). The reaction was monitored by exciting at 450 nm with a 480 nm emission cut-off filter. The addition of dUMP caused a decrease in fluorescence. The reaction was monitored until completion (~1 s) and the change in fluorescence was plotted versus free CH_2THF concentration and fit to a square hyperbola. The NADPH oxidase assay was used to determine the effective dissociation constant of CH_2THF to Y91A-ThyX. An aerobic solution of Y91A-ThyX (1 μM after mixing) was added to a solution of NADPH (150 μM after mixing) and varying concentrations of CH_2THF (0 – 80 μM after mixing), and the consumption of molecular oxygen was followed using a Hansetech Oxygrah DW1 oxygen electrode. Initial velocities were

plotted against CH_2THF concentration and fit to hyperbola to determine the effective dissociation constant.

Midpoint Potentials. Midpoint potentials for WT-ThyX, WT-ThyX•dUMP, and WT-ThyX•dTMP complexes were measured using the xanthine/xanthine oxidase method of Massey (*7*). Enzyme in 0.1 M Tris-HCl, 1 mM EDTA at pH 8.0 with 500 µM xanthine and 2 µM methylviologen was made anaerobic in a glass cuvette (*8*). After the solution was made anaerobic, a catalytic amount xanthine oxidase was tipped-in from a side-arm to initiate reduction. When determining the midpoint potential for WT-ThyX, 1-hydroxyphenazine was used as the indicator dye. The potential of 1-hydroxyphenazine was calculated to be -235 mV at pH 8.0 (*9*). When determining the midpoint potentials for the WT-ThyX•dUMP and WT-ThyX•dTMP complexes, phenosafranine was used as the redox indicator dye; its potential was calculated to be -283 mVat pH 8.0 (*9*).

Reductive Half-Reaction. Anaerobic solutions of enzyme active sites (15 µM after mixing) free or in complex with dUMP or dTMP (400 µM for WT; 1 mM for mutant enzymes) were mixed with various concentrations of either NADPH or NADH (0.25 – 5 mM after mixing) using a Hi-Tech Scientific KinetAsyst SF-61 DX2 stopped-flow spectrophotometer at 25 ºC. Alternatively, an anaerobic solution of WT-ThyX (15 µM) was mixed with various concentrations of NADPH (0.25 – 5 mM) with 400 µM dUMP using a stopped-flow spectrophotometer. Double-mixing experiments were also done by first mixing anaerobic WT-ThyX (15 µM after mixing) with dUMP (400 µM after mixing), aging for 0.1 s or 200 s, and then mixing with various concentrations of

NADPH (0.25 – 5 mM after mixing). A solution of anaerobic WT-ThyX (15 μM after mixing) was mixed with various concentrations of CH_2THF (0 – 400 μM after mixing) with 15 mM H_2CO and 1 mM of NADPH. Reduction of the enzyme-bound flavin was monitored by the absorbance at 450 nm, and reaction traces were fit using with Kinetic Studio (Hi-Tech Scientific) and KaleidaGraph. The reactions of WT-ThyX with NADPH and NADH, R90A-ThyX with NADPH, and WT-ThyX with NADPH and CH_2THF were fit using Equation 2, where ΔA is the absorbance change at 450 nm at any given ligand concentration and $\Delta A_{FAD,1\text{-}4}$ are the absorbance changes for each phase observed. This equation assumes reduction of active site flavin is sequential. All reactions were performed in 0.1 M Tris-HCl with 1 mM EDTA at pH 8.0.

$$\Delta A = \Delta A_{\infty} + \Delta A_{FAD,1}\exp^{-k_{red}tS} + \Delta A_{FAD,2}(k_{red}tS)\exp^{-k_{red}tS} + \Delta A_{FAD,3}(k_{red}tS)^2\exp^{-k_{red}tS} + \Delta A_{FAD,4}(k_{red}tS)^3\exp^{-k_{red}tS} \quad (2)$$

In an attempt to detect stable charge-transfer complexes, an anaerobic solution of NADPH (20 μM after mixing) was mixed from a side-arm of an anaerobic cuvette into an anaerobic solution of WT-ThyX (20 μM). The reduction was followed using a Hewlett-Packard 8453 photodiode array spectrophotometer. Once reduction was complete an anaerobic solution of $NADP^+$ (2 mM) was tipped-in from the second side-arm and absorbance spectra were recorded. Alternatively, anaerobic enzyme (~15 μM) was reduced with one equivalent of dithionite from a titrating syringe attached to the anaerobic cuvette. $NADP^+$ (2 mM) was added from a side-arm to the solution of enzyme either before or after reduction. Reactions were carried out in 0.1 M Tris-HCl, pH 8.0, 1 mM EDTA at 25 ºC.

Results

Ligand Binding and Midpoint Potentials. The dissociation constant for the oxidized WT-ThyX•dUMP and WT-ThyX•dTMP complexes was determined in titrations using the change in flavin fluorescence at 525 nm (Figure 2-3, Table 2-1 and 2-2). Data were fit to Equation 1, and enzyme concentrations were determined from this fit to be ~246 nM instead of the expected 337 nM. The dissociation constants were determined to be 24.8 nM and 17.5 nM for dUMP and dTMP, respectively. The dissociation constant for oxidized S88A-ThyX•dUMP complex was determined from the change in absorbance at 450 nm. Data were fit to a hyperbola giving a dissociation constant of 3.8 μM (Table 2-1). The dissociation constant for oxidized R90A-ThyX•dUMP was determined similarly to WT-ThyX•dUMP, however the change in fluorescence at 525 nm was fit to hyperbola, giving a dissociation constant of 3.7 μM. Effective dissociation constants for Q75A-ThyX•dUMP and R174A-ThyX•dUMP were determined using the NADPH oxidase assay because the absorbance change associated with binding was too small to determine the K_d (Figure 2-3 and Table 2-1). Plotting the change in initial velocity versus dUMP gave hyperbolic fits with effective dissociation constants of 6.6 μM and 60 μM for Q75A-ThyX•dUMP and R174A-ThyX•dUMP, respectively. The NADPH oxidase assay with Y91A-ThyX gave identical rates for each addition of dUMP (1 – 100 μM) suggesting a $K_d < 1$ μM (Table 2-1).

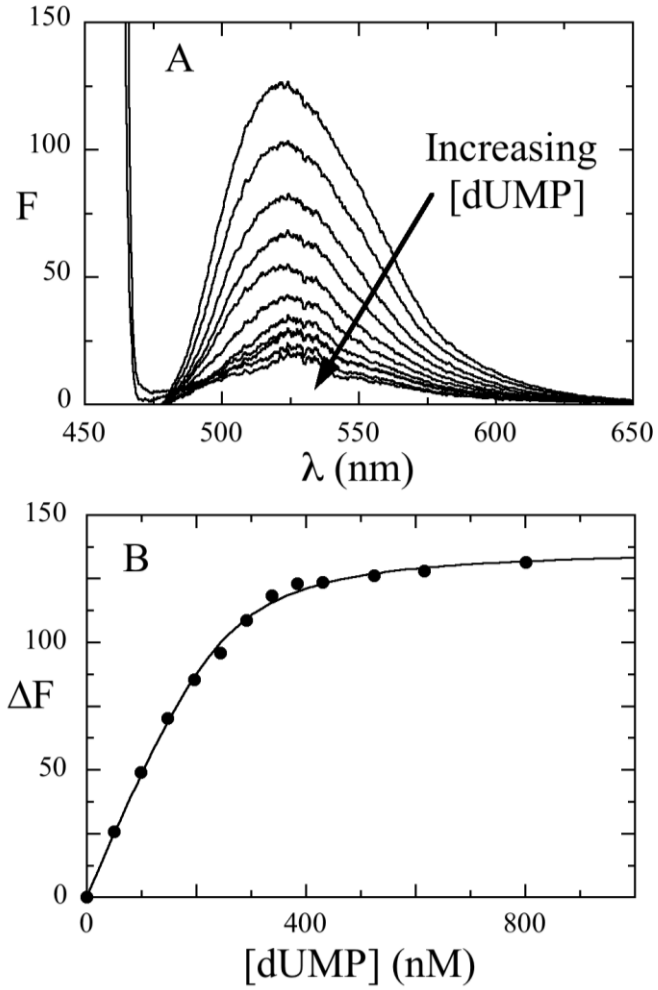

Figure 2-3. ***Binding Titration with dUMP.*** (A) WT-ThyX (337 nM) was titrated with dUMP (50 – 1005 nM) in 0.1 M Tris-HCl, 1 mM EDTA pH 8.0 at 25 ºC and the flavin fluorescence was recorded. Enzyme was excited at 450 nm and emission spectra were collected from 460 – 660 nm. (B) The fluorescence changes at 525 nm were plotted versus [dUMP]. Data were fit to Equation 1, giving a K_d of 24.8 nM.

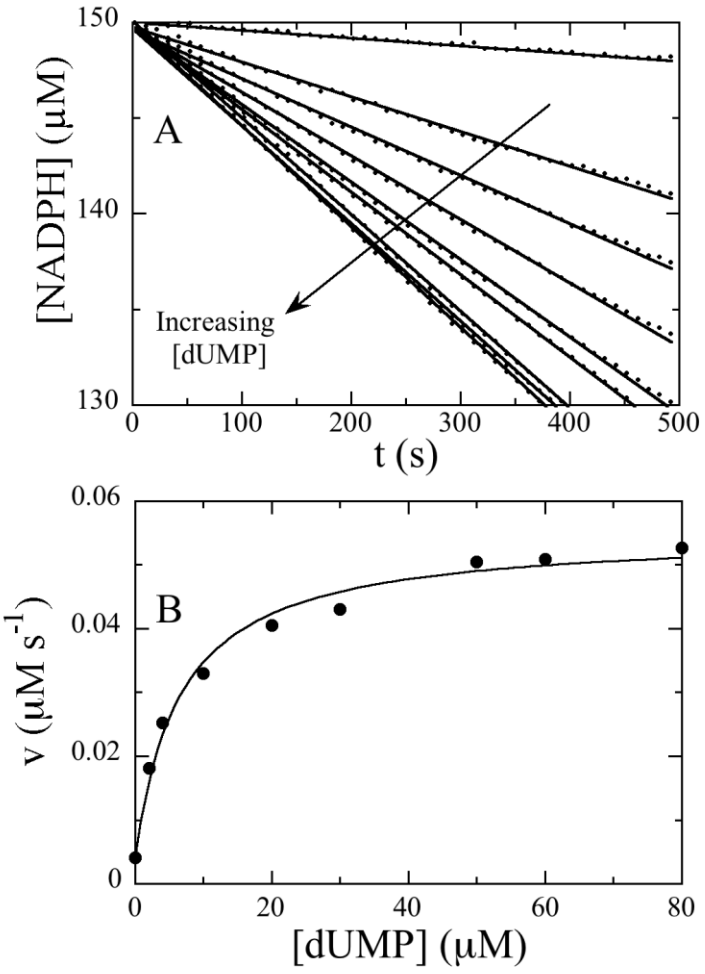

Figure 2-4. ***NADPH Oxidase Assay with Q75A-ThyX*****.** (A) A catalytic amount of Q75A-ThyX (1 μM final concentration) was mixed with NADPH (150 μM final concentration) with various concentrations of dUMP (0 – 80 μM final concentration). (B) Initial velocities were plotted as a function of dUMP concentration and fit to a square hyperbola, giving an effective dissociation constant of 6.5 μM.

Table 2-1. Kinetic constants for ligand binding to WT-ThyX.[a]

Ligand	k_{on} (M^{-1} s^{-1})[b]	k_{off} (s^{-1})[c]	$K_{d\ app}$	$K_{d,ox}$ (nM)[e]	$K_{d,red}$
dUMP	2.6 ± 0.2x 10^6	100 ± 28.7	38.5 ± 14.0	24. ± 5.6	1.4[a]
dTMP	2.3 ± 01 x 10^6	99.1 ± 5.3	43.1 ± 4.2	17.5 ± 6.5	1.2[a]
CH_2THF[g]	1.5 ± 0.1 x 10^6	37.5 ± 12.7	25.0 ± 10.1	n/a	n/a
THF[g]	1.5 ± 0.1 x 10^6	120 ± 20.8	80.0 ± 19.2	n/a	n/a

[a]Reactions were performed in 0.1 M Tris-HCl, pH 8.0, at 25 ºC. The reaction traces were fit to a single exponential and the observed rated constants were linearly fit versus substrate or product concentrations. [b]Second-order rate constants were determined from the slope. [c]Rate constants were determined from the y-intercept. [d]Dissociation constants determined from the ratio of k_{off} to k_{on}. [e]Dissociation constants determined from fluorescence binding titrations. [f]Dissociation constants determined by completing the thermodynamic box (Scheme 2). [g]Solutions were made anaerobic, and H_2CO was added to all CH_2THF solutions.

The dissociation constants for S88A-ThyX•CH_2THF, R90A-ThyX•CH_2THF, R174A-ThyX•CH_2THF, and Q75A-ThyX•CH_2THF were determined in titrations of each mutant enzyme with CH_2THF from the changes in flavin fluorescence observed in a stopped-flow instrument (Figure 2-5A). The dissociation constants were determined by plotting the change in fluorescence versus free CH_2THF and fitting to a square hyperbola (Figure 2-5B). The dissociation constants ranged from 8 µM to 34 µM (Table 2-2). The dissociation constant for CH_2THF with Y91A-ThyX could not be determined by using a stopped-flow spectrophotometer because the required enzyme concentration was too high to get a hyperbolic dependence. Therefore an effective dissociation constant for Y91A-ThyX•CH_2THF was determined from its NADPH oxidase assay (Table 2-2). A plot of initial velocities versus CH_2THF was fit to a square hyperbola, resulting in an effective dissociation constant of 6.3 µM.

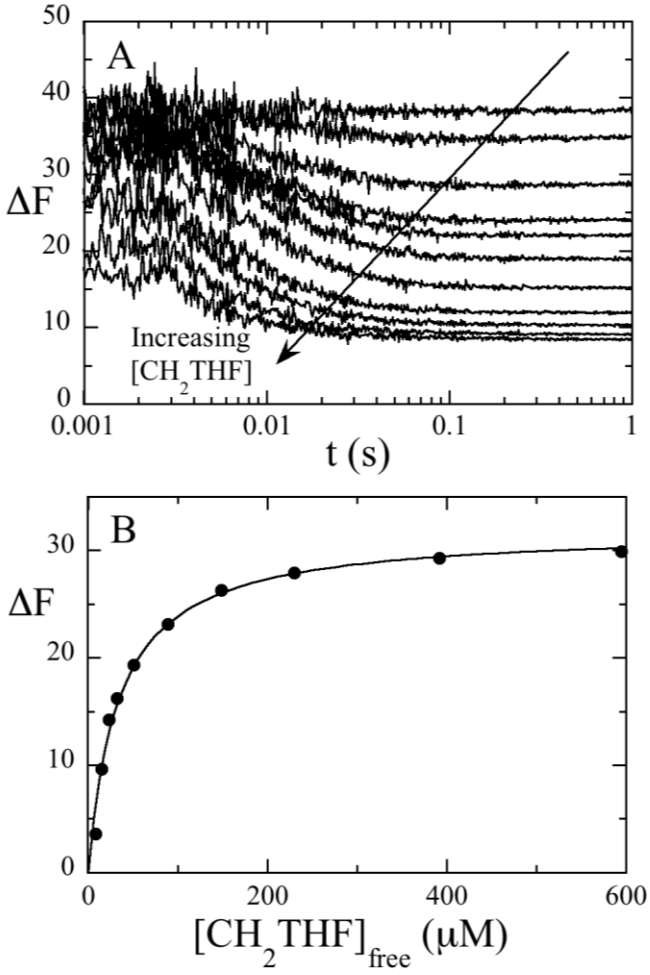

Figure 2-5. ***Titration with CH_2THF.*** (A) S88A-ThyX (10 μM after mixing) was mixed with varying concentrations of CH_2THF (6.3 – 600 μM after mixing) using a stopped-flow fluorometer. The fluorescence was monitored after excitation at 450 nm with a 480 nm cut-off filter. (B) The fluorescence change was plotted versus free [CH_2THF] and data were fit to a square hyperbola, giving a K_d of 31.9 μM

Table 2-2. A Comparison of the Dissociation constants for dUMP and CH_2THF

Enzyme	$K_{d,dUMP}$ (μM)	$K_{d,CH2THF}$ (μM)
WT	0.0076 ±0.00054	11.5 ± 3.3
Q75A	6.6 ± 0.9	8.0 ± 0.4
R90A	3.7 ± 0.3	19.7 ± 1.8
R174A	59.6 ± 13.2	22.3 ± 3.8
Y91A	< 10 μM	6.3 ± 1.9
S88A	3.8 ± 0.4	33.7 ± 3.1

All titrations were carried out in 0.1 M Tris, 1 mM EDTA at pH 8.0 at 25 ºC.

The kinetics of binding were determined for dUMP, dTMP, CH_2THF, and THF to oxidized WT-ThyX using stopped-flow fluorescence experiments (Figure 2-6). The decrease in fluorescence associated with binding was fit to one exponential (Table 2-1). The observed rate constants varied linearly with ligand concentration, giving the bimolecular rate constant, k_{on}, from the slope, ranging from (1.5 to 2.6) x 10^6 M^{-1} s^{-1} and a k_{off}, determined from the y-intercept, ranging from (38 to 100) s-1. The dissociation constants for all ligands, determined from the ratio of k_{off} and k_{on}, ranged from 25 μM to 80 μM. A difference in dissociation constants for dUMP and dTMP, determined from manual titrations and by stopped-flow spectroscopy, suggest binding occurs in at least two steps.

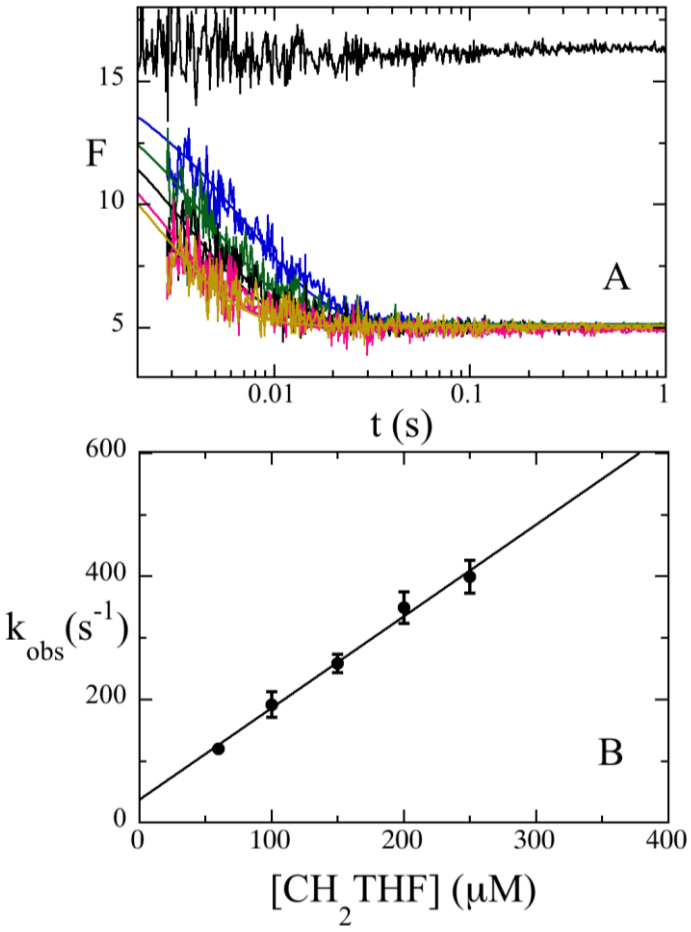

Figure 2-6. ***Kinetics of Binding*****.** Reactions were carried out in 0.1 M Tris-HCl, 1 mM EDTA, 15 mM H_2CO pH 8.0 at 25 ºC. (A) An anaerobic solution of WT-ThyX (6.6 µM after mixing) was mixed with various concentration of anaerobic CH_2THF (60 – 250 µM after mixing). The decrease in fluorescence emission was fit to one exponential. (B) The observed rate constants were plotted versus [CH_2THF], giving a rate constant for binding of 1.5 x 10^6 M^{-1} s^{-1} and a rate constant for dissociation of 38 s^{-1}.

Midpoint potentials of WT-ThyX were determined for the E_{ox}/E_{red}, E_{ox}•dUMP/E_{red}•dUMP, and E_{ox}•dTMP/E_{red}•dTMP couples using the xanthine/xanthine oxidase method (*7*) at pH 8.0 (Figure 2-7 and Table 2-3). The midpoint potential for the E_{ox}/E_{red} couple was -218 mV while that of the E_{ox}•dUMP/E_{red}•dUMP and

E_{ox}•dTMP/E_{red}•dTMP couples were ~50 mV lower with midpoint potentials of -270 mV and -273 mV, respectively. We were unable to determine the midpoint potential for the couple E_{ox}•CH_2THF/E_{red}•CH_2THF because no reduction of the E_{ox}•CH_2THF complex could be observed using the xanthine/xanthine oxidase method.

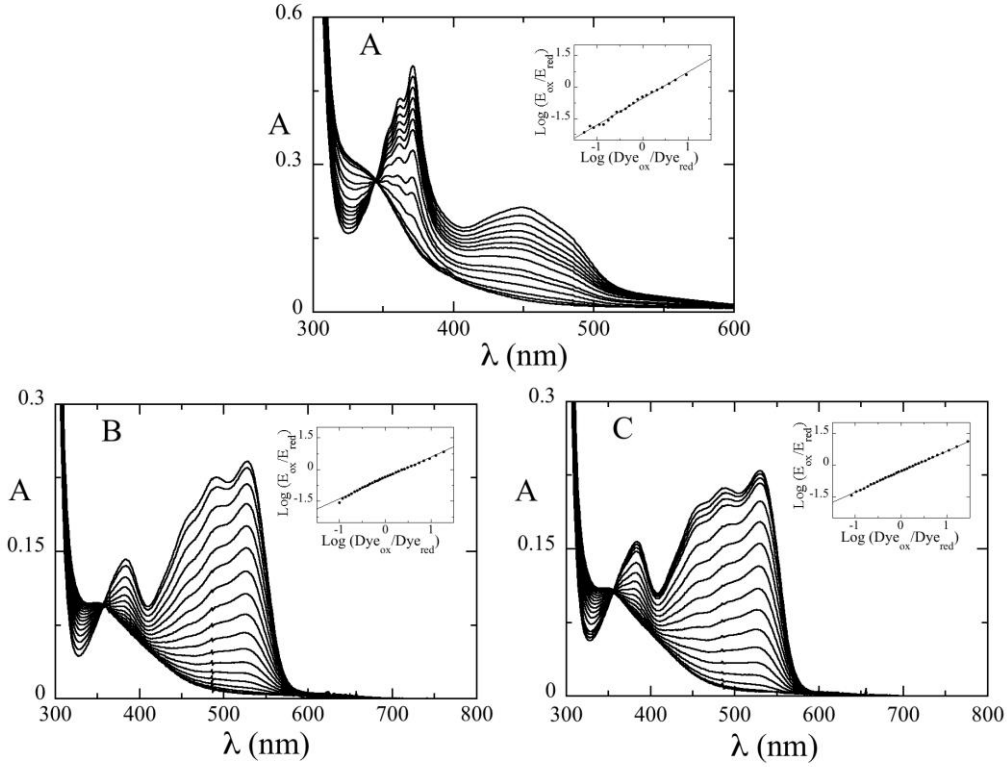

Figure 2-7. Midpoint potentials of WT-ThyX. The midpoint potentials were determined for the E_{ox}/E_{red} (-218 mM) (A), E_{ox}•dUMP/E_{red}•dUMP (-270 mV) (B), and E_{ox}•dTMP/E_{red}•dTMP (-273 mV) (C) couples using the xanthine/xanthine oxidase method in 0.1 M Tris-HCl, 1 mM EDTA pH 8.0.

Table 2-3. Midpoint potentials of WT-ThyX	
Redox couple	$E_{m8.0}$ (mV)[a]
E_{ox}/E_{red}	-218[b]
E_{ox}•dUMP/E_{red}•dUMP	-270[c]
E_{ox}•dTMP/E_{red}•dTMP	-273[c]

[a]Potentials were determined in 0.1 M Tris-HCl at pH 8.0, 25 ºC. [b]Midpoint potential determined using 1-hydroxphenazine ($E_{m8.0}$ = -235 mV). [c]Midpoint potentials determined using phenosafranine ($E_{m8.0}$ = -283 mV).

It was not possible to determine the dissociation constants of the reduced E_{red}•dUMP complex by direct spectral titration of E_{red} with dUMP because the concentration of enzyme required for an observable absorbance change would be well above the K_d. However, the K_d for this complex can be calculated from the difference in potentials for the E_{ox}/E_{red} and the E_{ox}•dUMP/E_{red}•dUMP couples and the dissociation constant measured for the E_{ox}•dUMP complex. Completing the thermodynamic box (Figure 2-8) gave dissociation constants for the E_{red}•dUMP and E_{red}•dTMP complexes of 425 nM, a ~53-fold decrease in affinity caused by flavin reduction.

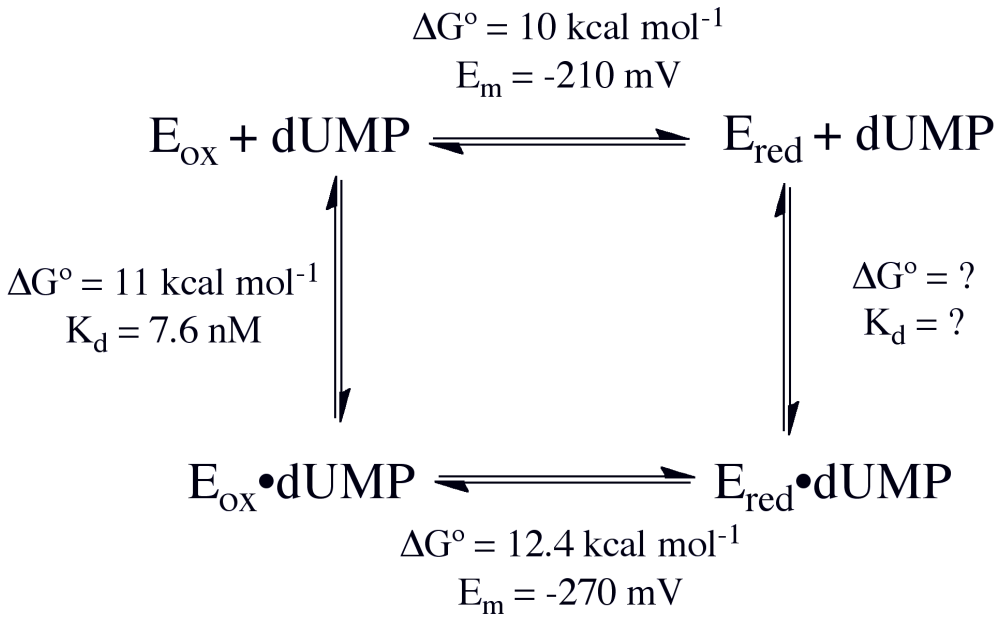

Figure 2-8. ***Thermodynamic Box of ThyX*****.** The thermodynamic box is used to determine the dissocation constants for the reduced enzyme•nucleotide complexes.

Reductive half-reaction. The reductive half-reaction was followed in the stopped-flow spectrophotometer by rapidly mixing an anaerobic enzyme solution with various concentrations of either NADPH or NADH and following the decrease of flavin absorbance at 450 nm (Figure 2-10 and 2-11). In the absence of bound deoxynucleotides, the reaction traces were too complex to be fit to the expected sums of exponentials, both when NADPH and NADH were used as reductants. However, a model is proposed where the reduction of each flavin of the tetramer is sequential - each active site requires the reduction of the previous one before being reduced (Figure 2-8). The data can be fit with each of the four steps being governed by identical rate constants using Equation 2. The observed rate constants were plotted versus pyridine nucleotide and fit to a hyperbola (Table 2-4). Reduction of WT-ThyX with NADPH gave a limiting rate constant of 0.6 s^{-1} with a K_d value of 1.1 mM (Figure 2-10). Reduction of WT-ThyX with NADH gave a limiting rate constant of 1.04 s^{-1} and K_d value of 1.8 mM (Figure 2-11).

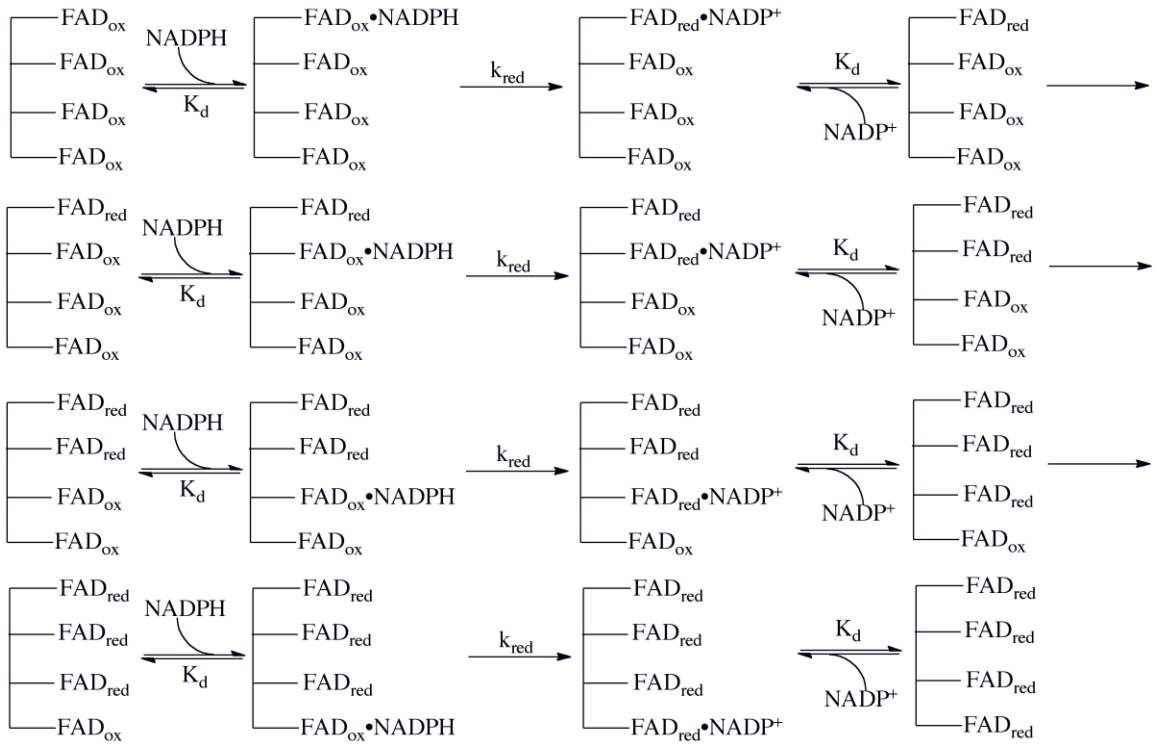

Figure 2-9: Reductive Half-Reaction Scheme. A sequential model for the reduction of the enzyme by NAD(P)H in the absence of nucleotide.

When dUMP was added to the anaerobic solution of WT-ThyX, reduction by either NADPH or NADH was simplified to a 2-exponential process, with each phase representing ~50 % of the total absorbance change. The observed rate constants were plotted as a function of pyridine nucleotide concentration and fit to a hyperbola (Table 2-4). The limiting rate constants for reduction by NADPH were 1.32 s^{-1} and 0.57 s^{-1} with K_d values of 0.45 mM and 0.99 mM, respectively (Figure 2-10). The limiting rate constants for reduction by NADH were slight less with 1.01 s^{-1} and 0.41 s^{-1} and K_d values were determined to be 0.85 mM and 1.5 mM, respectively (Figure 2-8). Similarly, when WT-ThyX•dTMP was reduced with NADPH, the reaction was fit to a sum of two exponentials with both phases representing ~ 50% of the total absorbance change. The

limiting rate constants for reduction by NADPH were 1.5 s^{-1} and 0.65 s^{-1} with K_d values of 0.72 mM and 1.2 mM, respectively (Table 2-4).

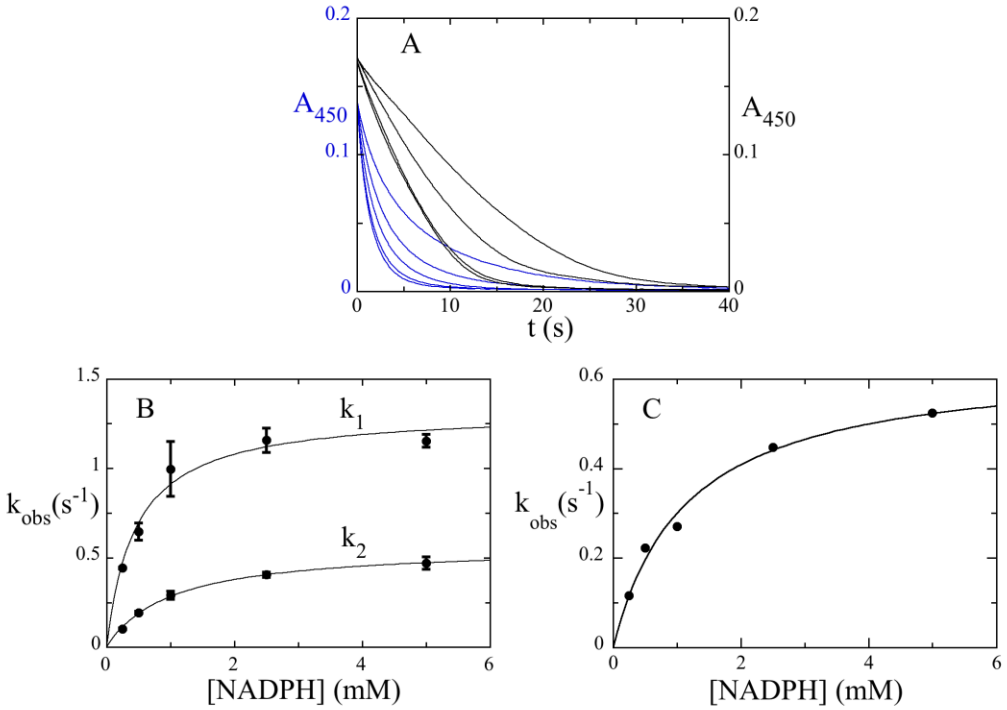

Figure 2-9. ***Reductive Half-Reaction of WT-ThyX with NADPH*****.** (A) A solution of WT-ThyX (~15 µM after mixing) with dUMP (400 µM after mixing, blue traces) or without (black traces) was mixed with varying concentrations of NADPH (0.25 – 5 mM after mixing). Reactions were carried out in 0.1 M Tris-HCl, 1 mM EDTA pH 8.0 at 25 ºC and were monitored at 450 nm using a stopped-flow spectrophotometer. (B) The reaction of WT-ThyX•dUMP with NADPH was fit to a sum of two exponentials. The observed rate constants were plotted as a function of NADPH concentration, giving limiting rate constants of 1.32 ± 0.08 s^{-1} and 0.57 ± 0.01 s^{-1} with K_d values of 0.45 ± 0.10 mM and 0.99 ± 0.07 mM, respectively. (C) Reaction of WT-ThyX with NADPH was fit using the stepwise model of reduction where each subunit is reduced sequentially (Equation 2, Scheme 2-3). The limiting rate constant for reduction was found to be 0.64 ± 0.04 s^{-1} with a K_d of 1.14 ± 0.20 mM.

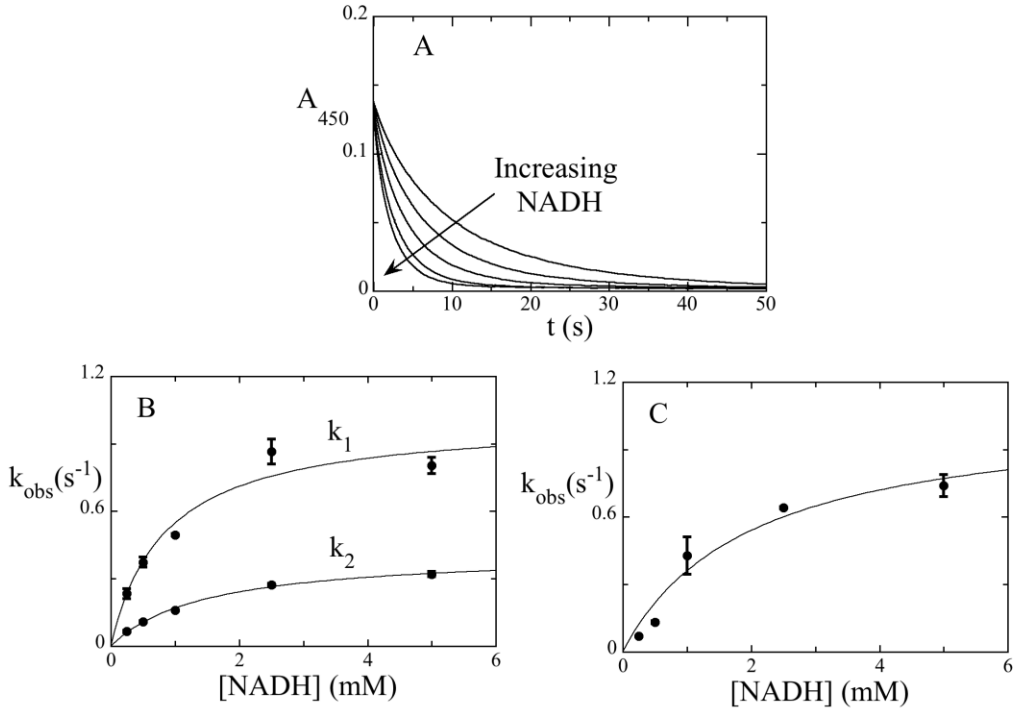

Figure 2-10. ***Reductive Half-reaction of WT-ThyX with NADH.*** (A) A solution of WT-ThyX (~15 µM after mixing) with or without dUMP (400 µM after mixing) was mixed with varying concentrations of NADH (0.25 – 5 mM after mixing). Reactions were performed in 0.1 M Tris-HCl, 1 mM EDTA pH 8.0 at 25 ºC. The reaction was monitored at 450 nm using a stopped-flow spectrophotometer. (B) When dUMP was present reaction traces were fit to a sum of two exponentials. The observed rate constants were plotted as a function of NADH concentrations with limiting rate constants of 1.02 ± 0.12 s^{-1} and 0.42 ± 0.02 s^{-1} with K_d values of 0.85 ± 0.29 mM and 1.48 ± 0.16 mM, respectively. (C) The reaction without dUMP was fit using the model for stepwise reduction (Equation 2, Scheme 3), with identical values for the reduction rate constant for each step. The observed rate constant for reduction was found to be 1.08 ± 0.21 s^{-1} with a K_d of 1.99 ± 0.89 mM.

The difference in the dissociation constant for dUMP determined by manual titration (K_d of 7.6 nM) and by stopped-flow methods (K_d of 38 µM) suggests at least two steps involved in binding. However, the complex formed during manual titration was allowed to incubate for times longer than would be catalytically relevant. In order

Table 2-4. Reductive half-reaction rate constants for WT-ThyX

	$k_{red,1}$ (s-1)	$k_{red,2}$ (s-1)	$K_{d,1}$ (mM)	$K_{d,2}$ (mM)
NADPH				
- dUMP	0.64 ± 0.04	-	1.14 ± 0.20	-
+ dUMP	1.32 ± 0.08	0.57 ± 0.01	0.45 ± 0.10	0.99 ± 0.07
+ dTMP	1.5 ± 0.09	0.65 ± 0.03	0.72 ± 0.14	1.23 ± 0.16
NADH				
- dUMP	1.04 ± 0.22	-	1.80 ± 0.94	-
+ dUMP	1.02 ± 0.12	0.42 ± 0.02	0.85 ± 0.29	1.48 ± 0.16

Enzyme (15 µM after mixing) or in complex with or without dUMP or dTMP (400 µM after mixing) was mixed with varying concentration of either NADH or NADPH (0.25 – 5 mM) in 0.1 M Tris-HCl, 1 mM EDTA, pH 8.0 at 25 ºC.

to determine which complex is catalytically relevant, the complex formed at 1 s or that formed after a long incubation, WT-ThyX was initially mixed with dUMP and allowed to age for either 0.1 s or 200 s before reaction with NADPH. With both age-times reduction of the enzyme was identical to the reduction observed when dUMP was premixed with WT-ThyX in a tonometer where it would sit for at least 60 minutes prior to reaction. Similarly, when a solution of WT-ThyX was reduced with NADPH (0.25 mM – 5 mM), in the presence of 400µM dUMP, reduction was identical to that when dUMP is incubated with the enzyme prior to reduction. This suggests reduction of the enzyme by NADPH does not require the complex formed after long incubation.

The reductive half-reactions of the mutant enzymes with NADPH was also studied (Table 5). Most mutants, except one, abolish this negative cooperativity. The mutants that abolish this negative cooperativity (Q75A-ThyX, Y91A-ThyX, R174A-ThyX, and S88A-ThyX) have two phases of reduction. However, reduction of R90A-ThyX by NADPH was similar to that of WT-ThyX with NADPH, only 5-fold slower.

When dUMP was bound to each of the variant enzymes, reduction with NADPH was similar to that of WT-ThyX. Reaction traces were fit to a sum of two exponentials (Table 2-5). The limiting rate constants ranged from 0.5 s^{-1} to 2.1 s^{-1} with K_d values from 0.5 mM to 4.2 mM for the first phase and 0.2 s^{-1} to 0.6 s^{-1} with K_d values from 1.0 mM to 6.1 mM for the second phase.

Table 2-5: A Comparison of the Reductive Half-Reaction Rate

Enzyme	$k_{1,red}(s^{-1})$	$k_{2,red}(s^{-1})$	$K_{d,1}$(mM)	$K_{d,1}$(mM)
Wt				
-dUMP	0.64 ± 0.04	-	1.14 ± 0.20	-
+dUMP	1.32 ± 0.08	0.57 ± 0.01	0.45 ± 0.10	0.99 ± 0.07
S88A				
-dUMP	1.12 ± 0.15	0.32 ± 0.01	1.77 ± 0.56	1.12 ± 0.13
+dUMP	0.58 ± 0.08	0.21 ± 0.05	3.95 ± 1.18	5.74 ± 2.97
Y91A				
-dUMP	0.71 ± 0.01	0.059 ± 0.002	0.63 ± 0.03	-
+dUMP	1.20 ± 0.07	0.36 ± 0.04	4.16 ± 0.46	6.05 ± 1.10
Q75A				
-dUMP	0.020 ± 0.003	0.004 ± 0.001	0.85 ± 0.42	-
+dUMP	1.05 ± 0.06	0.44 ± 0.05	1.95 ± 0.26	3.71 ± 0.77
R90A				
-dUMP	0.13 ± 0.015	-	1.91 ± 0.54	-
+dUMP	0.49 ± 0.02	0.20 ± 0.03	4.31 ± 0.38	5.78 ± 1.40
R174A				
-dUMP	0.071 ± 0.003	0.021 ± 0.002	1.10 ± 0.14	0.58 ± 0.22
+dUMP	2.12 ± 0.14	0.41 ± 0.04	1.39 ± 0.24	1.44 ± 0.36

Enzyme (15 µM after mixing) with or without dUMP present (400 µM after mixing) was mixed with various concentrations of NADPH (0.25 – 5 mM) in 0.1 M Tris-HCl, 1 mM EDTA, pH 8.0 at 25 ºC. S88A required a third exponential that was independent of concentration with a rate constant of 0.030 s^{-1}.

The effect of CH_2THF on reduction was also investigated. When an anaerobic solution of WT-ThyX was mixed with NADPH containing various concentrations of CH_2THF, reduction was inhibited (Figure 2-12). Absorbance traces collected at 450 nm were fit using the model for reduction of WT-ThyX without dUMP, using a single rate constant for the sequential reduction of each of the four active sites (Equation 2). The limiting rate constant of reduction at high CH_2THF concentration was 0.02 s^{-1} with an apparent inhibition constant of 11.5 μM.

It has been reported that $NADP^+$ remains bound to the reduced enzyme and forms a charge-transfer complex. This was checked by reducing an anaerobic solution of WT-ThyX with 1 equivalent of NADPH and recording absorbance spectra over time (Figure 2-13). Once reduction was complete, an anaerobic solution of $NADP^+$ (2 mM final) was added to the reduced enzyme. No absorbance increase was observed at wavelengths longer than 520 nm, where charge-transfer complexes would absorb. Alternatively, anaerobic enzyme was reduced with an equivalent of dithionite. A solution of anaerobic $NADP^+$ was added either before or after reduction from a side-arm and absorbance spectra were recorded. No charge-transfer complex was seen. Thus, there was no evidence for the charge-transfer complex reported previously (*10*).

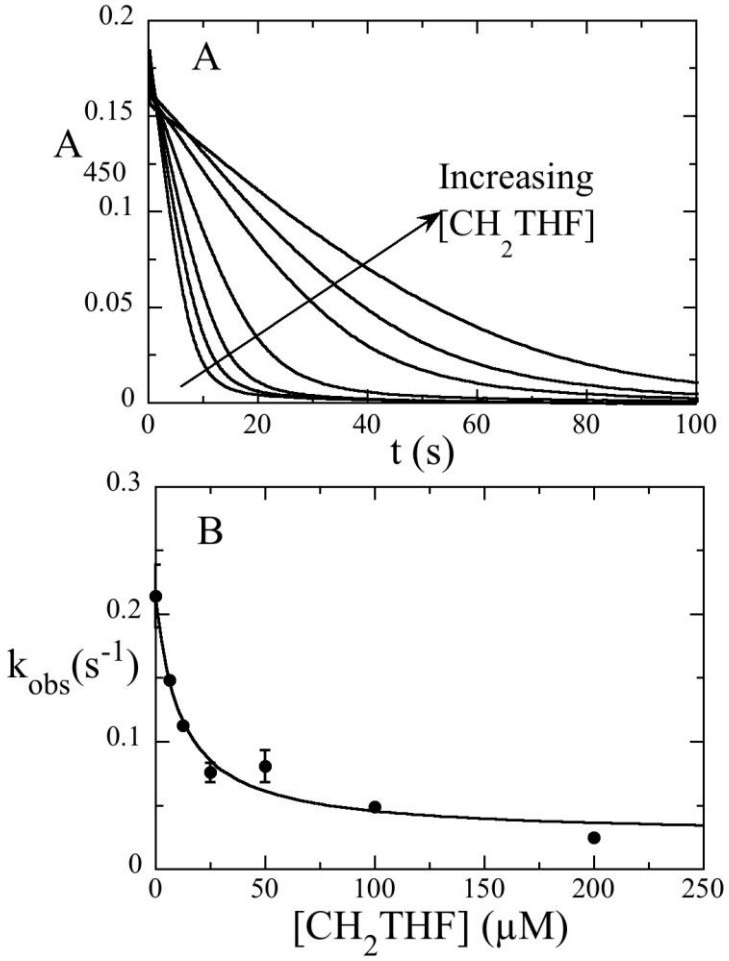

Figure 2-12. ***Reductive Half-Reaction of WT-ThyX NADPH and CH_2THF.*** (A) A solution of WT-ThyX (~15 μM after mixing) was mixed with both NADPH (1 mM after mixing) and various concentrations of CH_2THF (6.3 – 400 μM after mixing). Reactions were performed in 0.1 M Tris-HCl, 1 mM EDTA, 15 mM H_2CO pH 8.0 at 25 ºC. The reaction was monitored at 450 nm using a stopped-flow spectrophotometer and fit using a sequential model of reduction with a single rate constant for each of the four steps. (B) The observed rate constants were plotted as a function of CH_2THF concentration giving a limiting rate constant for reduction of 0.02 ± 0.002 s^{-1} with an apparent inhibition constant of 11.5 ± 3.3 μM.

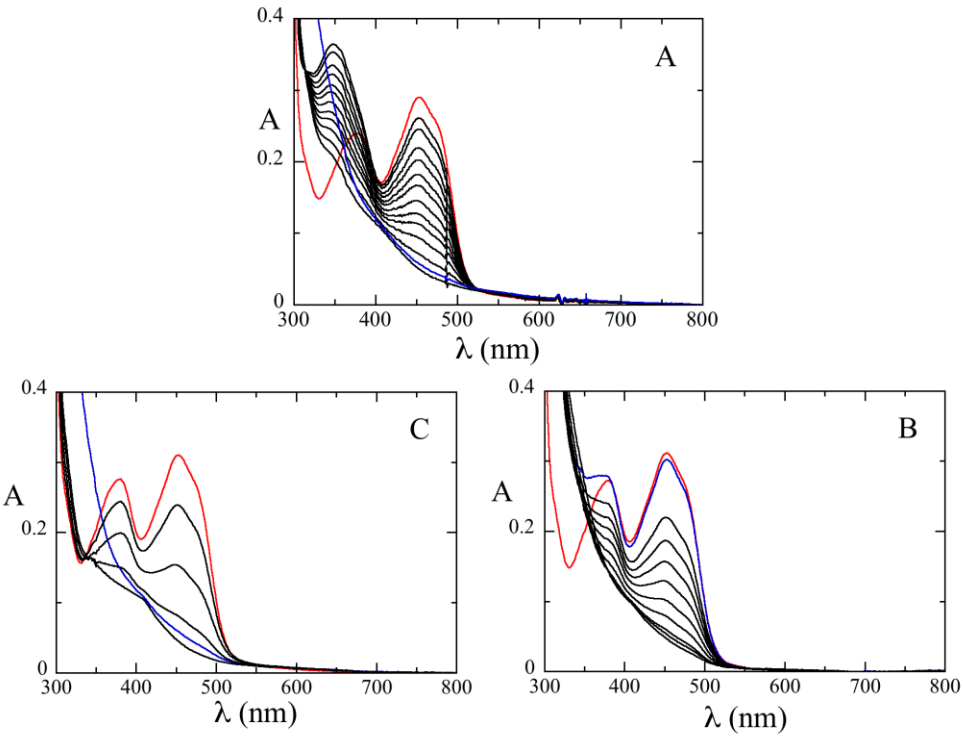

Figure 2-13. ***Spectral Change Associated with Reduction of Enzyme*****.** (A) An anaerobic solution of enzyme (~25 µM, red spectrum) was mixed with an anaerobic solution of NADPH (~25 µM) and absorbance spectra were recorded (black spectra). A solution of $NADP^+$ (2 mM) was added from the side-arm after reduction of the enzyme was complete (blue spectrum). (B) Anaerobic enzyme (~25 µM, red spectrum) was mixed with NADP+ (2 mM, blue spectrum). Enzyme was titrated with up to 1 equivalent of dithionite (black spectra). (C) Anaerobic enzyme (~25 µM red spectrum) was reduced with 1 equivalent of dithionite (black spectra). NADP+ (2 mM) was tipped in from the side-arm after reduction was complete (blue spectrum). All reactions were carried out in 0.1 M Tris-HCl, 1 mM EDTA, pH 8.0 at 25 ºC.

Discussion

ThyX requires both a reductant and a flavin prosthetic group for catalysis (*3*). In the reductive half-reaction a hydride is transferred from NADPH to the enzyme-bound FAD. The reduced enzyme then reduces the methylene group transferred from CH_2THF

to dUMP (*5*). Steady-state kinetics has been previously performed on a number of ThyX enzymes, resulting in numerous proposed kinetic and chemical mechanisms (*10-13*). These steady-state experiments were performed in the presence of molecular oxygen, which complicates the analysis because the reduced enzyme reacts with O_2. By looking specifically at the reductive half-reaction and the effects of the substrates we can suggest a binding order of the substrates (Figure 2-14).

The reductive half-reaction was studied with both NADPH and NADH. In the absence of dUMP or dTMP, each subunit appears to be reduced in succession, such that it is not until the first subunit is reduced before the next becomes reduced. Crystal structures of WT-ThyX without deoxynucleotide show that one of the active sites in a different conformation than the other three subunits (Figure 2-15). A mobile loop containing residues 86 – 97 is in a position that would allow NAD(P)H access to the isoalloxazine ring of FAD. Without deoxynucleotide present, reduction of WT-ThyX by NADPH exhibits a high degree of negatively cooperativity, with only one active site able to react at a time. When the reductive half-reaction was carried out with S88A-ThyX, R174A-ThyX, Y91A-ThyX, or Q75A-ThyX, reduction was similar to WT-ThyX when deoxynucleotide is bound suggesting a different mechanism for the variant ThyX enzymes. It is possible that a network that connects each of the subunits is disrupted in these variants.

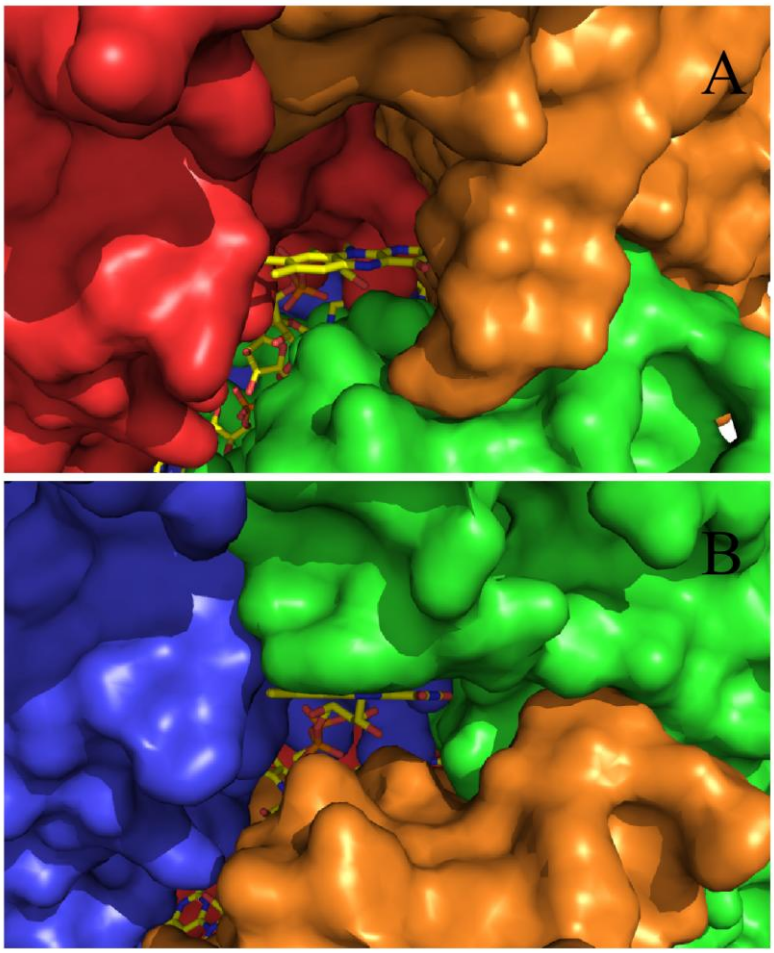

Figure 2-14. ***Active Site Structure of WT-ThyX from T. maritima (pdb 1O2B) Highlighting the Difference in ThyX Active Sites*****.** (A) Notice the position of the orange subunit that contains the active site loop, residues 86 – 97, is positioned away from the flavin. Only one of the active sites has this conformation. The other three active site of WT-ThyX are in the conformation shown in (B). Notice the green subunit, containing residues 86 – 97, position directly in front of the flavin.

The binding of either dUMP or dTMP increase the rate of reduction with either NADPH or NADH by ~2.2-fold compared to free ThyX. Similarly when ThyX is reduced with a solution of NADPH containing dUMP, the rate of reduction is identical to that observed when the ThyX•dUMP complex is reduced with NADPH. These results suggest that the dUMP complex is likely to form before reduction. The stimulation by

dUMP of the reduction of the enzyme by NAD(P)H suggests a preference for the ThyX•dUMP complex during the reductive half-reaction. The addition of dUMP also diminishes the negative cooperativity observed in its absence. In the presence of dUMP the reaction has two equal phases, suggesting two classes of inequivalent active sites. However, though distinct, each class of active site has a similar reduction rate constant and dissociation constants for NAD(P)H. Structures of the enzymes show that it is a homotetramer, with each active site being formed at the intersection of three subunits. Thus, it is plausible that in the presence of dUMP ThyX functions as a dimer of dimers in the reductive half-reaction.

The addition of either dUMP or dTMP lowers the midpoint potential of the flavin by ~50 mV. The decrease of the potential, a difference of ~2.5 kcal mol^{-1}, implies that reduction by NAD(P)H is less favorable thermodynamically when dUMP or dTMP are bound to the enzyme. This increase in ΔG^{o} does not lead to slower reduction when nucleotide is bound. Instead, reduction is faster and diminishes its negative cooperativety when nucleotide is bound to the enzyme (Figure 2-10).

Mutations to the active site greatly decreases the affinity of binding of dUMP by ~1000-fold. This is not surprising because dUMP makes many contacts with the surrounding residues (Figure 2-2). However, mutations to the active site do not appear to affect the binding of CH_2THF, suggesting that these residues are not involved in the binding of CH_2THF.

CH_2THF inhibits reduction by NADPH, indicating that in turnover, CH_2THF generally does not bind to the enzyme until after the reductive half-reaction. The WT-ThyX•CH_2THF complex could not be reduced using the xanthine/xanthine oxidase method, preventing the determination of midpoint potential of this complex. The inability of the WT-ThyX•CH_2THF complex to become reduced using NADPH or by the xanthine/xanthine oxidase method suggests that CH_2THF blocks the approach to the isoalloxazine. Consistent with this notion, previous studies have suggested that CH_2THF inhibits the reaction of the reduced enzyme with O_2 (*10*). The data presented here suggest that CH_2THF also inhibits the oxidase activity by inhibiting the reduction of the enzyme by NADPH.

Charge-transfer complexes were not observed before or after reduction by NADPH. When enzyme was reduced with an equivalent of NADPH, no evidence for charge-transfer species was observed despite addition of a large amount of $NADP^+$. This suggests that $NADP^+$ dissociates from the E_{red}•dUMP complex before CH_2THF binds to the reduced enzyme. It is difficult to imagine that $NADP^+$, dUMP, CH_2THF, and FAD can simultaneously occupy the active site of the enzyme.

The kinetic data presented here and work on the oxidative half-reaction (recently submitted) suggests the kinetic mechanism shown in Figure 2-14. Stopped-flow and acid quenching experiments on the oxidative half-reaction show the formation of 2 unidentified intermediates and a faster reaction when starting with the reduced ThyX•dUMP complex compared to starting with the reduced ThyX•CH_2THF complex.

This is consisted with kinetic experiments presented here on the reductive half-reaction. dUMP bind first followed by NADPH and reduction of the enzyme, and CH_2THF does not participate in the reductive half-reaction.

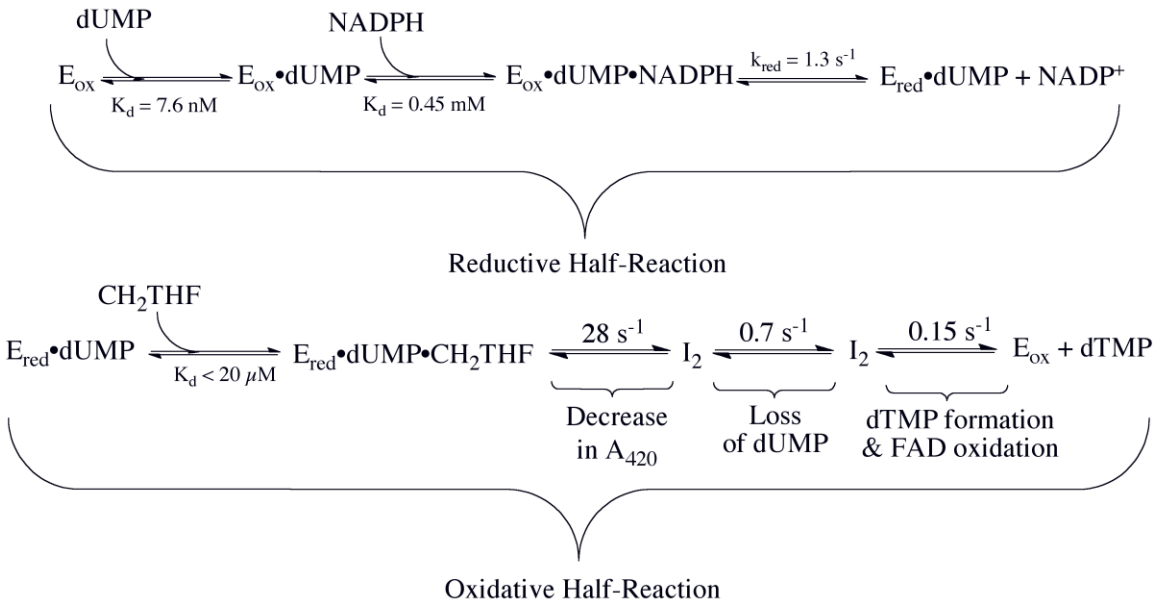

Figure 2-15: ***The Proposed Kinetic Mechanism of ThyX*****.** The kinetic mechanism was determined from the effects of the substrates on both the reductive (this chapter) and oxidative half-reaction (Chapter 3).

REFERENCES

1. Leduc, D., Escartin, F., Nijhout, H. F., Reed, M. C., Liebl, U., Skouloubris, S., and Myllykallio, H. (2007) Flavin-dependent thymidylate synthase ThyX activity: implications for the folate cycle in bacteria, *J Bacteriol 189*, 8537-8545.
2. Carreras, C. W., and Santi, D. V. (1995) The catalytic mechanism and structure of thymidylate synthase, *Annu Rev Biochem 64*, 721-762.
3. Myllykallio, H., Lipowski, G., Leduc, D., Filee, J., Forterre, P., and Liebl, U. (2002) An alternative flavin-dependent mechanism for thymidylate synthesis, *Science 297*, 105-107.
4. Mathews, II, Deacon, A. M., Canaves, J. M., McMullan, D., Lesley, S. A., Agarwalla, S., and Kuhn, P. (2003) Functional analysis of substrate and cofactor complex structures of a thymidylate synthase-complementing protein, *Structure 11*, 677-690.
5. Koehn, E. M., Fleischmann, T., Conrad, J. A., Palfey, B. A., Lesley, S. A., Mathews, II, and Kohen, A. (2009) An unusual mechanism of thymidylate biosynthesis in organisms containing the thyX gene, *Nature 458*, 919-923.
6. Lesley, S. A., Kuhn, P., Godzik, A., Deacon, A. M., Mathews, I., Kreusch, A., Spraggon, G., Klock, H. E., McMullan, D., Shin, T., Vincent, J., Robb, A., Brinen, L. S., Miller, M. D., McPhillips, T. M., Miller, M. A., Scheibe, D., Canaves, J. M., Guda, C., Jaroszewski, L., Selby, T. L., Elsliger, M. A., Wooley, J., Taylor, S. S., Hodgson, K. O., Wilson, I. A., Schultz, P. G., and Stevens, R. C. (2002) Structural genomics of the Thermotoga maritima proteome implemented

in a high-throughput structure determination pipeline, *Proc Natl Acad Sci U S A 99*, 11664-11669.

7. Massey, V. (1990) A Simple Method for the Determination of Redox Potentials, in *Flavins and flavoproteins* (Curti, B., S., R., and G., Z., Eds.), pp 59-66, Walter de Gruyter & Co, New York.

8. Williams, C. H., Jr., Arscott, L. D., Matthews, R. G., Thorpe, C., and Wilkinson, K. D. (1979) Methodology employed for anaerobic spectrophotometric titrations and for computer-assisted data analysis, *Methods Enzymol 62*, 185-198.

9. Clark, W. M. (1960) *Oxidation-reduction potentials of organic systems*, Williams & Wilkins, Baltimore,.

10. Wang, Z., Chernyshev, A., Koehn, E. M., Manuel, T. D., Lesley, S. A., and Kohen, A. (2009) Oxidase activity of a flavin-dependent thymidylate synthase, *FEBS J 276*, 2801-2810.

11. Graziani, S., Bernauer, J., Skouloubris, S., Graille, M., Zhou, C. Z., Marchand, C., Decottignies, P., van Tilbeurgh, H., Myllykallio, H., and Liebl, U. (2006) Catalytic mechanism and structure of viral flavin-dependent thymidylate synthase ThyX, *J Biol Chem 281*, 24048-24057.

12. Griffin, J., Roshick, C., Iliffe-Lee, E., and McClarty, G. (2005) Catalytic mechanism of Chlamydia trachomatis flavin-dependent thymidylate synthase, *J Biol Chem 280*, 5456-5467.

13. Agrawal, N., Lesley, S. A., Kuhn, P., and Kohen, A. (2004) Mechanistic studies of a flavin-dependent thymidylate synthase, *Biochemistry 43*, 10295-10301.

Chapter III

Oxidative Half-Reaction of the FAD-Dependent Thymidylate Synthase from *Thermotoga maritima*

One of the building blocks of DNA, 2'-deoxythymidine-5'-monophosphate (dTMP), is synthesized from 2'-deoxyuridine-5'-monophosphate (dUMP) and 5,10-methylenetetrahydrofolate (CH_2THF) by thymidylate synthase (TS). There are three classes of TS's. The first class is the flavin-independent TS (ThyA), encoded by the *thyA* gene (*1*). ThyA has been studied extensively and is expressed in organisms from bacteria to mammals. The second class is the bifunctional TS-dihydrofolate reductase. The bifunctional form has two distinct polypeptides, each containing its own active site (*2, 3*). This class of enzyme is found mainly in bacteria. The third, recently discovered, class is the flavin-dependent TS (ThyX) encoded by the *thyX* gene. ThyX is only expressed in microbes that include many pathogens associated with human diseases such as tuberculosis, anthrax, pneumonia, diarrhea, and syphilis, among others. Most bacteria that express ThyX lack the gene for ThyA. For the bacterial sources expressing both the *thyX* and *thyA* genes, it has been shown recently that expression of both genes is essential for bacterial survival (*4*). From those studies, it was concluded that the presence of ThyX

provides growth benefits under certain conditions where the concentration of reduced folate derivatives is compromised.

The crystal structures of ThyX have been solved from *Thermotoga maritima*, *Paramecium bursaria* chlorella virus-1, *Mycobacterium tuberculosis*, and *Corynebacterium glutamicum* (*5-8*). All these ThyX forms consist of a tetramer of single polypeptides where each of the four FAD binding sites is formed at the juncture of three of the four subunits. Furthermore, the crystal structure of ThyX from

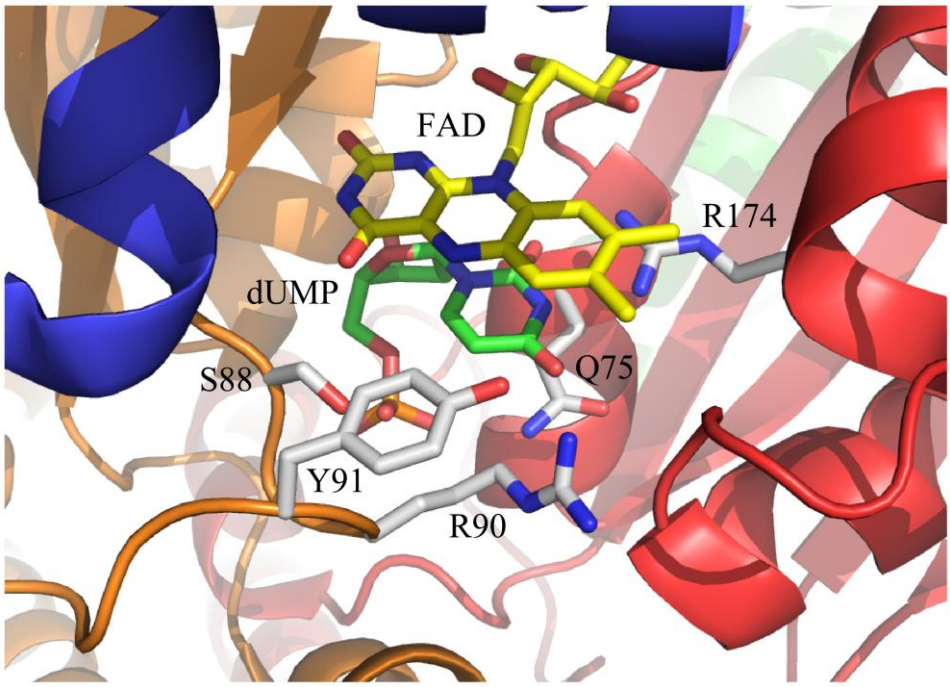

Figure 3-1. The Active Site of ThyX from T. maritima (pdb 1026). The crystal structure shows dUMP (green) bound in a polarized active site and stacks directly below the isollaxazine of the flavin (yellow). The subunits that make up the active site are colored differently to highlight the active site composed of three of the four subunits.

T. maritima in the presence of dUMP shows how dUMP binds in a pocket protected from solvent by a protein loop (residues 87-91) and by the isoalloxazine ring of the FAD

(Figure 3-1, (*5*)). The uracil ring of dUMP stacks against the isoalloxazine of FAD with its C6-position close to the N5 of the flavin. In the absence of dUMP, the deoxynucleotide binding site becomes disordered and acquires a different conformation.

The chemical mechanism of ThyA has been studied extensively for decades (*1*). The enzyme accomplishes several chemical tasks: activation of C5 of dUMP as a nucleophile by the Michael addition of a cysteine at C6; methylene transfer from CH_2THF to the nucleotide; and reduction of the methylene to methyl, to form dTMP, which is subsequently released from the enzyme adduct. Notably, ThyA uses the transiently formed THF to reduce the methylene group to form the methyl on the nucleotide, so that dihydrofolate is the folate product (1).

Although the mechanism of ThyX is not well understood, this reaction can be divided into two half reactions, the reductive and oxidative half-reaction. NADPH reduces the FAD of ThyX during the reductive half-reaction, while in the oxidative half-reaction, the reduced flavin is oxidized and dTMP is formed (*9*). The likely role of FAD in ThyX is to provide the reducing equivalents that ultimately lead to the reduction of the methylene (*10*). Several kinetic mechanisms have been postulated (summarized in (*11*)); however, data presented in this study show that the oxidative half-reaction is initiated by the addition of CH_2THF to the competent reduced ThyX•dUMP complex. Data from our laboratory suggest that the carbon-transfer step occurs prior to the redox reaction (*9*). We report here transient kinetic studies on ThyX from *T. maritima*. We propose that activation of dUMP does not require covalent catalysis, but instead, is caused by

polarizing the uracil moiety upon binding, consistent with previous data that suggested carbon transfer occurs before oxidation of the flavin (*9*).

EXPERIMENTAL PROCEDURES

Materials. dUMP, dTMP, sodium dithionite, EDTA, formaldehyde, and *L*-cysteine were purchased from Sigma Chemical Company. Dowex-1 was obtained from Bio-Rad. D_2O was from Cambridge Isotope Laboratory, Inc, and NaOD was from Aldrich. 6*R*-5,10-CH_2THF was kindly provided by Rudolf Moser from Merk-Eprova AG, Switzerland.

WT-ThyX from *Thermotoga maritima* (TM0449), and five variants containing the substitutions S88A, R90A, R174A, Q75A, and Y91A, were expressed with a His-tag in *E. coli* BL21 under the control of *L*-(+)-arabinose (*12*) and purified with a TALON metal affinity resin (Clontech) that uses Co^{2+}. ThyX was purified further by incubating at 65 ºC for 15 minutes followed by removal of the precipitate by cetrifugation for 10 min. at 14,000 rpms. Protocatechuate dioxygenase, purified from *Pseudomonas cepacia* DB01, was a gift from Professor David P. Ballou, University of Michigan (*13*). Prepurified dry argon and analytical mixtures of oxygen and nitrogen gases were from Matheson Coleman and Bell. Dry argon was passed through a column of OxiClear (LabClear) to remove traces of oxygen.

Transient Kinetics Monitored Through Absorbance. Stopped-flow kinetic studies were initiated by mixing reduced enzyme (14 μM) in the presence of saturating concentrations of either dUMP (300 μM) or CH_2THF (400 μM) with different concentrations of the other substrate. All concentrations reported for stopped-flow experiments are those after mixing. Anaerobic enzyme in a tonometer (with substrate present) was reduced by titrating with small aliquots of 6 mM sodium dithionite in 100 mM Tris-HCl buffer (pH 8.0). The reaction of the reduced enzyme•dUMP complex or the reduced WT-ThyX•CH_2THF complex with the other substrate was monitored at 25°C by following the absorbance of oxidized FAD at 420 nm with a photomultiplier detector or the diode-array mode using a Hi-Tech Scientific SF-61 DX2 double mixing stopped-flow spectrophotometer. All reactions were performed in 0.1 M Tris-HCl pH 8.0 with 1 mM EDTA and 15 mM H_2CO. As a control no reaction was observed between the reduced enzyme and H_2CO. The instrument was made anaerobic by flushing the system with an oxygen-scrubbing solution containing ~0.1 unit mL^{-1} protocatechuate dioxygenase (*13*) and 1 mM protocatechuate (3,4-dihydroxybenzoate) in 0.1 M KPi buffer (pH 7.0) and soaking overnight. The apparatus was thoroughly rinsed with anaerobic buffer prior use. Rate constants were calculated from exponential fits using Kinetic Studio (Hi-Tech Scientific), KaleidaGraph (Synergy Software, PA), KinTek Explorer, and Program A developed by Rong Chang, Chung-Yen Chiu, Joel Dinverno, and David Ballou, University of Michigan, which uses the Marquardt-Levenberg algorithm for fitting data to sums of exponentials (*14*). The reaction of R17A-ThyX•dUMP with CH_2THF was too slow to be observed by stopped-flow spectroscopy. Therefore, an anaerobic solution of R17A-thyX was reduced with one equivalent of dithionite in an anaerobic cuvette that

housed both dUMP (300 µM) and CH_2THF (400 µM) in separate side-arms. The solution dUMP was added to the reduced enzyme followed by CH_2THF to initiate the reaction. The reaction was monitored with a scanning spectrophotometer and the reaction trace at 420 nm was fit to single exponential.

The pH Dependence of the Oxidative Half-Reaction. The oxidative half-reaction of WT-ThyX was studied over a range of pH (6-10). WT-ThyX was exchanged into the appropriate buffer (pH 6 – 7.5, the buffer was 0.1 M KPi; for pH 7.5 – 9 the buffer was 0.1 M Tris-HCl; and for pH 9 – 10 the buffer was 0.1 M glycine) using an Econo-Pac 10DC disposable desalting column (Bio-Rad). For each pH used, an anaerobic solution of WT-ThyX (14 µM) was reduced with one equivalent of dithionite followed by the addition of dUMP (400 µM). The reduced WT-ThyX•dUMP complex was mixed with various concentrations of CH_2THF (100, 200, 400, 800 µM) using a stopped-flow spectrophotometer. The reaction was monitored at 420 nm and reaction traces were fit to a sum of exponentials to determine the limiting rate constants. The limiting rate constants were plotted versus pH and were fit to equation 1, for the first phase, and equation 2, for the second phase, to determine the pKa values.

$$k_{ox} = \frac{k_{ox,\lim}}{1+10^{pH-pKa}} \qquad (1)$$

$$k_{ox} = \frac{k_{ox,\lim}}{1+10^{0.5(pH-pKa)}} \qquad (2)$$

The Oxidative Half-Reaction of WT-ThyX with the Substrate Analogue 5-dUMPS. The reaction of the phosphorothioate analogue of dUMP (5-dUMPS) in the oxidative half-reaction of WT-ThyX was carried out using a stopped-flow spectrophotometer. A solution of anaerobic WT-ThyX (14 μM) in the presence of 5-dUMPS (400 μM) was reduced with one equivalent of dithionite. The reduced WT-ThyX-5-dUMPS complex was mixed with a saturating concentration of CH_2THF (400 μM) and monitored at 420 nm. The reaction traces were fit to a sum of exponentials using KaleidaGraph.

Oxidative Half-Reaction of Reconstituted 5-deaza-FAD-WT-ThyX. FAD from WT-ThyX was removed from the protein using previous published methods (*5*). Apo-WT-ThyX was reconstituted with an equivalent of 5-deaza-FAD. The reconstituted 5-deaza-FAD-WT-ThyX was reduced with a 6-fold excess of NADPH and reduction of enzyme was monitored using a scanning spectrophotometer to ensure complete reduction. Excess NADPH was removed using a desalting column. A solution of dUMP (300 μM) was added to the reduced 5-deaza-FAD-WT-ThyX (20 μM) followed by the addition of CH_2THF (300 μM) to initiate the oxidative half-reaction, which was monitored using a scanning spectrophotometer. Alternatively, the reduced 5-deaza-FAD-WT-ThyX (14 μM) with bound dUMP (300 μM) was mixed with various concentrations of CH_2THF (100, 200, 400, and 800 μM) using a stopped-flow spectrophotometer. The reaction was monitored at 408 nm and reaction traces were fit to single exponentials. The Oxidative half-reaction was carried out in 0.1 M Tris-HCl at pH 8.0 with 1 mM EDTA and 15 mM H_2CO at 25 ^oC.

Formation of the WT-ThyX•5F-dUMP•CH_2THF Complex. An anaerobic solution of WT-ThyX (87 µM) in an anaerobic cuvette, in the presence of both 5F-dUMP (300 µM) and CH_2THF (400 µM), was reduced with one equivalent of dithionite. 5F-dUMP was added to the reduced WT-ThyX. A solution of CH_2THF was then added to the WT-ThyX•dUMP complex. The complex formations were observed using a scanning spectrophotometer and performed in 0.1 M Tris pH 8.0 with 1 mM EDTA and 15 mM H_2CO at 25 ºC.

Acid Quenching. Rapid quench-flow experiments were initiated by mixing reduced WT-ThyX (50 µM) in the presence of dUMP (300 µM) with 400 µM CH_2THF under anaerobic conditions using a Hi-Tech Scientific SF-61 DX2 double mixing stopped-flow spectrophotometer equipped with a qPOD prototype cell especially designed for quenching (TgK Scientific). Concentrations are those after the first mix. Anaerobic enzyme in a tonometer (with dUMP present) was reduced as stated above. Oxygen contamination was prevented by including in the tonometer the PCA (50 µM)/PCD system. The reaction of reduced ThyX•dUMP complex with CH_2THF was quenched with 1 M HCl at different age times (0.045 – 199.96 s). The quenched reactions (80 µL) were collected by flushing the cell with 500 µL of anaerobic buffer.

HPLC analysis. The pH of the acid-quenched samples (580 µL) was adjusted to 7.0 with 6 µL of 2.5 M NaOH. The solution was spun in a microcentrifuge and the supernatant was filtered with millex-GV filter units. The pellet (denatured enzyme) was

stored at -80°C until further analysis. Pellets were digested with trypsin and analyzed by the Biomedical Mass Spectroscopy Facility by MADLI-TOF. A volume of 25 µL for each filtrate was injected into a WATERS HPLC system controlled by the EmpowerPro software and analyzed using a WATERS C-18 Symmetry column (3.9x150 mm) with 5 µm pore size under 200 mM triethylammonium bicarbonate (pH 7.0) . The HPLC system included: Alltech on-line degassing system, WATERS 717plus auto sampler, WATERS 600 pump, and WATERS 490E detector. The chromatograms showed many peaks corresponding to dTMP, dUMP, and acid-degraded folates (e.g., CH_2THF, THF); the elution time for the peaks was dependent on pH. The peaks for dUMP and dTMP at pH 7.0 eluted at 7.34 and 15.0 min, respectively. The assignment of the dUMP and dTMP peaks was confirmed by co-injecting standards. Concentrations of dUMP and dTMP were determined from standard curves of peak area as a function of nucleotide concentration. The concentration of dUMP consumed or dTMP produced in reactions was plotted *vs*. time and the kinetic traces were fit to a single exponential using KaleidaGraph.

Confirmation of dTMP Synthesis by Mutant Enzymes by HPLC. An anaerobic solution of mutant enzyme (~25 µM) was reduced with one equivlalent of dithionite in an anaerobic cuvette. An anaerobic solution of dUMP (500 µM) was added from a side-arm followed by the addition of CH_2THF (500 µM) from a second side arm to initiate the oxidative half-reaction. The reaction was monitored until completion by absorbance. The enzyme was removed using a 10,000 MWCO (molecular weight cutoff filter) microcentrifugal spin filter (Millipore) and 10 µL of the flow-through was injected on a

Shimadzu HPLC fitted with a 3.9 x 150 mm, 5 µm Symmetry C18 column (Waters). dTMP was eluted at 5.3 min under isocratic conditions at 1 ml/min with 200 mM ammonium phosphate pH 5.0.

RESULTS

Transient Kinetics Monitored Through Absorbance. The oxidative half-reaction of WT-ThyX in the presence of saturating dUMP or CH_2THF was studied using a stopped-flow spectrophotometer. The reaction was observed with an initial small decrease, followed by a large increase due to oxidation (Figure 3-2A). While we observed the initial small decrease at 450 nm this decrease in absorbance was largest at 420 nm, so this wavelength was chosen for our single-wavelength data collection. The reaction of the reduced WT-ThyX•dUMP with CH_2THF is faster than the reaction of the reduced WT-ThyX•CH_2THF complex with dUMP, suggesting a preference for the WT-ThyX•dUMP complex (Figure 3-2). If the reduced WT-ThyX•dUMP complex must form prior to CH_2THF binding, then the reaction of the reduced ThyX•CH_2THF complex with dUMP would require the dissociation of CH_2THF from the reduced enzyme as the initial step (Figure 3-4)

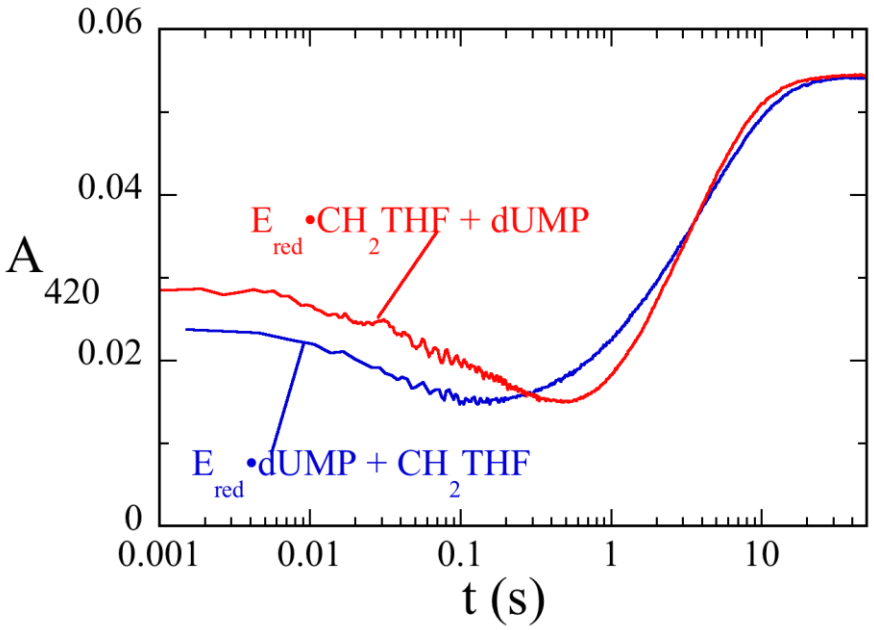

Figure 3-2. ***Comparison of Absorbance Traces of the Oxidative Half-Reaction at 420 nm.*** The reaction of the reduced WT-ThyX•dUMP complex with 400 µM CH_2THF is shown in the red trace. The reaction of the reduced WT-ThyX•CH_2THF complex with 300 µM dUMP is shown in the blue trace. The reactions were studied by stopped-flow spectroscopy in 0.1 M Tris-HCl (pH 8.0) with 1 mM EDTA and 15 mM H_2CO at 25 ºC..

The reaction of the reduced WT-ThyX•CH_2THF complex with various concentrations of dUMP (0.1, 0.4, 0.8, 1.6, 3.2, and 6.4 mM) was followed at 420 nm using a stopped-flow spectrophotometer. The kinetics can be described with two phases (Figure 3-3A). The fast phase, the initial decrease in absorbance, is hyperbolically dependent on dUMP concentration with a limiting rate constant of 5.6 s^{-1} with a non zero intercept of 0.86 s^{-1} and half-saturating concentration of 2.1 mM (Figure 3-3B) this is consistent with the mechanism in Figure 3-4. The second phase, corresponding to flavin oxidation, was hyperbolically dependent on dUMP concentration with a saturating rate constant equal to 0.28 s^{-1} and a half-saturating concentration of dUMP of 39.7 µM (Figure 3-3C). The comparison of the oxidation half-reaction starting with the reduced ThyX•dUMP complex and the reduced WT-ThyX•CH_2THF complex (Figure 3-2), suggests the preference for the reduced WT-

ThyX•dUMP as the initial starting complex. Although, the overall k_2 is essentially unaffected at high concentrations of dUMP. The reaction of the reduced ThyX•CH_2THF complex with dUMP would require the dissociation of CH_2THF from the reduced enzyme as the initial step. The reduced WT-ThyX binds dUMP and the reaction is initiated by CH_2THF (Figure 3-4). This is consistent with the hyperbolic dependence, with a non-zero intercept, for the first phase, which suggests at least two steps occur prior to oxidation of the enzyme.

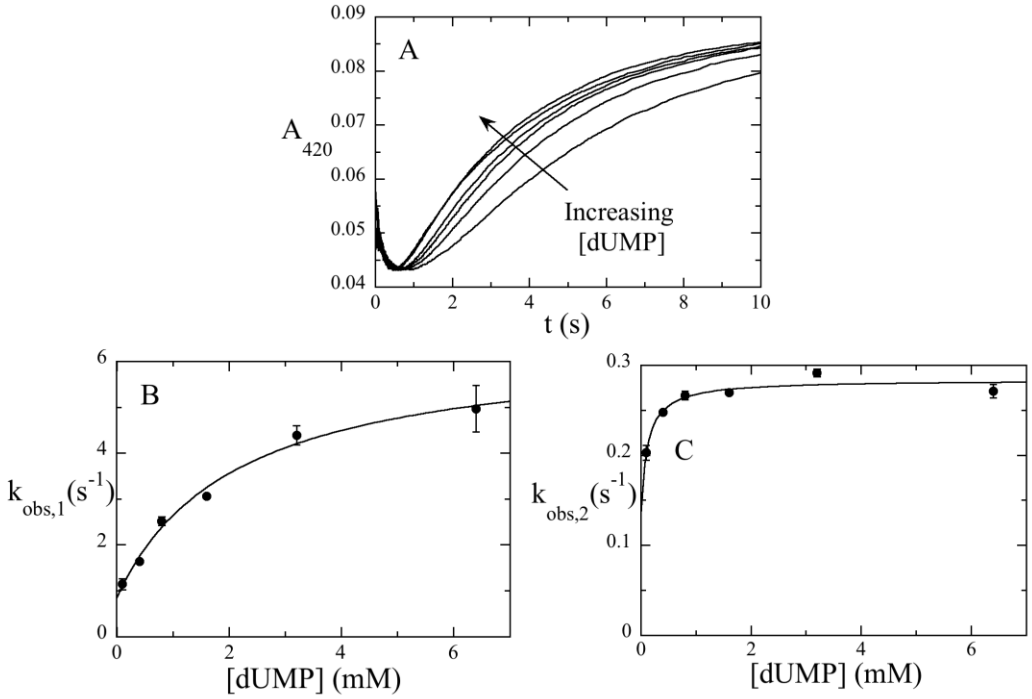

Figure 3-3. ***The Reaction of the Reduced WT-ThyX•CH_2THF Complex with dUMP.*** *Reaction of the reduced WT-ThyX•CH_2THF complex with dUMP.* A) Kinetic traces at 420 nm from the reaction of the reduced WT-ThyX (14 µM) with bound CH_2THF (400 µM) with various concentrations of dUMP (0.1, 0.4, 0.8, 1.6, 3.2, and 6.4 mM). B) The observed rate constants for the initial decrease in absorbance were plotted versus dUMP concentration. The limiting rate constant was 5.6 s^{-1} with a half-saturating concentration of 2.1 mM and a non-zero intercept of 0.86 s^{-1}. C) The observed rate constants for the second phase were plotted versus dUMP concentration and fit to hyperbola with a limiting rate constant of 0.2 s^{-1} and a half-saturation concentration of 39 µM. The reaction was performed by stopped-flow spectroscopy in 0.1 mM Tris-HCl (pH 8.0) with 1 mM EDTA and 15 mM H_2CO at 25 ºC

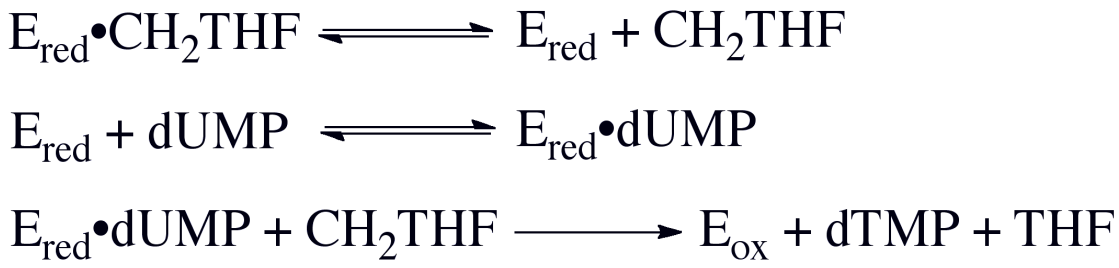

Figure 3-4: ***A Model Describing the Reaction of the Reduced WT-ThyX•CH_2THF complex with dUMP.***

The reaction of the reduced WT-ThyX•dUMP complex with different concentrations of CH_2THF (100, 200, 400, and 800 μM) was followed at 25 ºC in diode array and single wavelength modes. The reaction was observed as a fast decrease in absorbance followed by a large slower increase in absorbance (Figure 3-5A). The initial decrease in absorbance can be fit to a single exponential and is independent of CH_2THF concentration with a limiting rate constant of 28.4 s^{-1} (Figure 3-5B). A concentration-independent first step suggests that binding of CH_2THF is fast and occurs within the dead time of the instrument (1.6 ms) and therefore sets a limit of < 20 μM for the dissociation constant of CH_2THF with the reduced WT-ThyX•dUMP complex. The second phase is also independent of CH_2THF concentration, having limiting rate constant of 0.2 s^{-1} (Figure 3-5B).

The absorbance spectrum of the intermediate was deconvoluted by singular-value decomposition from diode-array data (Figure 3-6A and 3-6B). The spectrum calculated for the reduced WT-ThyX•dUMP•CH_2THF complex is different from that of the reduced WT-ThyX•dUMP complex. A small spectral change was then observed. The

spectrum of the intermediate is similar to anionic flavin, which requires deprotonation at N1 of the flavin (*15*). However, this is inconsistent with the pH dependence showing an increased rate constant at low pH (see below). Isoalloxazine spectra are sensitive to the environment of the chromophore, but not in a rigorously understood way. Therefore reason for this spectral change remains unknown.

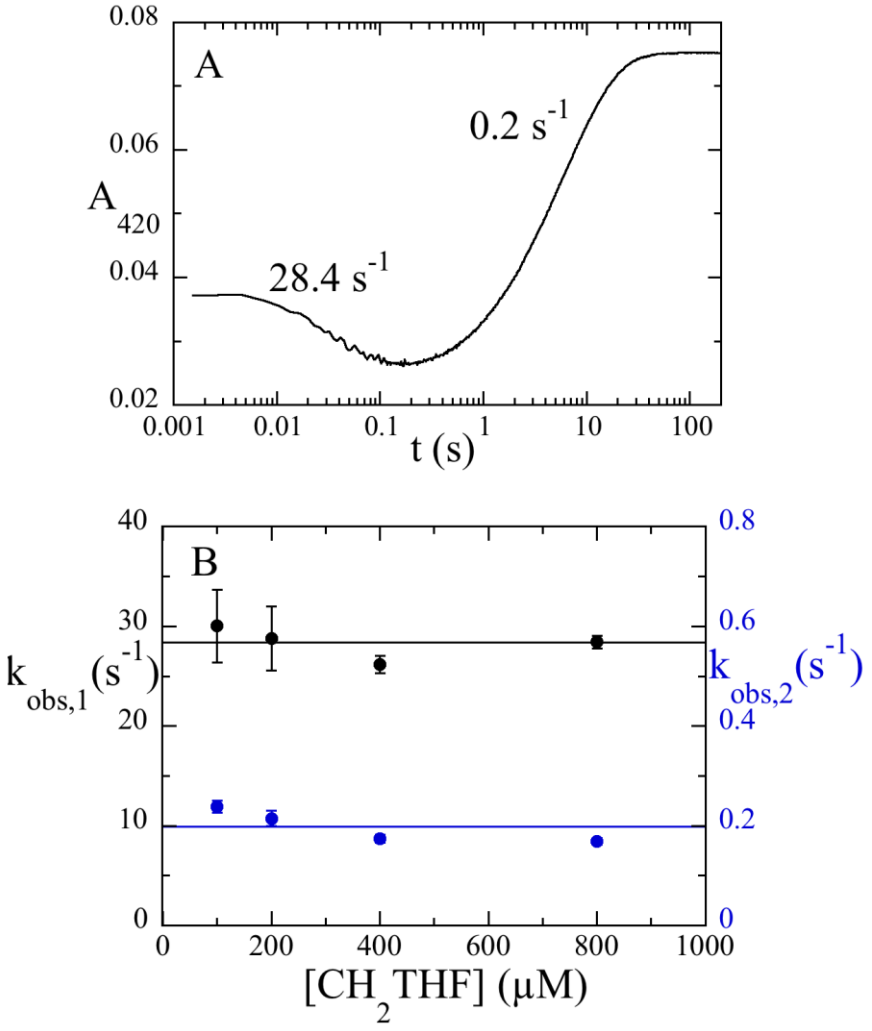

Figure 3-5. ***The Reaction of the Reduced WT-ThyX•dUMP with CH_2THF.*** The reduced WT-ThyX (14 μM) with dUMP bound (300 μM) was mixed with various concentrations of CH_2THF (100, 200, 400, or 800 μM) using a stopped-flow spectrophotometer. The reaction was carried out in 0.1 M Tris-HCl (pH 8.0) with 1 mM EDTA and 15 mM H_2CO

at 25 ºC. A) A kinetic trace from the oxidative half-reaction at 420 nm. B) The observed rate constants for both phases were plotted as a function of CH_2THF concentrations and both fit to a line. The rate constants for the first and second phase were 28.4 s^{-1} and 0.2 s^{-1}, respectively.

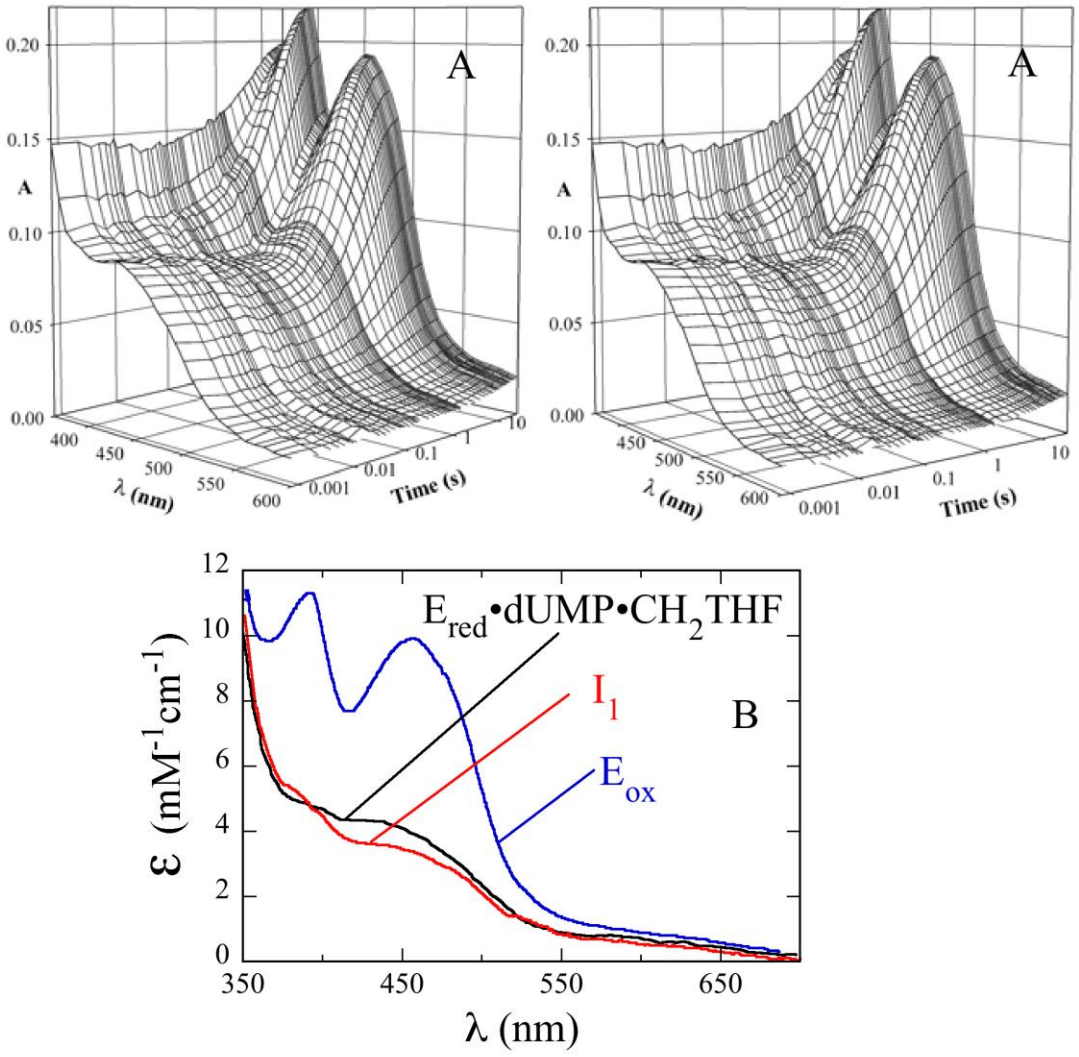

Figure 3-6. ***The Intermediates of the Oxidative Half-Reaction.*** The reaction of the reduced WT-ThyX (14 µM) with bound dUMP (300 µM) was mixed with 400 µM CH_2THF using a stopped-flow spectrophotometer in diode array mode. A) A stereo view of the oxidative half-reaction in diode array mode. B) The deconvoluted intermediate spectra from the reaction of reduced WT-ThyX•dUMP complex with CH_2THF using diode array and fitting the reaction to the rate constants of 28.4 s^{-1} and 0.2 s^{-1}.

Figure 3-7: ***A Model for the Reaction of the Reduced Enzyme•dUMP Complex with CH_2THF.***

Acid Quenching. The reaction of the reduced WT-ThyX•dUMP complex with 400 μM CH_2THF was quenched with acid at a series of delay times as described under Experimental Procedures. Analysis of HPLC chromatograms of the quenched reactions show a single exponential decay for dUMP with an observed rate constant equal to 0.7 s^{-1}, and a single exponential rise for dTMP with an observed rate constant of 0.15 s^{-1} (Figure 3-8A). Correlation of the concentration of dUMP and dTMP detected by HPLC analysis with the corresponding absorbance trace at 420 nm indicates that dUMP consumption takes place after the initial small decrease in absorbance at 420 nm, and production of dTMP occurs with a concomitant increase of absorbance at 420 nm, corresponding to the first phase of FAD oxidation. The rate constants for the loss of dUMP and the formation of dTMP suggests an intermediate, different from that observed by stopped-flow spectroscopy, having a maximum formation at 2.6 s (Figure 3-8B). Data from both stopped-flow spectroscopy and quenching reactions are interpreted in Figure 3-9. Mass spectrometry was used to detect any protein adduct formed from the quenched

reaction; however, no change in molecular weight was observed, suggesting that the quenching did not cause the accumulation of significant protein adducts.

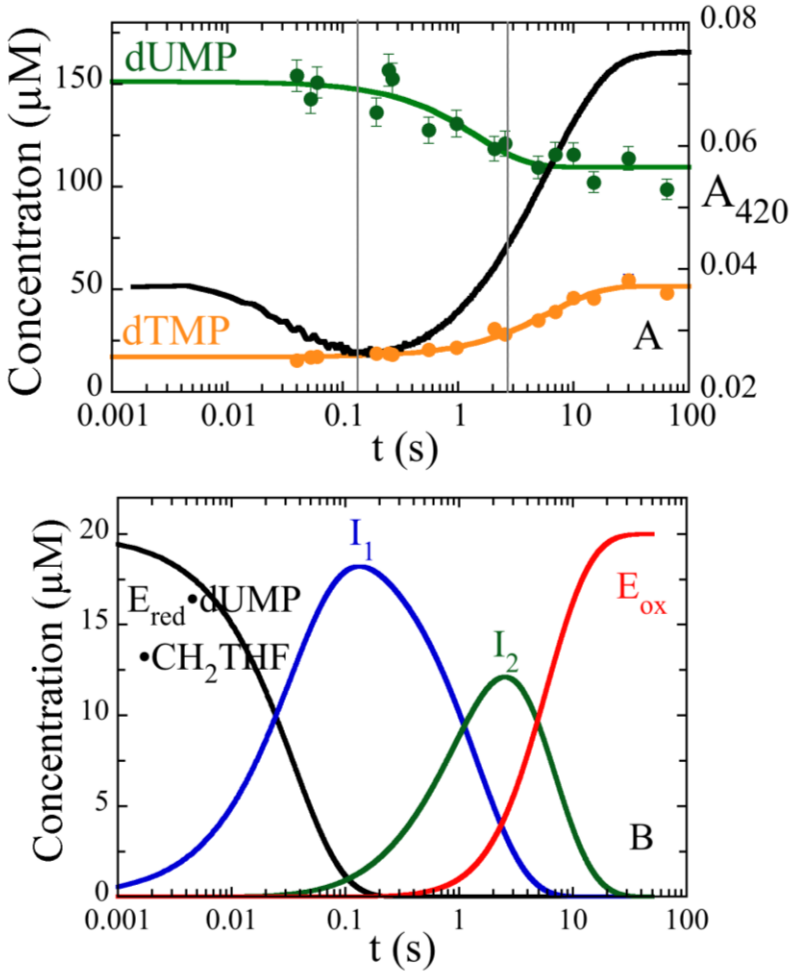

Figure 3-8. ***The Oxidative Half-Reaction of WT-ThyX.*** A) Reduced WT-ThyX (50 μM) with bound dUMP (300 μM) was mixed with 400 μM CH_2THF. The reaction was quenched with acid at different times, and the concentrations of dUMP (green trace) and dTMP (orange trace) were calculated from the area under the peaks of HPLC chromatograms. The reduced WT-ThyX (14 μM) with bound dUMP (300 μM) was mixed 400 μM CH_2THF using a stopped-flow spectrophotometer and the reaction was monitored at 420 nm (black trace). The vertical lines at 0.13 s and 2.6 s highlight the time of maximum accumulation of both intermediates I_1 and I_2. B) The accumulation of intermediates formed during the oxidative half-reaction is shown in the bottom panel. The rate constants from the oxidative half-reaction, 28.4 s^{-1} and 0.2 s^{-1}, and the rate constant from the loss of dUMP, 0.7 s^{-1}, observed by quenching, were used to simulate the formation of the two intermediates. The simulation used an enzyme concentration of 20 μM and shows that intermediates accumulate maximally at 0.13 s and 2.6 s.

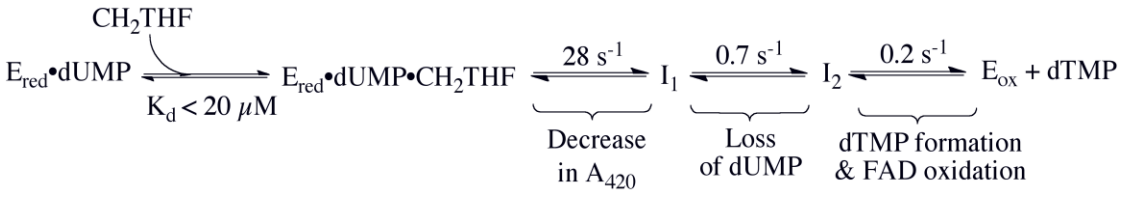

Figure 3-9. ***The Kinetic Mechanism of the Oxidative Half-Reaction of ThyX from T. maritima.***

The Oxidative Half-Reaction of WT-ThyX with the Substrate Analogue 5-dUMPS. The importance of the phosphate moiety of dUMP during the oxidative half-reactions was examined using a phosphorothioate analogue of dUMP (5-dUMPS). The sulfur atom of the analog is more nucleophilic than the oxygen it replaces and also disperses the negative charge compared to the concentrated charge o the small, more electronegative oxygen. The reaction of the reduced WT-ThyX•5-dUMPS complex with a saturating concentration of CH_2THF (400 μM) was monitored at 420 nm using a stopped-flow spectrophotometer (Figure 3-10). The reaction was similar to the reaction with WT-ThyX•dUMP, an initial decrease followed by a large increase in absorbance. The reaction could be fit to a sum of two exponentials with a rate constant for first phase of 3 s^{-1} and a rate constant for the second phase of 0.08 s^{-1}, 9-fold and 2.5-fold less than the rate constants for WT, respectively. The production of the phosphorothioate analogue of dTMP was confirmed by HPLC. These data suggest that the reaction is favored by the more concentrated negative charge of oxygen rather than the more nucleophilic sulfur.

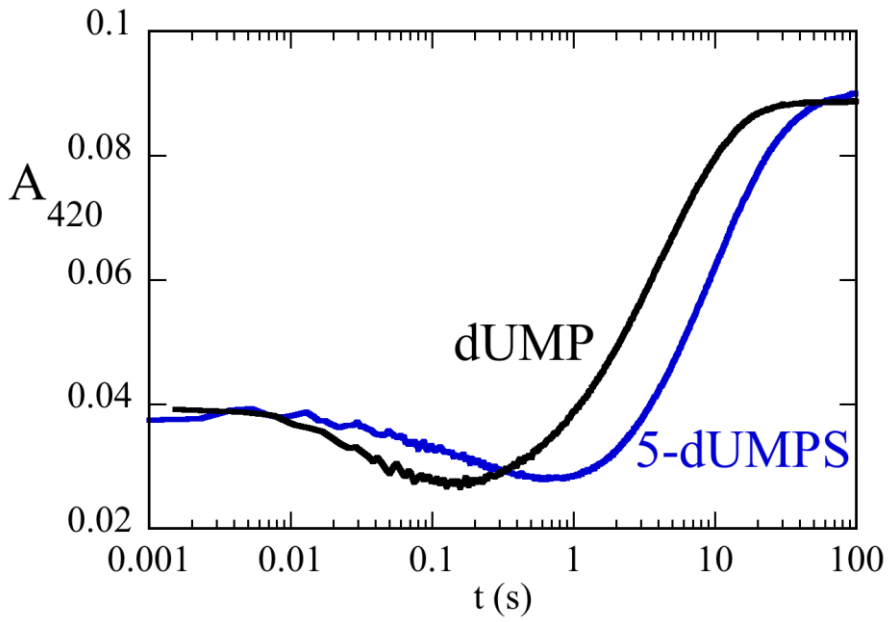

Figure 3-10. ***The Reaction of Reduced WT-ThyX•dUMPS with CH_2THF.*** The oxidative half-reaction of WT-ThyX was studied with a phosphothioate analogue of dUMP as substrate. Reduced WT-ThyX (14 µM) bound with dUMP (black trace) or with dUMPS (blue trace) was mixed with 400 µM CH_2THF using a stopped-flow spectrophotometer. The reactions were carried out in 0.1 M Tris-HCl (pH 8.0) with 1 mM EDTA and 15 mM H_2CO at 25 ºC.

The pH Dependence on the Oxidative Half-Reaction. The reaction of the reduced WT-ThyX•dUMP complex with CH_2THF was also examined over a range of pH values (6-10). The pH range was limited by the stability of the enzyme. The reaction traces at all pH values were qualitatively similar to those observed at pH 8.0, with a small decrease followed by a large increase in absorbance at 420 nm (Figure 3-11A). The rate constants for both phases increased with decreasing pH. The rate constants for the initial phase was fit to Equation 1, giving a limiting rate constant of 61.5 s^{-1} and a pKa value of 8.3 (Figure 3-11B). Opening of the ring of CH2THF to form the iminium ion would require the protonation of N10 (1); thus we ascribe the first observed rate constant to this

process. Curiously, the second phase could not be fit using Equation 1, which assumes the ionization of one proton. Instead, the plot of the logarithm of the rate constant as a

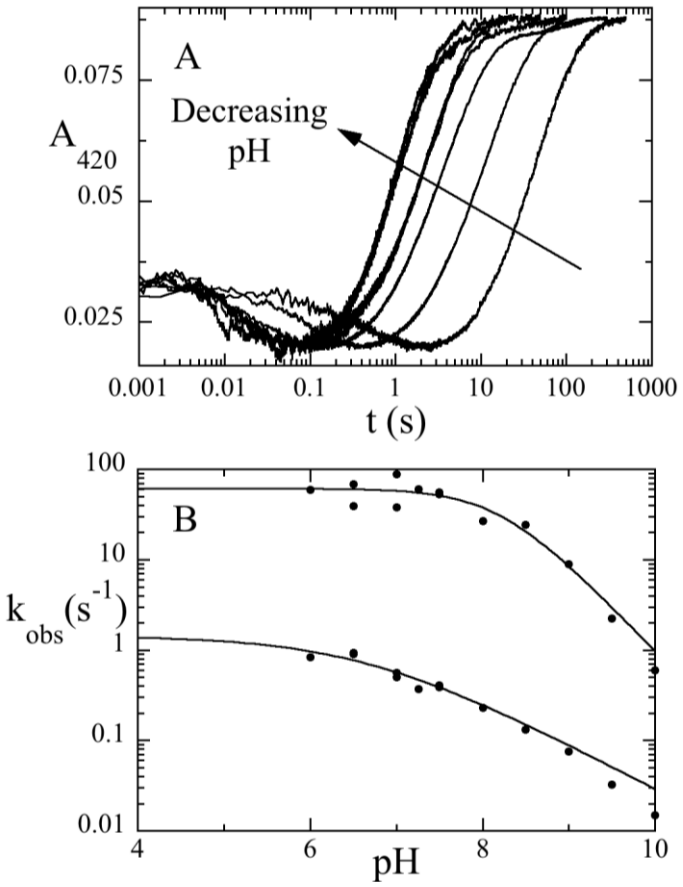

Figure 3-11. ***The pH Dependence of the Oxidative Half-Reaction***. The oxidative half-reaction of WT-ThyX at various pH values (6 - 10). A) Absorbance traces at 420 nm from the reaction of the reduced WT-ThyX•dUMP complex with CH_2THF at various pH values. B) The relationship between pH and observed rate constants for both phases. The limiting rate constants for the first phase were plotted versus pH and fit to Equation 1, giving a limiting rate constant of 62 s^{-1} and a pK_a value of 8.2. The limiting rate constants for second phase were plotted versus pH and fit to Equation 2 giving a limiting rate constant of 1.4 s^{-1} and a pK_a value of 6.6.

function of pH at pH values above the plateau appears to have a slope of 0.5. Empirically, this fits Equation 2, giving a limiting rate constant at low pH of 1.4 s^{-1} and pK_a value of 6.6 (Figure 3-11). The elimination of THF from the methylene bridging complex would be

assisted by the protonation of N5 of THF (1). The reason for the apparent slope of 0.5 is not yet clear. It could indicate a pKa at pH value slightly higher than maximum allowed by enzyme stability, perturbing the dependence in the accessible range; further work will be needed to clarify this.

Oxidative Half-Reaction of Reconstituted 5-deaza-FAD-WT-ThyX. The structure shows that N5 of FAD in a position to activate dUMP by nucleophilic attack on C6 (Figure 3-1). UDP-galactopyranose mutase was proposed to use reduced FAD as a nucleophile (16); that possible role was tested in ThyX. The FAD bound to WT-ThyX was replaced with 5-deaza-FAD, which, when reduced, does not have a lone pair of electrons at the 5-position for a nucleophilic attack on dUMP. An anaerobic solution of the reduced 5-deaza-FAD-WT-ThyX•dUMP complex was mixed with CH_2THF using either a stopped-flow spectrophotometer or by manually mixing using a scanning spectrophotometer (Figure 3-12A and 3-12B). The reaction was followed at 408 nm and could be fit to a single exponential with a limiting rate constant of 0.02 s^{-1} (Figure 3-12A). The formation of dTMP still occurs and oxidation of the enzyme was only 10-fold slower than with FAD.

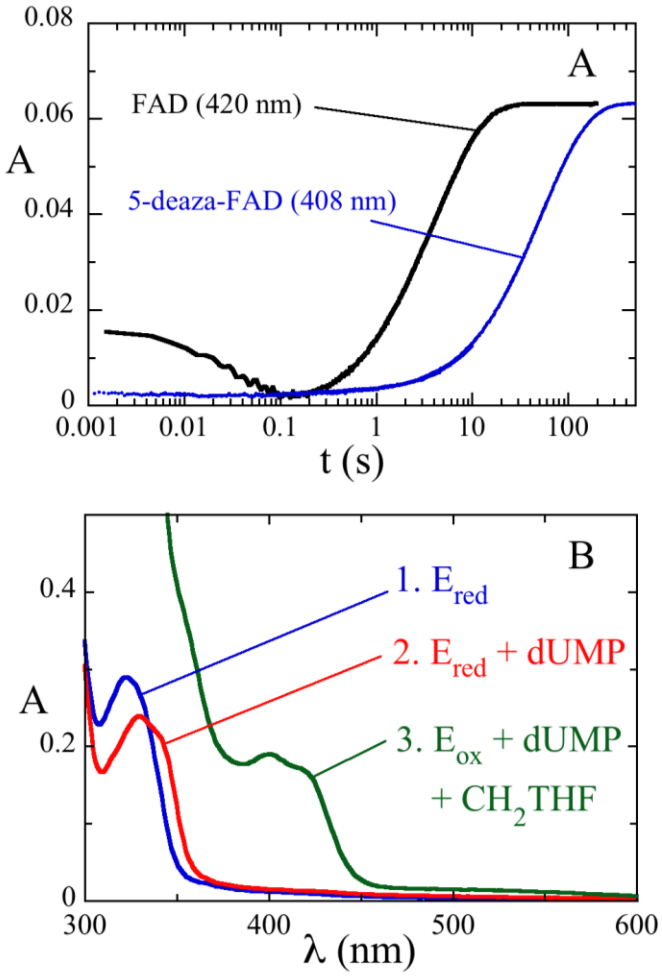

Figure 3-12. ***The Reaction of the Reduced 5-deaza-FAD-WT-ThyX•dUMP Complex with CH_2THF.*** A) The reaction of the reduced WT-ThyX•dUMP complex (420 nm, black trace) or the reduced 5-deaza-FAD-WT-ThyX•dUMP complex (408 nm, blue trace) with 400 µM CH_2THF. The reactions were carried out by stopped-flow spectroscopy. B) The spectrum of the reduced 5-deaza-FAD-WT-ThyX is shown in blue. The spectrum of the reduced 5-deaza-FAD-WT-ThyX•dUMP complex is shown in red. The final absorbance spectrum obtained after the reaction of the reduced 5-deaza-FAD-WT-ThyX•dUMP with CH_2THF is shown in green. Reactions were carried out in 0.1 M Tris-HCl (pH 8.0) with 1 mM EDTA and 15 mM H_2CO at 25 ºC using a stopped-flow spectrophotometer.

Formation of the WT-ThyX•5F-dUMP•CH_2THF Complex. The fluorouracil moiety of 5F-dUMP can be reduced, but not dehalogenated which prevents C-C bond

scission between the 5-methylene adduct of dUMP and THF (*1*). Therefore 5F-dUMP is useful for probing the relative timing of flavin oxidation and carbon transfer. Reduced WT-ThyX was incubated with 5F-dUMP and CH_2THF and monitored over time using a scanning spectrophotometer. Spectral changes associated with the binding of both 5F-dUMP and CH_2THF were observed (Figure 3-13), but not flavin oxidation, suggesting that the fluorine substituent blocks the reaction pathway at a step prior to redox chemistry.

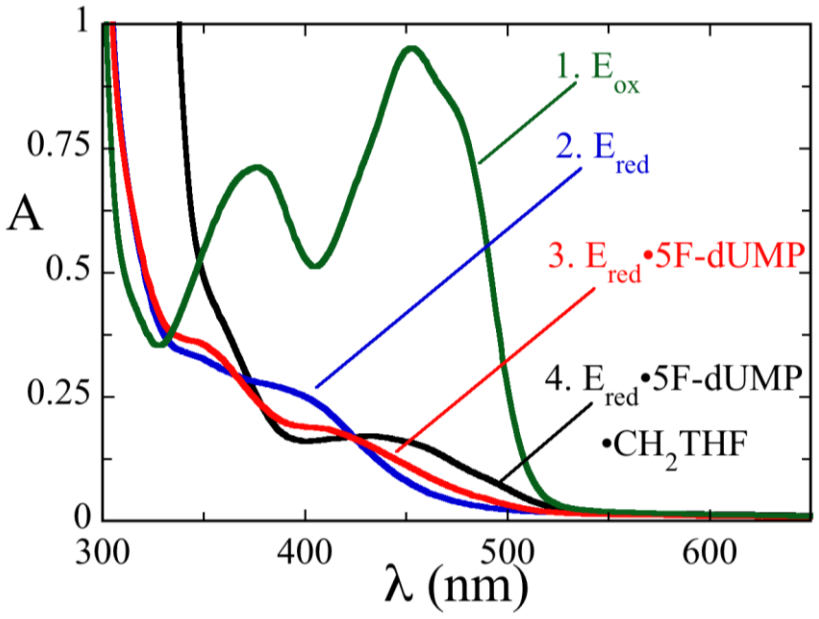

Figure 3-13. ***Formation of the Reduced WT-ThyX•5F-dUMP•CH₂THF Complex***. An anaerobic solution of WT-ThyX (87 µM green spectrum) was reduced (blue spectrum) with one equivalent of dithionite. An anaerobic solution of 5F-dUMP (300 µM) was added to form the reduced WT-ThyX•5F-dUMP complex (red spectrum). The addition of an anaerobic solution of CH_2THF (400 µM) formed the reduced WT-ThyX•5F-dUMP•CH_2THF complex (black spectrum). The spectra were recorded using a scanning spectrophotometer.

Transient Kinetics of Variant Enzymes Monitored Through Absorbance. The crystal structure of *T. maritima* ThyX (Figure 1) shows that dUMP makes several contacts in the active site (*5*). In order to investigate the role of these active site residues they were replaced by alanine and their effects on the oxidative half-reaction were determined. All variant enzymes synthesized dTMP, as detected by HPLC. The reaction of the reduced enzyme•dUMP complex with CH_2THF was studied for each variant using a stopped-flow spectrophotometer (Table 3-1). Except for R174A, all reactions showed an initial decrease followed by a large increase in absorbance at 420 nm. The residue R174 hydrogen bonds to dUMP at N3 and at the C4 oxygen, potentially, stabilizing the build-up of the negative charge at C5 and correctly positioning the uracil moiety above the isoalloxazine of the flavin. Substituting R174 by alanine caused a drastic effect on the oxidative half-reaction. Only one phase, a large increase in absorbance, was observed and had a rate constant of 6.8×10^{-5} s^{-1}, ~400,000-fold slower than the second phase of the WT reaction. The loss of the initial phase and the drastic decrease in rate constant suggest that a reaction before flavin oxidation has become rate-limiting. The residue R90, which also hydrogen bonds to the C4 oxygen of dUMP, could stabilize a buildup of negative charge at the C4 oxygen. The oxidative half-reaction of the R90A variant enzyme shows a greater effect on the first phase compared to the second, 86-fold and 7.6-fold, respectively. The residues Q75 and S88 are in hydrogen bonding distance to the phosphate oxygen of dUMP, 2.9 Å and 2.6 Å, respectively. Substitutions of these residues showed rate constants that were less by 13-fold - 35-fold on the first phase and by 2.7-fold – 3.3-fold on the second phase compared to the WT reaction. The residue Y91 is 4.6 Å away from N5 of the flavin. The Y91A variant also had a greater effect on

the first phase than on the second phase, 53-fold and 28-fold slower, respectively, than the WT reaction.

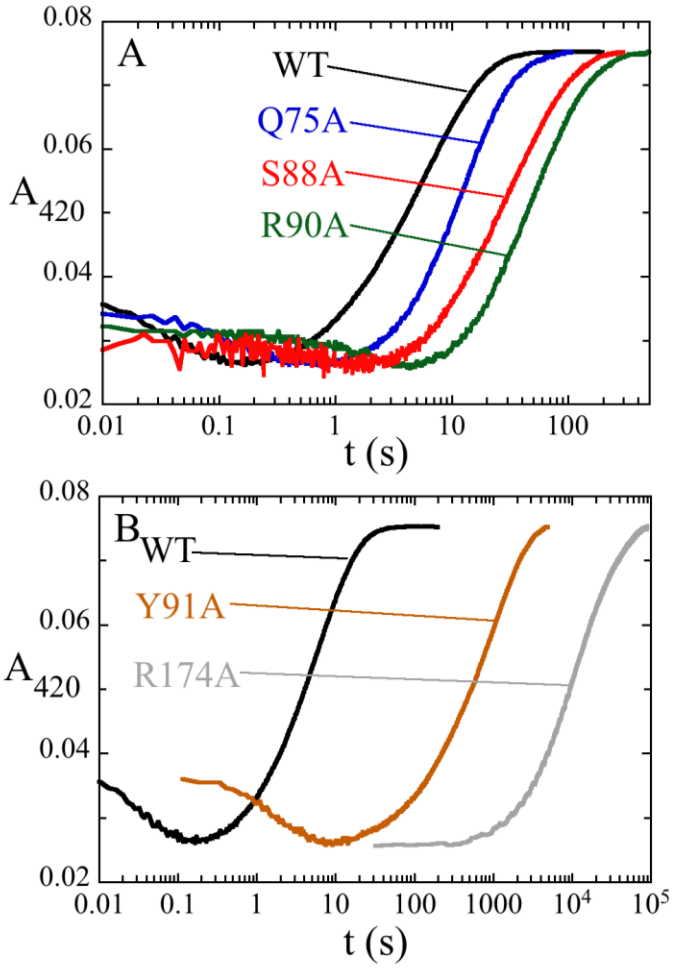

Figure 3-14. ***The Oxidative Half-Reaction of Mutant Enzymes.*** The reduced mutant enzyme•dUMP complexes were mixed with saturating concentrations CH_2THF using a stopped-flow spectrophotometer. The reactions were monitored at 420 nm. The reactions were performed in 0.1 M Tris-HCl (pH 8.0) with 1 mM EDTA and 15 mM H_2CO at 25 ^oC.

Table 3-1. Comparison of the Oxidative Half-Reaction Rate Constants[a]			
Enzyme	k_1 (s^{-1})	k_2 (s^{-1})	k_3 (s^{-1})[b]
WT	28.4 ± 0.8	0.20 ± 0.01	-
Q75A	2.2 ± 0.3	0.074 ± 0.002	0.003 ± 0.0005
R90A	0.33± 0.01	0.026 ± 0.01	-
R174A	6.8 x 10^{-5} ± 1.6 x	-	-
Y91A	0.53 ± 0.04	0.007 ± 0.0001	0.001 ± 0.0002
S88A	0.82 ± 0.05	0.06 ± 0.002	0.019 ± 0.0005

[a]An anaerobic solution of reduced enzyme (14 µM) with dUMP (400 µM) was mixed with various concentrations of CH_2THF (100, 200, 400, and 800 µM) using a stopped-flow spectrophotometer. The reactions were monitored at 420 nm and the traces were fit to a sum of exponentials. Reactions were carried out in 0.1 M Tris-HCl at pH 8.0 with 1 mM EDTA and 15 mM H_2CO at 25 ºC.

[b]The reaction traces required a third exponential to fit a small increase in absorbance at the end of the reaction.

DISCUSSION

The kinetic and chemical mechanisms of the flavin-dependent ThyX have generated interest recently, both in order to learn how they differ from those of the classic enzyme ThyA, and to learn how these differences may be exploited for design of inhibitors to treat of infections caused by the numerous pathogens that rely on ThyX. All TSs must accomplish the same chemical tasks: activation of both dUMP and CH_2THF followed by transfer of the methylene from CH_2THF to dUMP and its subsequent reduction. However, ThyX is unrelated to ThyA both in either sequence or structure, and accomplishes its chemistry using pyridine nucleotide as an electron source and FAD as a prosthetic group. ThyX, therefore, has distributed the chemistry to additional reactive species that could be the object of drug candidates.

A major question is how dUMP becomes activated. In order to attack the iminium of CH_2THF, the nucleophilicity of C5 of dUMP must be increased. In the classic

thymidylate synthase, including ThyA and the bifunctional TS-DHFR (*1, 3*), the enzymes use an active site cysteine to activate dUMP through a Michael addition at C6. There is no cysteine in the active site of *T. maritima* ThyX. The only conceivable nucleophilic residue is an active site serine (*16*). We substituted this serine residue, S88 in *T. maritima* ThyX, with an alanine to eliminate the putative nucleophile and activation of dUMP. This should have a drastic effect on the oxidative half-reaction. However, the S88A variant was still active (*10*). In fact, the oxidative half-reaction was similar to that of WT-ThyX. Both phases were only slightly slower than those of WT-ThyX, verifying that S88 is not a critical nucleophile (Figure 3-14A).

Conceivably, water could act as a nucleophile. However activation of the water molecule by deprotonation would be required. However, the active site contains no residues or metals that could activate water, and the pH dependence on the oxidative half-reaction shows that the rate constants for both observable phases are greater at low pH (Figure 3-11). We can conclude that water is not the nucleophile because if it were, the rate constants should have increased at high pH. The phosphate of dUMP could also be considered as a nucleophile. The structure of ThyX shows that dUMP is in an unusual curled conformation, with the phosphate oxygen 4 Å away from C6 of the uracil moiety (Figure 3-1). Conceivably a phosphate oxygen could attack the uracil moiety in a Michael addition. However, the phosphorothioate analog, of dUMP, with a more nucleophilic sulfur atom available to attack the uracil moiety, reacts more slowly, not faster, than dUMP, which is not expected if the phosphate oxygen of dUMP is the nucleophile.

Recently a mechanism for another flavoprotein, UDP-galactopyranose mutase, has been proposed in which the N5 of a reduced flavin acts as a nucleophile (*17*).

In the crystal structure of *T. maritima* ThyX, N5 of the flavin is in a position to react by a Michael addition (Figure 3-1). Replacing FAD with 5-deaza-FAD eliminated the possibility for the reduced form to act as a nucleophile. While this reaction is somewhat slower that with FAD, the 5-deaza-FAD-substituted enzyme still reacted (Figure 3-13). The substantial reactivity of the 5-deaza-FAD-substituted enzyme also eliminates mechanisms invoking flavin radicals, because 5-deaza-FAD radicals are extremely unfavorable.

A hydride, transferred from the reduced flavin, has been proposed to activate dUMP (*10*). NMR analysis clearly shows that a hydride is transferred from the flavin to C6 of dUMP, but several experiments show that it does not take place until after activation of dUMP and transfer of the methylene from CH_2THF. Activation of dUMP by a hydride transfer from the reduced flavin would result in oxidation of the flavin as an early event of the oxidative half-reaction. Addition of dUMP to the reduced enzyme (in the absence of CH_2THF) causes no flavin oxidation. Neither does incubating the reduced enzyme with 5F-dUMP and CH_2THF. The fluoro-substitution would not prevent redox chemistry, but would prevent the breakdown of a nucleotide-folate adduct. This is consistent with previously published data with *C. jejuni* ThyX that show 5F-dUMP and CH_2THF do not oxidize the reduced enzyme (*9*). Furthermore, direct observation of dUMP and CH_2THF reacting with reduced enzyme by stopped-flow methods shows at least one reaction occurring before flavin oxidation. Chemical quenching shows another - the loss of dUMP, implying the formation of another intermediate - prior to flavin oxidation. All of these results show that dTMP synthesis cannot be initiated by reductive enolization of dUMP.

We propose that activation of dUMP does not occur by a Michael addition or other chemistry. Instead, dUMP binds to the enzyme in a polarizing site, with the negative charge of the phosphate of dUMP close to its N1 and C6, and the positive charges of R90 and R174 close to the carbonyl oxygen of C4 (Figure 3-1). This electrostatic environment would favor the polarized resonance description in Scheme 3-4, which has a higher electron density on C5 than the usual non-polarized resonance description. The higher electron density of could C5 accelerates attack on the iminium carbon of CH_2THF. It is noteworthy that uracil can react without any promotion of a nucleophile in aqueous solution with formaldehyde (*18, 19*).

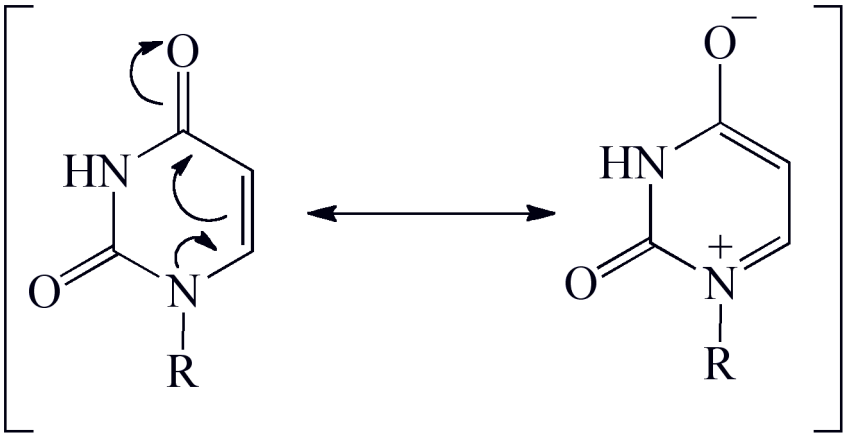

Figure 3-15: ***Polariation of dUMP***. The proposed mode of activation of dUMP occurs through the polarization of dUMP .

This concept leads to the chemical mechanism for the oxidative half-reaction shown in Figure 3-16. Steps whose arrows are colored red (1-3) are suggested to occur in the first phase observed in stopped-flow experiments, while those in blue (4-5) occur in the second phase as the flavin becomes oxidized. Polarization of dUMP occurs upon binding. We propose that activation of CH_2THF, nucleophilic attack of dUMP on

CH_2THF, and deprotonation of C5 occur during the first observed phase. The replacement of R90 and R174 with alanines diminishes polarization of dUMP so that the negative charge build-up at the C4 oxygen of dUMP is not stabilized. Thus, the first phase for these variants is slower than WT. The phosphate of dUMP must be in the correct position to enable efficient polarization and stabilization of the positive charge at N1 of the uracil moiety. Q75 and S88 both hydrogen-bond to the phosphate oxygen of dUMP, positioning it above N1 and C6 of dUMP. Mutations to either of residues slows this first step, presumably because the phosphate is not positioned effectively. The nucleotide analogue 5-dUMPS, that has a phosphate with a more dispersed negative charge, also slows this first step, suggesting inefficient polarization of the uracil ring (Figure 7). The mechanism is also consistent with the observation (quenching experiments) that the disappearance of dUMP occurs before flavin oxidation is observed. It also predicts that there is no protein-nucleotide covalent adduct, and none was found by mass spectroscopy. Activation of CH_2THF, step 1, also occurs in the first phase. The rate constant for this phase increased at lower pH, as would be expected for formation of the iminium ion of CH_2THF by protonation of N10.

Flavin oxidation occurs in the second phase observed in stopped-flow experiments. In Figure 3-16, the elimination of THF from the bridging complex between THF and dUMP accompanies flavin oxidation (step 4) and would be assisted by the protonation of N5 of THF, consistent with the observed acid-catalysis of flavin oxidation as well as previous studies suggesting that a hydride from the reduced flavin is transferred to C6 of the nucleotide (*10, 20*). Lastly, a 1,3-sigmatropic rearrangement has been previously proposed as the final step (step 5) based on NMR analysis of label

incorporation (*10*). This reaction would very likely not significantly perturb the absorbance spectrum of the oxidized flavin, and so would not be detected in stopped-flow experiments. Furthermore, if the reaction is fast relative to the time required for HPLC analysis of acid-quenched samples, both tautomers of the nucleotide product would be detected as dTMP.

In conclusion, the search for a nucleophile in the ThyX reaction has been unsuccessful because, we believe, there is no nucleophile. The chemical mechanism in Figure 3-16 proposed for the synthesis of dTMP is consistent with the data presented here and as well as results published previously. The novelty of this scheme shows that multiple mechanisms are likely to have evolved to solve the biochemical problem of reductive methylation of uracil using CH_2THF as a carbon donor. These results suggest that inhibition could be developed that prevents activation of dUMP or electron transfer from the reduced flavin.

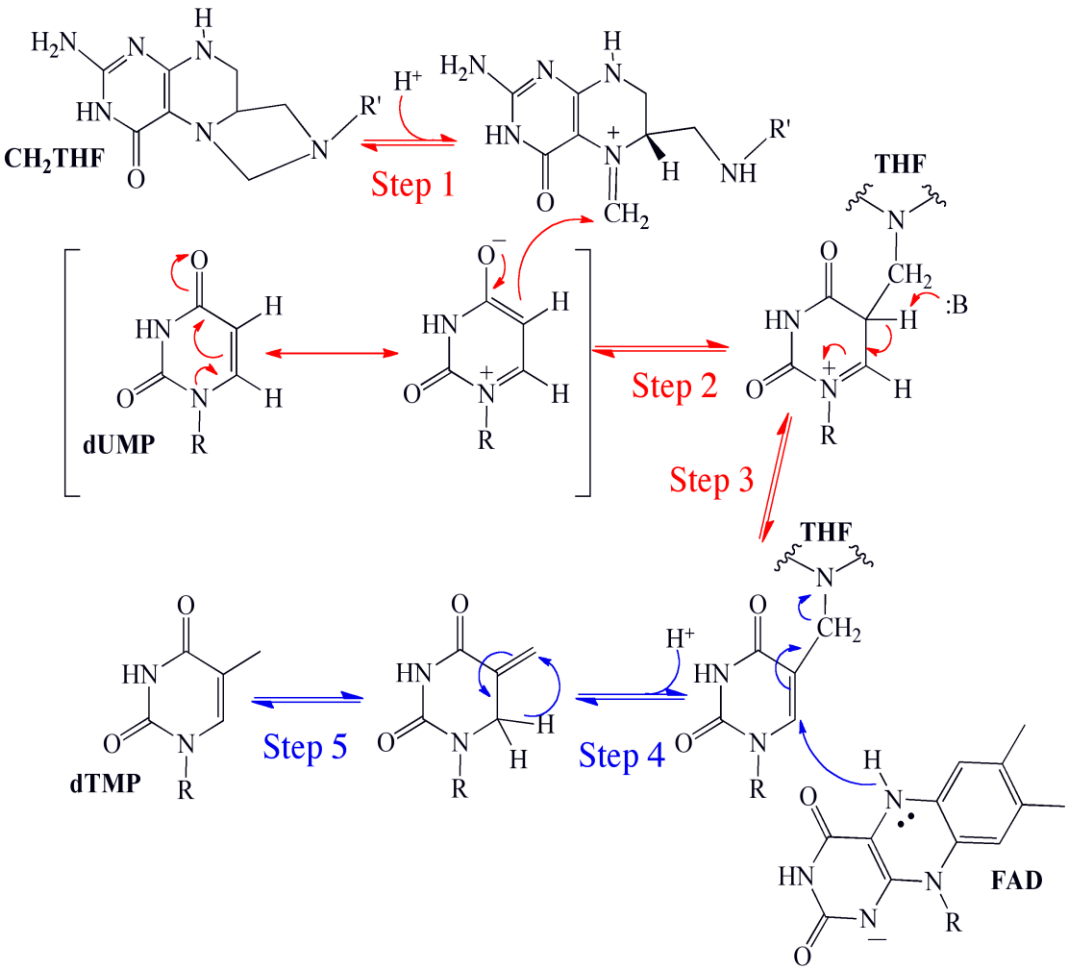

Figure 3-16. ***The Proposed Chemical Mechanism for the Synthesis of dTMP by ThyX.*** The steps in red are the proposed steps that occur before oxidation of the flavin. The steps in blue that include and proceed after oxidation of the flavin.

REFERENCES

1. Carreras, C. W., and Santi, D. V. (1995) The catalytic mechanism and structure of thymidylate synthase, *Annu Rev Biochem 64*, 721-762.
2. Atreya, C. E., Johnson, E. F., Williamson, J., Chang, S. Y., Liang, P. H., and Anderson, K. S. (2003) Probing electrostatic channeling in protozoal bifunctional thymidylate synthase-dihydrofolate reductase using site-directed mutagenesis, *J Biol Chem 278*, 28901-28911.
3. Atreya, C. E., and Anderson, K. S. (2004) Kinetic characterization of bifunctional thymidylate synthase-dihydrofolate reductase (TS-DHFR) from Cryptosporidium hominis: a paradigm shift for ts activity and channeling behavior, *J Biol Chem 279*, 18314-18322.
4. Leduc, D., Escartin, F., Nijhout, H. F., Reed, M. C., Liebl, U., Skouloubris, S., and Myllykallio, H. (2007) Flavin-dependent thymidylate synthase ThyX activity: implications for the folate cycle in bacteria, *J Bacteriol 189*, 8537-8545.
5. Mathews, II, Deacon, A. M., Canaves, J. M., McMullan, D., Lesley, S. A., Agarwalla, S., and Kuhn, P. (2003) Functional analysis of substrate and cofactor complex structures of a thymidylate synthase-complementing protein, *Structure 11*, 677-690.
6. Graziani, S., Bernauer, J., Skouloubris, S., Graille, M., Zhou, C. Z., Marchand, C., Decottignies, P., van Tilbeurgh, H., Myllykallio, H., and Liebl, U. (2006) Catalytic mechanism and structure of viral flavin-dependent thymidylate synthase ThyX, *J Biol Chem 281*, 24048-24057.

7. Sampathkumar, P., Turley, S., Ulmer, J. E., Rhie, H. G., Sibley, C. H., and Hol, W. G. (2005) Structure of the Mycobacterium tuberculosis flavin dependent thymidylate synthase (MtbThyX) at 2.0A resolution, *J Mol Biol 352*, 1091-1104.

8. Wang, W. C., Liu, J.S, Chang, C.M., . (PDB ID: 3FNN) Biochemical and structural analysis of atypical ThyX: Cornebacterium glutamicum NCHU 87078 depends on ThyA for thymidine biosynthesis.

9. Gattis, S. G., and Palfey, B. A. (2005) Direct observation of the participation of flavin in product formation by thyX-encoded thymidylate synthase, *J Am Chem Soc 127*, 832-833.

10. Koehn, E. M., Fleischmann, T., Conrad, J. A., Palfey, B. A., Lesley, S. A., Mathews, II, and Kohen, A. (2009) An unusual mechanism of thymidylate biosynthesis in organisms containing the thyX gene, *Nature 458*, 919-923.

11. Chernyshev, A., Fleischmann, T., Koehn, E. M., Lesley, S. A., and Kohen, A. (2007) The relationships between oxidase and synthase activities of flavin dependent thymidylate synthase (FDTS), *Chem Commun (Camb)*, 2861-2863.

12. Lesley, S. A., Kuhn, P., Godzik, A., Deacon, A. M., Mathews, I., Kreusch, A., Spraggon, G., Klock, H. E., McMullan, D., Shin, T., Vincent, J., Robb, A., Brinen, L. S., Miller, M. D., McPhillips, T. M., Miller, M. A., Scheibe, D., Canaves, J. M., Guda, C., Jaroszewski, L., Selby, T. L., Elsliger, M. A., Wooley, J., Taylor, S. S., Hodgson, K. O., Wilson, I. A., Schultz, P. G., and Stevens, R. C. (2002) Structural genomics of the Thermotoga maritima proteome implemented in a high-throughput structure determination pipeline, *Proc Natl Acad Sci U S A 99*, 11664-11669.

13. Patil, P. V., and Ballou, D. P. (2000) The use of protocatechuate dioxygenase for maintaining anaerobic conditions in biochemical experiments, *Anal Biochem 286*, 187-192.

14. Bevington, P. R. (1969) *Data reduction and error analysis for the physical sciences*, McGraw-Hill, New York,.

15. Ghisla, S., Massey, V., Lhoste, J. M., and Mayhew, S. G. (1974) Fluorescence and optical characteristics of reduced flavines and flavoproteins, *Biochemistry 13*, 589-597.

16. Leduc, D., Graziani, S., Lipowski, G., Marchand, C., Le Marechal, P., Liebl, U., and Myllykallio, H. (2004) Functional evidence for active site location of tetrameric thymidylate synthase X at the interphase of three monomers, *Proc Natl Acad Sci U S A 101*, 7252-7257.

17. Soltero-Higgin, M., Carlson, E. E., Gruber, T. D., and Kiessling, L. L. (2004) A unique catalytic mechanism for UDP-galactopyranose mutase, *Nat Struct Mol Biol 11*, 539-543.

18. Dworkin, J. P. (1997) Attempted prebiotic synthesis of pseudouridine, *Orig Life Evol Biosph 27*, 345-355.

19. Choughuley, A. S., Subbaraman, A. S., Kazi, Z. A., and Chadha, M. S. (1977) A possible prebiotic synthesis of thymine: uracil-formaldehyde-formic acid reaction, *Biosystems 9*, 73-80.

20. Agrawal, N., Lesley, S. A., Kuhn, P., and Kohen, A. (2004) Mechanistic studies of a flavin-dependent thymidylate synthase, *Biochemistry 43*, 10295-10301.

Chapter IV

Conclusions and Future Directions

All TSs catalyze the reductive methylation of dUMP. The synthesis of dTMP by ThyX, however, is unique in that it does not use the transiently formed THF as a reductant, but requires both an FAD prosthetic group and reducing equivalents from NADPH. This enzyme is drastically different from ThyA in both sequence and structure. The work presented in this thesis shows the mechanism of ThyX also has important differences than the mechanism of ThyA.

My thesis work focused on both the kinetic and chemical mechanism of ThyX from *T. maritima*. In Chapters 2 and 3, by looking at the effects of substrates on the reductive and oxidative half-reactions, I was able to determine the preferred order of binding. In the reductive half-reaction the enzyme•dUMP complex usually precedes reduction by NADPH. No charge-transfer complex between the reduced enzyme•dUMP complex and $NADP^+$ was observed, suggesting that $NADP^+$ does not remain bound after reduction. In the oxidative half-reaction the reduced enzyme•dUMP complex reacts with CH_2THF to form dTMP and THF. These experiments focused on the preferred binding order, but did not focus on order of product release. Further experiments will be required in order to determine the order of product release. A full steady-state workup could

determine the order of product release, but such experiments will require a strict anaerobic environment to ensure no off pathway reactions between the reduced enzyme and molecular oxygen.

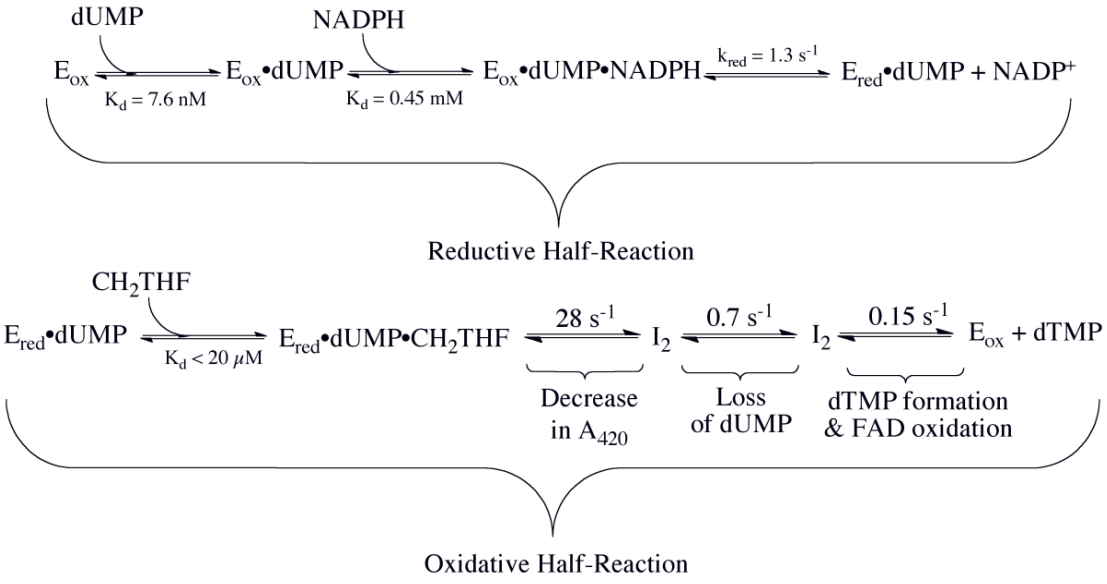

Figure 4-1. ***The Kinetic Mechanism of ThyX from T. maritima***. The kinetic mechanism of ThyX shown as two half-reactions.

A number of active site mutations were also made. These residues drastically affected the binding of dUMP. However, these mutations had little effect on the reduction of the enzyme•dUMP complex by NADPH and binding of CH_2THF to the oxidized enzyme. While it is clear were dUMP binds in the active site, as observed in crystal structures of the enzyme•dUMP complex, it is unclear where NAD(P)H or CH_2THF bind. It has been proposed, using docking models (*1*), that the flavin moves to allow binding of CH_2THF in the active site; however, location of NADPH and CH_2THF in the active site remain elusive. Further structures of ThyX, specifically with NADPH or CH_2THF, would greatly enhance our understanding of where these substrates bind.

The work presented in Chapter 3 focused on the activation of dUMP. Earlier work suggested that activation of dUMP occurs through a Michael addition using a conserved serine, similar to activation of dUMP by ThyA, which uses an active site cysteine (*2, 3*). This hypothesis was ruled out by experiments, using site directed mutagenesis of this serine to an alanine, carried out by our lab and that of Kohen and co-workers (*4*). In that work it was suggested that a hydride transfer from the reduced flavin to C6 of dUMP activates the nucleotide (*4*), but that hypothesis is inconsistent with data on the oxidative half-reaction in this dissertation that shows at least two observable intermediates occurring prior to oxidation of the flavin (Chapter 3). I examined the effects of pH, mutagenesis, and dUMP and FAD analogues on the oxidative half-reaction. These studies suggested that activation occurs through the polarization of the substrate (Figure 4-2), accomplished by binding to a polarized active site. Presumably, activation by polarization occurs concomitant with binding of dUMP in the active site; however, further experiments will be required to confirm this notion. In principle, using ^{15}N-dUMP, the polarization, facilitated by binding, would be observable by NMR.

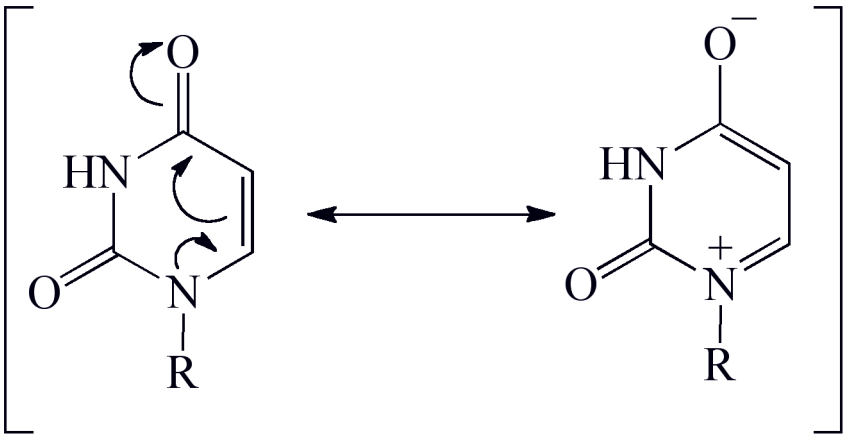

Figure 4-2. ***Activation of dUMP by ThyX***. The activation of dUMP, by ThyX is proposed to occur by the polarization of dUMP through the binding in a polarized active site.

In Chapter 3 results of studies of the oxidative half-reaction by stopped-flow spectroscopy and acid quenching revealed the accumulation of two intermediates prior to oxidation of the flavin. These results suggests that carbon transfer occurs before oxidation of the flavin; however, the identity of these intermediates is unknown. The proposed mechanism is shown below in Figure 4-3.

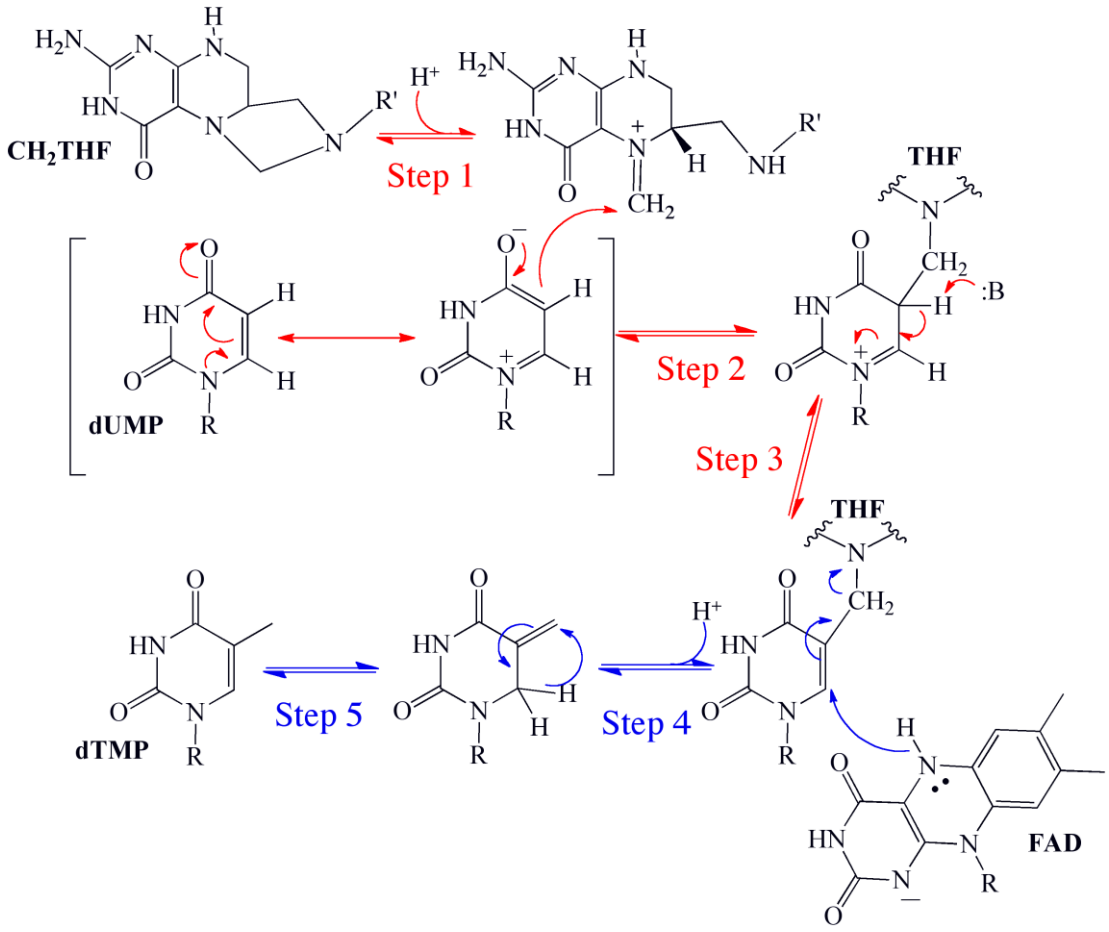

Figure 4-3. ***The Proposed Chemical Mechanism of ThyX***. The steps in red are the proposed steps that occur before flavin oxidation.

The first intermediate, observable by stopped-flow spectroscopy by the rapid decrease in absorbance at 420 nm, is proposed here as the accumulation of the product from step 2. This step is affected by the formation of the active forms of both substrates, i.e., polarization of dUMP and formation of the iminium ion of CH_2THF. Presumably, the formation of the iminium ion is facilitated by the protonation of N10 of CH_2THF, as indicated by the increase in rate constant at low pH. It is conceivable the protonation of N10 of CH_2THF could be facilitated by a glutamate residue (glutamate 144 in *T.*

maritima ThyX). The elimination of the acidic residue should result in a lesser rate constant for this first observable step on the oxidative half-reaction.

The formation of the second intermediate of the oxidative half-reaction was observed by rapid reaction acid quenching experiments as the loss of dUMP; however, this step was not observable by stopped-flow spectroscopy. This intermediate has been proposed here as the formation of the product from step 3. The formation of this intermediate requires deprotonation at C5 of dUMP; however, further experiments would be required in order to test this hypothesis. This deprotonation step requires a base and thus should be faster at high pH. A pH dependence of this reaction performed by acid quenching should make the formation of this intermediate faster at high pH and would be observable as an increase in rate constant for the loss of dUMP. Alternatively, this step should slow down if the proton at C5 is replaced with deuterium. Using $5H^2$-dUMP in the oxidative half-reaction, performed by acid quenching, should result in a decrease in rate constant for the loss of dUMP.

The final phase, observable by both stopped-flow spectroscopy and acid quenching, is the formation of dTMP and oxidation of the flavin. This mechanism proposes the second intermediate is the accumulation of the product from step 3. Therefore, this final phase should be the reaction of this intermediate with the reduced FAD. A derivative of this compound, 5-thyminyl-5,6,7,8-tetrahydrofolate, has been shown to be stable in aqueous solution (*5*). However further modification to form the dUMP-5,6,7,8-tetrahydrofolate would be required. This compound when bound should

react solely with the reduced enzyme. Alternatively, this final phase has been shown to be faster at low pH. It was suggested that this is the result of the protonation of N5 of THF that facilitates its elimination from the complex. A glutamate residue (glutamate 144 in *T. maritima* ThyX) could facilitate this protonation. Elimination of this acidic residue by site directed mutagenesis should hinder this step during the oxidative half-reaction and should be observable by stopped-flow spectroscopy as a decrease in rate constant for this step.

While the study of ThyX is still in its infancy greats steps have been made in order to determine the mechanism. The drastic differences in the sequence, structure, and the unique mechanism of ThyX, compared to ThyA, should lead to it being a promising drug target.

References

1. Agrawal, N., Lesley, S. A., Kuhn, P., and Kohen, A. (2004) Mechanistic studies of a flavin-dependent thymidylate synthase, *Biochemistry 43*, 10295-10301.
2. Leduc, D., Graziani, S., Lipowski, G., Marchand, C., Le Marechal, P., Liebl, U., and Myllykallio, H. (2004) Functional evidence for active site location of tetrameric thymidylate synthase X at the interphase of three monomers, *Proc Natl Acad Sci U S A 101*, 7252-7257.
3. Ulmer, J. E., Boum, Y., Thouvenel, C. D., Myllykallio, H., and Sibley, C. H. (2008) Functional analysis of the Mycobacterium tuberculosis FAD-dependent thymidylate synthase, ThyX, reveals new amino acid residues contributing to an extended ThyX motif, *J Bacteriol 190*, 2056-2064.
4. Koehn, E. M., Fleischmann, T., Conrad, J. A., Palfey, B. A., Lesley, S. A., Mathews, II, and Kohen, A. (2009) An unusual mechanism of thymidylate biosynthesis in organisms containing the thyX gene, *Nature 458*, 919-923.
5. Gupta, V. S., and Huennekens, F. M. (1967) Thyminyl derivatives of tetrahydrofolate, *Biochemistry 6*, 2168-2177.